Summer 8-18-2017

Molecular mechanisms of C-terminal Eps15 Homology Domain containing (EHD) protein function

Kriti Bahl
University of Nebraska Medical Center

Molecular mechanisms of C-terminal Eps15 Homology Domain containing (EHD) protein function

By

Kriti Bahl

A DISSERTATION

Presented to the Faculty of

The Graduate College in the University of Nebraska

In Partial fulfillment of Requirements

For the degree of Doctor of Philosophy

Department of Biochemistry and Molecular Biology

Under the Supervision of Professor Steve Caplan

University of Nebraska Medical Center

Omaha, Nebraska

June, 2017

Supervisory Committee:

Richard MacDonald, Ph.D. Justin Mott, M.D., Ph.D.

Laurey Steinke, Ph.D.

TITLE

Molecular mechanisms of C-terminal Eps15 Homology Domain containing (EHD) protein function

BY

Kriti Bahl

APPROVED	DATE
Steve Caplan, Ph.D.	**June 23rd 2017**
Richard MacDonald, Ph.D.	**June 23rd 2017**
Justin Mott, M.D., Ph.D.	**June 23rd 2017**
Laurey Steinke, Ph.D.	**June 23rd 2017**

SUPERVISORY COMMITTEE

GRADUATE COLLEGE **UNIVERSITY OF NEBRASKA**

Molecular mechanisms of C-terminal Eps15 Homology Domain containing (EHD) protein function

Kriti Bahl, Ph.D.

Advisor: Steve Caplan, Ph.D.

Endocytic trafficking is not only an essential process for the maintenance of cellular homeostasis but also plays a vital role in regulating diverse cellular processes such as signaling, migration and cell division. The C-terminal Eps 15 Homology Domain proteins (EHD1-4) play pivotal roles in regulating distinct steps of endocytic trafficking. Among the EHDs, EHD2 is disparate both in terms of sequence homology (70%) and its subcellular localization at the caveolae. The crystal structure of EHD2 has been solved and it contains an unstructured loop consisting of two proline-phenylalanine (PF) motifs: K**PF**RKLN**PF**. However, the other paralogs EHD1, EHD3 and EHD4 contain a single KPF or RPF motif, but no NPF motif. In this study, we sought to elucidate the precise role of the two PF motifs of EHD2 in homo-dimerization, binding with the protein partners, and subcellular localization. We demonstrated that an EHD2 NPF-to-NAF mutant that mimics the homologous sequences of EHD1 and EHD3, lost its ability to dimerize and bind to Syndapin2. However, it continues to localize primarily to the cytosolic face of the plasma membrane. On the other hand, EHD2 NPF-to-APA mutants maintained their ability to dimerize and bind to Syndapin2, but exhibited markedly increased nuclear localization and decreased association with the plasma membrane. Hence, the EHD2 NPF phenylalanine residue is crucial for EHD2 localization to the plasma membrane, whereas the proline residue is essential for EHD2 dimerization and binding. These studies also support the recently proposed model in which the EHD2 N-terminal region may regulate the availability of the unstructured loop for interactions with neighboring EHD2 dimers, thus promoting oligomerization. We further hypothesized that the single PF motif of EHD1 might be responsible for both binding and localization

functions of EHD1. Indeed, the EHD1 RPF motif was required for dimerization, interaction with MICAL-L1 and Syndapin2, as well as localization on tubular recycling endosomes. Moreover, recycling assays demonstrated that EHD1 RPF-to-APA was incapable of supporting normal receptor recycling. The biogenesis of tubular recycling endosomes (TRE), their role in cargo-sorting and subsequently their vesiculation are essential for receptor recycling. EHD proteins have been implicated in the bending and fission of TRE, thus regulating endocytic recycling. Recent studies from our lab have demonstrated that asparagine-proline-phenyalanine (NPF)-containing binding partners of EHD1 and EHD3, such as molecules interacting with CasL-like1 (MICAL-L1) and Syndapin2, are indispensable for TRE biogenesis. Also vital for TRE biogenesis is the generation of phosphatidic acid (PA), an essential lipid component of TRE that serves as a docking point for MICAL-L1 and Syndapin2. EHD1 and EHD3 have 86% amino acid identity; they homo-and heterodimerize and partially co-localize to TRE. Despite remarkable identity between EHD1 and EHD3, they have disparate mechanistic functions. EHD1 induces membrane vesiculation, whereas EHD3 supports TRE generation and/or stabilization by an unknown mechanism. While using phospholipase D inhibitors (which block the conversion of glycerophospholipids to PA) to deplete cellular TRE, we observed that, upon inhibitor washout, there was a rapid and dramatic regeneration of TRE, as observed by immunostaining with MICAL-L1 antibodies. This “synchronized” TRE biogenesis system has enabled us to determine that EHD3 is involved in the stabilization of TRE rather than in their biogenesis. Moreover, we have identified residues Ala-519/Asp-520 in the EH domain of EHD1 and Asn-519/ Glu-520 in the EH domain of EHD3 as being important for that dictating the preference of these two paralogs for NPF-containing binding partners. Overall, we have delineated a model to explain the atomic basis for understanding the differential roles of EHD3 and EHD1 in stabilization and vesiculation of TRE, respectively.

Table of Contents

Table of Figures

CHAPTER 1

CHAPTER 3

List of Tables

CHAPTER I

CHAPTER III

Abbreviations

ACAP1	Arf GAP with coiled-coil ankyrin repeat and PH domains 1
AMPA	2-amino-3 (3-hydroxy-5-methyl-isoxazol-4-yl) propanoic acid
AMPPNP	Adenylyl Imidodiphosphate
AP-2	Adaptor Protein-2
ARF	ADP-Ribosylation Factor
ARH	Autosomal Recessive Hypercholestrolemia Protein
B2AR	β2 Adrenergic Receptor
BAR	Bin-Amphiphysin-Rvs
BSA	Bovine Serum Albumin
C-terminus	Carboxyl-Terminal
C.elegans	*Caenorhabditis elegans*
CCIE	Clathrin and Caveolae-Independent Endocytosis
CCP	Clathrin-Coated Pit
CCV	Clathrin-Coated Vesicle
Cdc42	Cell Cycle Dependent 42
CI	Clathrin-Independent

CIE	Clathrin-Independent Endocytosis
CLASPs	Clathrin-Associated Sorting Protein
CLICs	Clathrin-Independent Tubulovesicular Intermediate
CME	Clathrin-Mediated Endocytosis
COPI	Coat Protein Complex I
CORVET	Class C core vacuole/endosome tethering
cPLA2α	Cytosolic Phospholipase A2-α
CSC	Cargo-Selective-Complex
CTxB	Cholera toxin B subunit
DAB2	Disabled Homolog 2
DAG	Diacylglycerol
[DE] XXXL [LI]	Dileucine-based Motifs
DMEM	Dulbecco’s Modified Eagle Medium
dSTORM	Direct Stochastic Optical Reconstruction Microscopy
EE	Early Endosome
EGF	Epidermal Growth Receptor
eGFPC3	Green Fluorescent Protein
EH	Eps15
EHBP1	EHD2 Binding Protein1
EHD	C-terminal Eps15 Homology domain containing Protein
ERC	Endocytic Recycling Compartment

ESCRT	Endosomal Sorting Complexes Required for Transport
FBS	Fetal Bovine Serum
FCH	Fps/Fes/Fer/CIP4 Homology
FCHO	FCH Domain Only
FIPI	5-Fluoro-2-indolyl des-chlorohalopemide
FRAP	Fluorescence recovery after photobleaching
FYVE	Fab1, YOTB, Vac1, and EEA1
GAP	GTPase-activating protein
GDF	GDI displacement factor
GDI	GDP dissociation inhibitor
GDP	Guanosine-5'-Diphosphate
GEEC	GPI-AP-enriched Early Endosomal Compartment
GEF	Guanyl nucleotide factor
GGA	Golgi-localized γ-ear-containing ARF-binding
GPCR	Gprotein-coupled receptor
GPI	Glycosylphosphatidylinositol
GPI-AP	GPI-anchor linked proteins
GRAF1	GTPase Regulator Associated with Focal Adhesion Kinase-1
GST	Glutathione-S-transferase
GTP	Guanosine-5'-Triphosphate
GTPase	Guanosine-5'-Triphosphatase

h	Hour
Hrs	Hepatocyte growth factor-regulated tyrosine kinase substrate
HOPS	Homotypic fusion and protein sorting
Hsc70	Heat Shock Cognate 70
IF	Immunofluorescence
IL-2	Interleukin-2
ILV	Intraluminal Vesicle
IPTG	Isopropyl β-D-1-thiogalactopyranoside
KD	Knockdown
K_D	Binding constant
Km	Michaelis Constant
LDLR	Low-Density Lipoprotein Receptor
LE	Late Endosome
LRP	LDLR-Related Protein
MHC I	Major Histocompatibility Complex I
MICAL-L1	Molecules Interacting with CasL-Like1
min	Minute
MTOC	Microtubule Organizing Center
MVB	Multivesicular Bodies
N	Amino-terminal
N-WASP	Neural Wiskott-Aldrich syndrome protein

NgCAM	Neuron-glia Cell Adhesion Molecule
NMR	Nuclear Magnetic Resonance
NPF	Asparagine-Proline-Phenylalanine
NSF	N-ethylmaleimide-sensitive fusion protein
O.D.	Optical Density
P-loop	Phosphate Binding-Loop
PA	Phosphatidic Acid
PAGE	Polyacrylamide Gel Electrophoresis
PAST1	Putative Achaete-Scute Target 1
PDZ	PSD-95, DLG and ZO-1
PF	Proline-Phenylalanine
PH	Plecksterin Homology
PI	Phosphoinositide
PI (3,5) P2	Phosphatidylinositol 3,5 bisphosphate
PI (3)K	Phosphatidylinositol-3-kinase
PI (3)P	Phosphotidylinositol (3) phosphate
PIKfyve	Phosphoinositide kinase
PIP2	Phophotidylinositol 4,5 bisphosphate
PIP5K	Phosphatidylinositol 4,5 kinase
PLD	Phospholipase D
PLD2	Phospholipase D2

PM	Plasma Membrane
PRD	Proline-rich Domain
PTB	Phosphotyrosine-Binding
PX	Phox-Homology
Rab11-FIPs	Rab11-family Interacting Proteins
Rac1	Ras-related C3 Botulinum Toxin Substrate
RE	Recycling Endosome
RILP	Rab7-interacting Lysosomal Protein
RME-1	Receptor-Mediate Endocytosis-1
RTK	Receptor Tyrosine Kinase
S. cerevisiae	*Saccharomyces cerevisiae*
SDS	Sodium Dodecyl Sulphate
SE	Sorting Endosome
SH3	Src Homology Domain 3
STAM2	Signal-transducing Adaptor Molecule 2
SIM	Structured Illumination Microscopy
SNAP-29	Synaptosome-associated Protein 29
SNAREs	Soluble-NSF Attachment Protein
SNX	Sorting nexin
SV40	Simian Virus 40
TBC1D10C	TBC Domain member 10C

TfR	Transferrin receptor
TGN	Trans-Golgi Network
TRE	Tubular Recycling Endosome
TrkA	Nerve Growth Factor Receptor
Tsg101	Tumor susceptibility gene 101
UIM	Ubiquitin-interacting Motif
Vps	Vacuolar protein sorting
WB	Western blot
YXXϕ	Tyrosine-based Motifs

Acknowledgements

I wish to express my sincere appreciation to those who have made significant contribution to this dissertation and supported me in one way or another during this amazing journey.

First and foremost, I would like to thank God for giving me the strength to complete this Ph.D. program. Secondly, I would like to express my sincere gratitude to my mentors, Dr. Steve Caplan and Dr. Naava Naslavsky, for their guidance, support, patience, time, motivation and encouragement during my years of training. They have been great mentors and have made these five years a productive and stimulating experience.

I am fortunate to have been helped in different capacities by the past and present members of my lab. I would also like to sincerely thank Dr. Sai Srinivas Panappakam Giridharan and Dr. Shuwei Xie for their friendship and for training me in performing experiments and analyzing results. I would also like to thank Trey Farmer for being an amazing frend and junior in the lab. I would also like to thank Dr. Bishuang Cai, Dr. Jing Zhang, Dr. Laura Simone, Dawn Katafiaz, Dr.James Reinecke. I would also like to give a special thanks to Dr. Gaelle Spagnol and Andrew Trease from Dr. Sorgen's laboratory for helping me with protein purifications.

I am indebted to my supervisory committee members Dr. Richard MacDonald, Dr. Justin Mott, and Dr. Laurey Steinke for their guidance, encouragement, and support.

I am grateful to my comprehensive exam committee members Dr. Kaustabh Datta, Dr. Xu Luo and Dr. Terrence Donohue for guiding me during the rigors of the comprehensive exam process.

I would also like to thank everyone at the University of Nebraska Medical Center, especially the Department of Biochemistry and Molecular Biology for their support and collegial environment to pursue my graduate studies. I would specifically like to thank Karen Hankins in the BMB office for being an amazing friend, and for her support in the tumultuous times. I would also like to thank Graduate Studies at UNMC for funding.

Words are short to express my heartfelt thanks to my family for their unparalleled love, help, and support. I would also like to especially thank my mom, who raised me with a love of science, supported me in all my pursuits, and has been a constant source of determination and inspiration in the last five years. Thanks to my Dad for always believing in me and encouraging me to follow my dreams. To my sister Agrima and my brother Vikram for being there for me always, showing me the importance of being a free spirit and having a fresh perspective on every aspect of life.

I also want to thank my amazing friends here at UNMC, Sohini Roy, Swati Surkar, Shreya Roy and Mary Anne Smith, for taking out time for me from their busy schedules for talking to me, offering me advice, constantly encouraging me, warm hugs and being there for me when I needed a friend. I also want to thank my friends back in India, Soumya Menon, Ruchika Bharadwaj and Priyanka Arora for being just a text and phone call away, despite the time difference between us.

Last but not the least, I would like to acknowledge the most important person in my life – my husband and best friend, Suprit Gupta, for his endless love, humor, and encouragement throughout this journey. Without him, I would have struggled to find the inspiration, motivation, sanity, and bliss needed to complete this dissertation.

CHAPTER I

Introduction

1. Endocytic trafficking

1.1 Overview

The plasma membrane (PM) is a lipid bilayer that forms a permeability barrier between the interior of the cells and the extracellular environment (Conner and Schmid, 2003). The PM not only regulates the selective transport of ions and macromolecules in and out of the cell but also mediates communication with neighboring cells and the extracellular environment. Hence, the composition of the PM needs to be tightly regulated to generate appropriate responses to the cues from the extracellular environment. The dynamic interplay between endocytic trafficking and exocytic events is crucial for the precise regulation, and maintenance of the surface area and composition of the PM (Doherty and McMahon, 2009).

Endocytosis or endocytic trafficking refers to the process of internalization of receptors, proteins, and nutrients along with extracellular fluid enclosed in an invaginated portion of the PM, which culminates in pinching off of the membrane to form a vesicle (Conner and Schmid, 2003). The internalized lipids and proteins are returned to the PM by the process of exocytosis. Internalization of PM containing lipids, proteins, and receptors can occur through mechanistically diverse pathways regulated by distinct molecular players (detailed explanation in section 2). Irrespective of the mode of internalization, endocytosed cargo is packaged into a vesicle and delivered to a common "sorting station" known as the sorting endosome (SE) or the early endosome (EE) (Mayor et al., 1993; Mellman et al., 1996), where initial sorting events decide the fate of incoming cargo (Hauotari and Helenius, 2011). From here, cargo destined for degradation is transported to the late endosome (LE) and the lysosome, bound for recycling to the PM, or transported to the *trans*-Golgi network (TGN). While the receptors

and some of the lipids are destined for recycling; the ligands, soluble proteins of the PM are generally transported for degradation (Maxfield and MacGraw, 2004) (Fig 1.1).

Endocytic trafficking plays a vital role in regulating diverse processes, including nutrient uptake, regulation of surface receptors, cellular signaling, cytokinesis (Schmid and Conner, 2003; Skop et al., 2001), maintenance of cell polarity, cell adhesion and migration (Wang et al., 2000; Caswell and Norman, 2008), and synaptic vesicle retrieval in neurons (Kjaerulff et al., 2002). In addition, elegant studies have confirmed that pathogens exploit distinct endocytic pathways for their internalization in the cell (Mercer et al., 2010). Dysregulation of endocytic transport is related to diverse diseases including cancer, neurodegeneration, and heart disease (Conner and Schmid 2003; Stein et al., 2003). Thus, elucidation of the underlying mechanisms of endocytic trafficking will ultimately provide novel avenues for developing innovative therapeutic strategies and drug discovery.

2. Routes of Internalization

Internalization can occur through various mechanisms primarily governed by the size of the molecules and particles that the cell uptakes. Small molecules including amino acids, sugars and ions can enter through the channels and protein pumps. However, the macromolecules are endocytosed through the membrane invaginations and budding of the PM. Endocytosis is broadly classified into two main types based on the size of the endocytic vesicle: 1) *phagocytosis* involves large particles (>250) nm including microbial pathogens and cellular debris (Addermen and Underhill, 1999) 2) *pinocytosis* involves the uptake of fluid and low-molecular-weight solutes (<150) nm

Figure 1.1. Pathways of endocytosis and endocytic recycling.

Itinerary of cargo proteins and lipids internalized in cells by clathrin-mediated endocytosis (CME) (blue cargo) and clathrin-independent endocytosis (CIE) (red cargo) and subsequent routes of cargo to the early endosome (EE), endocytic recycling compartment (ERC) and recycling endosome (RE) is shown.

Figure 1.1

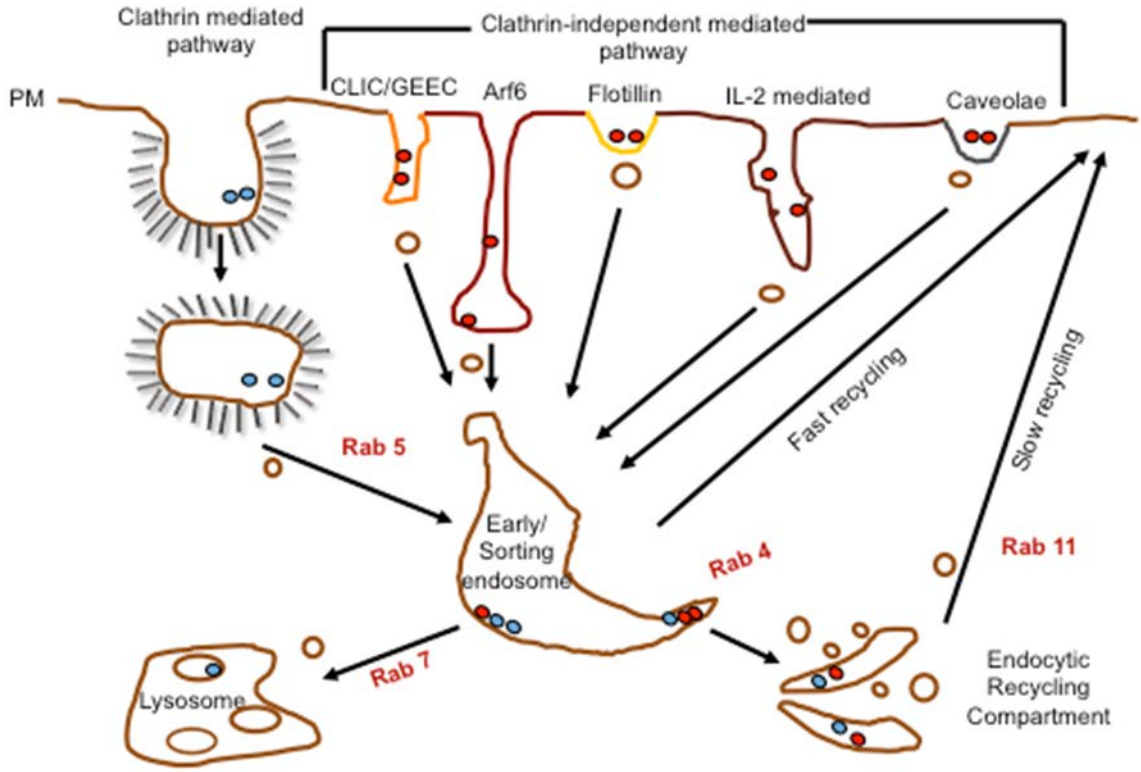
Clathrin mediated pathway
Clathrin-independent mediated pathway
PM
CLIC/GEEC
Arf6
Flotillin
IL-2 mediated
Caveolae
Rab 5
Fast recycling
Slow recycling
Early/ Sorting endosome
Rab 4
Rab 11
Rab 7
Lysosome
Endocytic Recycling Compartment

(Schmid and Conner, 2003). Pinocytosis, also known as “cell drinking” can be further classified based on the endocytic machinery recruited by the cargo molecules into clathrin-mediated endocytosis (CME) and clathrin-independent endocytosis (CIE). CIE is further subdivided into caveolae-mediated endocytosis, clathrin-independent endocytosis and caveolae-independent endocytosis (CCIE) (Conner and Schmid, 2003; Mayor and Pagano,2007) (Mayor, Parton and Donaldson, 2014).

2.1 Clathrin-mediated endocytosis (CME)

CME is the most extensively characterized route of internalization from the PM. The seminal discovery of clathrin and purification of clathrin-coated vesicles (CCVs) by Barbara Pearse forms the basis of our current understanding of CME (Pearse, 1987). Over the past 40 years, much work has shed light on the mechanism by which receptors and their bound ligands are internalized into clathrin-coated pits (CCPs) and eventually form the CCVs (Sorokin, 2004; Robinson, 2015). CCV formation is divided into a five-stage process: initiation, cargo selection, coat assembly, scission, and uncoating. The first stage of pit formation (CCP) is the assembly of a putative “nucleation module” consisting of Fps/Fes/Fer/CIP4 homology (FCH) domain only (FCHO) proteins, EGFR pathway substrate 15 (Eps15) and Intersectins at the PM (McMahon and Boucrot, 2011; Boucrot and McMahon, 2011). Furthermore, recent studies have demonstrated, proteins in the “nucleation module” are responsible for recruiting a tetrameric Adaptor Protein-2 (AP-2) that is a hub of interactions as it binds to both cargo and lipids in the PM (preferentially phosphatidylinositol (4, 5) bisphosphate (PIP2)). AP-2 is a complex composed of two large adaptin subunits-α and β2, one medium-μ2 and one small σ2 subunit (Owen et al., 2004). The AP-2 complex recognizes two types of motifs on the cytoplasmic tail of receptors (cargo): tyrosine-based motifs with a consensus sequence YXXΦ, where Y is a tyrosine residue, X stands for any amino acid residue and Φ is a

bulky hydrophobic amino acid residue, and the dileucine-based sorting signals with a consensus sequence [aspartic acid-glutamic acid]-X stands for any amino acid residue-X-X-leucine- [leucine-isoleucine] [DE] XXXL [LI] (Bonifacino and Traub, 2003). The binding site for the tyrosine-based motifs is on the carboxyl terminus (C) of the μ2 domain (Ohno et al.,1995), while the α/σ2 hemi-complex and potential β2 subunit bind to the dileucine-based sorting signal sequence (Chaudri et al., 2007; Doray et al., 2007). There are other specialized adaptor proteins known as clathrin-associated sorting proteins (“CLASPs”), that recognize diverse sorting signals on the respective cargo receptors thus facilitating a large repertoire of distinct cargo to be endocytosed (Linton and Bonifacino, 2013). For instance, cargo receptors such as the low-density lipoprotein receptor (LDLR) have an phenyalanine-X stands for any amino acid residue-asparagine -proline-X-tyrosine (FXNPXY) motif, that doesn’t directly bind to AP-2; hence the cooperation with CLASPs containing a phospho-tyrosine binding (PTB) domain such as disabled homolog 2 (Dab2) or autosomal recessive hypercholesterolemia protein (ARH) contributes to the process (Maurer and Cooper, 2006; Hawryluk et al., 2006). Post-translational modifications such as phosphorylation and ubiquitination can also recruit adaptor proteins to receptor tails as in the case of binding of Epsin to the ubiquitinated Epidermal Growth Factor Receptor (EGFR). Epsin is another example of a CLASP and it primarily regulates EGFR internalization (Polo et al., 2002; Kazazic et al., 2009). Once the cargo is selected and packaged by AP-2 or CLASPs, the assembly of the clathrin coat is initiated. AP-2 and accessory proteins recruit clathrin on the nascent CCP. Clathrin is a trimer of a dimers of three heavy chains and three light chains assembled as a triskelion (three-legged) that has an intrinsic ability to form cage-like structures, which facilitate membrane invagination (Kirchhausen, 2000). Next, accessory proteins such as Bin-Amphiphysin-Rvs (BAR) containing proteins are recruited to generate and stabilize the curvature of maturing CCPs (Quallmann B et. al, 2011). In addition, a large

and modular guanosine tri-phosphatases (GTPase) known as Dynamin, together with other curvature sensing proteins including Amphiphysin, Endophilins and Sorting nexin 9 (SNX9), facilitates the release of CCVs from CCPs (Lee et al., 1999; Vallis et al., 1999; van der Bliek et al., 1993; Yoshida et al., 2004). Dynamin oligomerizes as collar-like structures around the neck of CCPs and undergoes guanosine tri-phosphate (GTP) hydrolysis to mediate membrane fission and generate CCVs. After vesicle scission, the clathrin coat is disassembled by the action of an adenosine tri-phosphatase (ATPase) known as Heat shock cognate 70 (Hsc70) and its cofactor Auxillin (Braell et al., 1984; Prasad et al., 1993; Ungewickell et al., 1995). LDL receptor and the iron-laden transferrin receptor (Tf) are examples of signature cargo internalized by CME.

2.2 Clathrin-Independent Endocytosis (CIE)

CME is the predominant endocytic paradigm by which receptors are internalized; however, cells utilize mechanisms beyond clathrin-coated pits, collectively known as CIE. A common feature of CIE is their dependence upon cholesterol (Sandvik and vanDeurs, 1994; Mayor and Pagano, 2007).

2.2.1 Caveolae-mediated pathway

The caveolae-mediated pathway is the best-characterized clathrin-independent endocytic pathway (Rothberg et al., 1992). Caveolae are flask-shaped invaginations of 50-100 nm that are concentrated in microdomains of PM enriched in cholesterol, sphingolipids, and phosphatidylinositol (4,5)-bisphosphate (PIP2) (Andereson 1998; Pitto et al., 2000; Simone et al., 2014). Caveolin-1, an integral membrane protein that oligomerizes as well as inserts itself as a loop in the PM to generate the framework of caveolae (Bastini and Parton, 2010). At the PM, caveolin-1 recruits multimeric complexes of cavin proteins (cavin 1-4) that aid in shaping and stabilizing the caveolar

invaginations (Hill et al., 2008; Hansen et al., 2009; et al., 2009. Additionally, Syndapin2 (also known as Pacsin2), a BAR domain-containing protein that can sense and modulate membrane curvature, shapes the caveolar invagination (Senju et al., 2011 and Koch et al., 2012). Syndapin2 also has a Src homology 3 (SH3) domain that facilitates its binding to the proline-rich domain (PRD) of Dynamin and a tripeptide sequence containing, asparagine-proline-phenylalanine (NPF) motif that mediates binding with C-terminal Eps15 homology domain containing (EHD) protein 2 (EHD2). Recently, a series of reports have firmly established the caveolar localization of EHD2 and caveolar stabilization occurs in an adenosine triphosphate (ATP)-dependent manner. Previous studies from our lab have shown that the localization of EHD2 on caveolae is independent of its interaction with Syndapin2 and dependent on PIP2 in the PM (Moren et al., 2012; Stoeber et al., 2012; Simone et al., 2013). Caveolae are specifically enriched in certain cell types including smooth muscle cells, fibroblasts, adipocytes, and endothelial cells (Parton and Simons, 2007). The cargo that are internalized in caveolin-positive structures include simian virus 40 (SV40) virions, cholera toxin B subunit (CTxB), and glycosylphosphatidylinositol (GPI)-linked proteins (Cheng et al., 2006; Kirkham and Parton, 2005; Parton and Simons, 2007).

2.2.2 Clathrin-Independent Carriers/GPI-AP-enriched early endosomal compartment (CLIC/GEEC)

Proteins that are attached to the membrane by GPI-anchor-linked proteins (GP1-AP) are internalized independent of clathrin and caveolin coats however they require cholesterol enriched microdomains (Sabharjanek et al., 2002). GPI-APs are internalized through specialized EE-like structures termed, GPI-AP-enriched early endosomal compartment (GEEC). They are formed by the fusion of cell surface-derived clathrin independent (CI) tubulovesicular intermediates termed CLICs (Kirkham et al., 2005).

CLIC formation is regulated by small GTPases including cell cycle dependent 42 (Cdc42) and adenosine di-phosphate (ADP)-ribosylation factor1 (Arf1) (Kumari and Mayor, 2008). These structures are Dynamin-independent and their budding mechanism is not clear. However, recently a specific marker and regulator of these CLICs has been identified, a protein called GTPase regulator associated with focal adhesion kinase-1 (GRAF1). GRAF1 has distinct domains capable of regulating membrane deformation, a scission-BAR domain (membrane and curvature sensing), a pleckstrin homology (PH) domain (directly interacts with PIP2 in PM) and an SH3 domain (which can bind to a PRD domain in Dynamin) (Lundmark et al., 2008). Furthermore, previous work from our lab has led to a model that suggests the formation of a vesiculation complex that comprises Molecules Interacting with CAsL-Like1 (MICAL-L1) and C-terminal Eps15 homology domain containing (EHD) protein 1(EHD1) on tubular recycling endosome (TRE) and supports TRE vesiculation (Cai et al., 2012; Cai et al., 2014). Thus, GRAF1 could also be a potential vesiculator of this pathway. Cargo that are internalized by this pathway are GPI-APs, CTxB and fluid phase markers (Mayor and Pagano, 2007; Doherty and MaMahon, 2009).

2.2.3 Arf6 Associated Pathway

Another clathrin-independent pathway for the internalization of cell surface integral proteins lacking adaptor protein recognition sequences is associated with ATPase, ADP-ribosylation factor 6 (Arf6). Arf6 is localized at the PM and it regulates the flow of trafficking into and out of the cell, and the actin cytoskeleton at the PM. Arf6 is responsible for activating phosphatidylinositol 4,5 kinase (PIP5K) for generation of PIP2. The tubule-vacuolar carriers of cargo in this pathway are enriched in PIP2. Furthermore, PIP2 can also stimulate the actin polymerization machinery and drive the endocytic pathway. Thus, Arf6 indirectly regulates endocytic events through PIP2. The GPI-AP,

CD59, CD55 and major histocompatibility complex class I (MHC I) proteins are the primary cargo internalized by this pathway (Naslavsky et al., 2003).

2.2.4 Flotillin-Dependent Pathway

Flotillins are proteins localized to specific microdomains or lipid rafts in the PM and mediate yet another clathrin-independent endocytosis pathway that is regulated by the Src family tyrosine kinase Fyn (Gleebov et al., 2005; Otto and Nicholas, 2005). The flotillin family comprises flotillin 1 and flotillin 2 proteins, which are highly homologous (sharing 50% sequence identity). Flotillin 1 and flotillin 2 assemble in almost equal amounts at the PM for generation of the transport carriers (Otto and Nicholas, 2005). The cargo that utilize this pathway are CTxB, GPI-AP CD59, and fluid-phase markers.

2.2.5 Other routes

Another clathrin-independent pathway is the endocytic mechanism used by the interleukin-2 (IL-2) receptor. The concentration and internalization of IL-2 receptors occurs via small non-coated invagination (Mayor et al., 2014). The process is dependent upon RhoA and consequently ras-related C3 botulinum toxin substrate 1(Rac1) (Lamaze et al., 2001; Gesbert et al., 2004)(Fig 1.1).

3. Sorting of Cargo at EE/SE

Regardless of which of the many pathways receptors are internalized in mammalian cells, the internalized cargo enters a well-defined endomembrane or organellar system. The endocytic system decides the direction of flow and ultimately the fate of the cargo. Accordingly, a unique mechanism has evolved to converge differentially internalized cargo to a common sorting station for the initiation of sorting. This common sorting station localized to the cell is known as the EE or SE (see Fig 1.1) (Mayor et al., 1993;

Maxfield and McGraw, 2004). Rab5 is a key component of the cytosolic surface of EE, and together with its effector Vps34/p150, forms a phosphatidylinositol 3-kinase (PI(3)K) complex. Activation of PI(3)K complex leads to phosphorylation of phosphoinositidyl inositol (PI) and its conversion to phosphatidylinositol (3) Phosphate (PI(3)P), PtdIns(3)P, which is the most abundant phosphoinositide in the EE membrane. The simultaneous presence of Rab5 and PtdIns(3)P helps to EE to initiate a signaling cascade, which regulates the homotypic fusion in EE and motility of EE on actin and microtubular tracks(Zerial and Mcbride, 2001; Behnia and Munro, 2005).

EE have a mildly acidic luminal pH (≈6.3-6.5), thereby facilitating the uncoupling of ligands from their receptors within minutes of internalization. The uncoupling of receptors from the ligands is the first step of sorting (Maxfield and McGraw, 2004). Additionally, the EE is a highly dynamic structure with a strong propensity to undergo homotypic fusion (Gruenberg et al., 1989). It is a highly complex and pleomorphic organelle that consists of morphologically distinct elements, thin tubules (≈60 nm diameter) and large vesicles (≈300-400 nm diameter) with membrane invaginations and a multi-vesicular appearance. This precise subdomain morphology provides a platform for efficient “geometric sorting” of the cargo (Mayor et al., 1993). The tubular elements that have a high surface-to-volume ratio preferentially cluster cargo targeted for recycling. On the other hand, cargo concentrated in large vesicles (that eventually form multi-vesicular bodies (MVBs)) is shunted for degradation (Mellman, 1996). In most cases, the receptors are recycled back to the PM for additional rounds of ligand binding and the ligand is transported to lysosomes for degradation (Maxfield and McGraw, 2004). For instance, Tf and LDL receptors are recycled from EE, whereas the LDL itself and EGFR coupled to its ligand are transported for degradation (Jovic et al., 2009).

3.1 Sorting to the lysosomes for degradation

EE is responsible for sorting the soluble ligands and signaling receptors for degradation in a regulated manner. The soluble ligands are automatically sorted for degradation as the EE matures into LE. However, the sorting of signaling receptors for degradation in lysosomes requires specific sorting signals in the cytosolic domain. The signaling receptors are targeted to the lysosomes through the LE in order to attenuate their signals. Epidermal growth factor (EGF)-laden EGFR is a prototypic receptor tyrosine kinase (RTK) having specific cytosolic domain recognized by the sorting machinery for degradation (Haglund et al., 2003; Mosseson et al., 2003). The mono-ubiquitinylation of one or more lysine residues in the cytoplasmic tail of EGFR serves as an important intracellular sorting signal for the degradative pathway (Barriere et al., 2006; Haglund et al., 2003; Huang et al., 2006; Levkowitz et al., 1999; Umebayashi et al., 2008). The ubiquitylated receptors are recognized by several ubiquitin-interacting motif (UIM)-containing proteins, endosomal sorting complexes required for transport-0 (ESCRT-0) component, hepatocyte growth factor regulated tyrosine kinase substrate (Hrs), Eps15R, signal transducing adaptor molecule 2 (STAM2) and the ESCRT-I component, tumor susceptibility gene 101 (Tsg101) (Raiborg et al., 2002). Hrs also interacts with the flat clathrin lattice to form clustered Hrs microdomains for specialized recognition of ubiquitylated membrane proteins and their efficient sorting for degradation (Raiborg et al, 2002). Concomitantly, the ESCRT-I component, Tsg101, promotes the recruitment of ESCRT-II complex and initiation of the budding process of the MVB. Upon recruitment ESCRT-II initiates the oligomerization of the ESCRT-III complex on the endosomal membrane (Raiborg et al., 2009). ESCRT-III complex sequesters the cargo in nascent MVB and catalyzes the scission of MVB (Babst et al., 2002 a and b; Bonifacino and Hurley, 2008; Schmidt and Ties, 2012). Once the MVB formation is completed, Vps4, an *ATPases* associated with various cellular activities (AAA ATPase) is recruited, which catalyzes the disassembly of ESCRT-III from the MVB membrane.

The disassembly of ESCRT-III is essential for termination of cargo sorting and MVB release. Newly formed MVB fuses with either LEs or lysosomes and results in degradation of EGFR and other sorted receptors (Shestakova et al., 2010). A recent study from our lab has highlighted the role of C-terminal Eps15 homology domain containing (EHD) protein 4 (EHD4) in the trafficking of receptors from EE to the lysosomes (Sharma et al., 2008).

3.2 Sorting for Recycling

The majority of the internalized receptors from the surface of mammalian cells are recycled back to the PM via EE. Simplistically, the recycling of receptors from EE has been divided into two distinct pathways: “fast recycling” and “slow recycling”. Recycling kinetics of TfR confirmed the existence of a faster route ($t_{1/2}$ = 5 min) and a slower route ($t_{1/2}$ = 15-30 min) for recycling (Daro et al., 1996; Mayor et al., 1993). While some of the receptors are directly returned to the PM from EE through the fast recycling pathway, the majority of receptors traversing the slow recycling pathway are first transported to an additional organelle, endocytic recycling compartment (ERC) localized near the microtubular organizing center (MTOC) in the perinuclear area (Maxfield and McGraw, 2004; Grant and Donaldson, 2009). Rab4 and Rab11 are the most prominent markers for the fast and slow recycling processes, respectively (Van der Suljs et al., 1992; Ulrich et al., 1996). The process of efficient recycling through the ERC is coordinated through an elaborate network of endosomes known as TREs (detailed explanation in section 3.2.1).

Previously, it was thought that no sorting motif is necessary for receptor recycling. However, recent studies have demonstrated that a GTPase-activating protein (GAP) for ADP ribosylation factor (Arf6), Arf GAP with coiled-coil ankyrin repeat and PH domains 1 (ACAP1), serves as a sorting molecule involved in direct binding to two

phenylalanine-containing sorting motifs in the TfR; leucine-phenylalanine (LF) or arginine-phenylalanine (RF) (Dai et al., 2004). Indeed, there was delay in the recycling of TfR upon disruption of the binding between Tf and ACAP1 (Dai et al., 2004). Recent studies have demonstrated that Sorting Nexin 17 (SNX17) directly binds to an asparagine-X stands for any amino acid-proline-tyrosine (NPXY) motif in the cytoplasmic domain of LDLR-related proteins (LRPs) and promotes LRP recycling (Van Kerkhof et al., 2005). Another study demonstrated that SNX27 acts as an adaptor that links the coat protein retromer to a prototypical G-protein coupled receptor (GPCR) cargo, the β2 adrenergic receptor (B2AR), by recognizing its PDZ domain (named after the first three proteins in which it was identified, PSD-95, DLG and ZO-1) to sort for recycling (Lauffer et al., 2010). Thus, there are clearly instances where recycling can be dictated by select sorting motifs.

3.2.1 Significance of TREs in Recycling

The composition, structure, and mode of functioning of ERC in endocytic recycling are poorly understood, despite the importance of the recycling process. Recent studies from our lab employing Structured Illumination Microscopy (SIM), dual channel 2D-direct Stochastic Optical Reconstruction Microscopy (dSTORM), and 3D dSTORM, have shed new light on the ERC morphology and cargo segregation. The ERC is composed of an array of dynamic, densely situated, yet independent, tubular and vesicular recycling endosomes radiating from the MTOC (Xie et al., 2015). It has been well established that the high surface area-to-volume ratio of tubular carriers effectively serves to segregate the integral membrane proteins from the luminal content (Maxfield and Macgraw, 2004). However, our recent studies suggest that the ERC maintains cargo segregation acquired upon exit from the SE. Hence, the ERC serves as a focal point for vesicular transport to the PM (Xie et al., 2015). TREs are crucial for the recycling of

internalized receptors and lipids. Previous studies from our lab have demonstrated that MICAL-L1-decorated TREs can be generated from regions of SE that are enriched in a Rab-5 effector, Rabenosyn-5, indicating that TREs are responsible for the movement of CIE cargo from peripheral SE to the perinuclear ERC (Xie et al., 2015). Moreover, current models from our lab support the finding that the fission of TREs leads to formation of vesicle carriers (vesiculation) that carry recycled receptors back to the PM (Cai et al., 2012; Cai et al., 2013; Cai et al., 2014).

Owing to the significance of TRE in endocytic recycling, multiple studies from our lab have focused on identifying the molecular players involved in TRE generation, fission, fusion, and function. Previous studies from our lab have demonstrated that MICAL-L1 is a protein localized to the outer TRE leaflet (Sharma et al., 2009). MICAL-L1 acts as a hub that recruits and stabilizes a battery of proteins that directly impact membrane shaping. For instance, the F-BAR domain containing protein Syndapin2 (Giridharan et al., 2013). MICAL-L1 also interacts with the C-terminal Eps15 homology domain containing (EHD) protein 3 (EHD3) and EHD1 (Sharma et al., 2009; Kieken et al., 2010), which are involved in TRE stabilization and vesiculation, respectively (Cai et al., 2013; Bahl et al., 2016). Also crucial for TRE biogenesis is the high local concentration of phosphatidic acid (PA), an essential lipid component of TRE tubules, which binds and recruits MICAL-L1 and Syndapin2. Syndapin2 has an SH3 domain, which mediates stable interaction with the PRD domain of MICAL-L1. Syndapin2 also has an F-BAR domain that can sense and bend the membranes to induce tubulation (Giridharan et al., 2013). EHD1 subsequently joins this complex on TRE, where it interacts with both MICAL-L1 and Syndapin2 and initiates vesiculation, giving rise to newly formed vesicles (Cai et al., 2012; Giridharan et al., 2013; Cai et al., 2013; Cai et al., 2014).

3.3 Sorting for TGN

EEs not only serve as stations to sort receptors for recycling and degradation but also function as a common junction that connects various endocytic and biosynthetic routes. Trafficking from the EE to the biosynthetic routes is known as retrograde transport. Retromer-mediated tubulation is required for the retrograde transport from EE to the TGN and these retromer-mediated tubules are distinct from the TREs that facilitate the recycling process from EE to ERC (Bonifacino and Rojas, 2006). Retromer machinery is preferentially recruited to EEs which are maturing towards LE and contain increasing concentrations of phosphatidylinositol 3,5 bisphosphate (PI(3,5)P2), generated by phosphoinositide kinase (PIKfyve) (Rutherford et al., 2006) and an increasing number of intralumenal vesicles (ILVs) (Arighi et al., 2004).

Pioneering studies by Seamen et al., 1998, in the yeast endolysosomal system were instrumental in the identification of the protein coat “retromer”. Retromer was shown to mediate the endosome-to-Golgi retrieval of the vacuolar hydrolase receptor (Vps10p), the yeast functional equivalent of the mannose 6-phosphate (M6PR) receptor. Retromer is a heteropentameric complex consisting of a sorting nexin (SNX) dimer composed of SNX 1/2 and SNX 5/6 and a trimer consisting of Vps proteins namely, Vps26, Vps29 and Vps35 (Bonifacino and Hurley, 2008; Bonifacino and Rojas, 2006; Seaman, 2005; Rojas et al., 2007). The SNX protein dimer possesses a phox-homology (PX) domain and a BAR domain. While the PX domain is involved in binding to PI(3)P and other phosphoinositides in the EE membrane, the BAR domains (that can sense and induce membrane curvature) mediate dimerization and attachment to the curved membranes (Bonifacino and Rojas, 2006). The Vps26, 29 and 35 heterotrimer is involved in recognizing cargo proteins and is therefore termed as the cargo-selective-complex (CSC). Vps35 provides the interface for the recognition of cargo. Vps29 is indispensable for the interaction of the CSC with the SNX dimer and functions as a

scaffold for retromer assembly by binding the carboxyl (C)-terminal half of Vps35. Vps26 binds to the amino (N)-terminal half of Vps35 (Seamen et al., 2007). The CSC, unlike the SNX dimer, lacks lipid-binding domains; hence, its recruitment on the endosome is dependent on the interaction of Rab7 with Vps35. Furthermore, Rab7/Vps35 interaction not only stabilizes the CSC on the endosome membrane, but also synchronizes the timing of cargo export with endosome maturation (explained in detail in section 3.1) (van Weering et. al, 2012). The mechanism by which CSC recognizes cargo is also poorly understood. However, it is well established that the cargo destined for retromer-dependent sorting possesses at least one simple hydrophobic motif phenylalanine/tryptophan-leucine-methionine/valine (F/W-L-M/V) (Seamen et al., 2007). Recent studies have also implicated the involvement of Vps26 in recognizing cargo by a FANSHY sorting signal and the role of SNX27 in cargo sorting (Fjorback et al., 2012; Steinberg et al., 2013). The best-studied examples of cargo proteins transported through the retromer-mediated pathway include the vacuolar hydrolase transport receptors, Vps10 in yeast and M6PR in mammals (Bonifacino and Rojas 2006; Johannes and Popoff 2008).

EHD1 is yet another important regulator of retromer-mediated transport. EHD1 colocalizes and interacts with Vps26 and Vps35 on retromer tubules, and affects the retrieval of M6PR mediated by the retromer (Gokool et al., 2007). However, no direct binding between EHD1 and the retromer has been detected. We have identified Rabankyrin-5, a Rab5 effector, as a novel NPF-interaction partner for EHD1. Rabankyrin-5 also interacts with Vps26 and Vps35 thus facilitating the association of EHD1 with the retromer complex (Zhang et al., 2012 (a) and (b))(McKenzie et al., 2012). EHD3, another member of the EHD protein family and the closest paralog of EHD1, also mediates endosome-to-Golgi transport and retromer trafficking (Naslavsky et al., 2009).

4. Regulators of Endocytic Trafficking

The endosomal system is an elaborate and dynamic network of membrane-bound organelles interconnected by vesicular “vehicles” that transport lipids and proteins. The process of endosomal transport can be divided into four distinct steps: vesicle budding from the donor organelle, transport, tethering with the acceptor organelle and finally, fusion of the lipid bilayers of the vesicle and the acceptor organelle (Fig 1.2) (Bonafacino and Glick, 2004). A conserved arsenal of regulatory proteins coordinates these fission and fusion events.

The budding process is initiated by recruitment of coat proteins onto the donor membrane to induce the formation of the vesicle. Coat subunits are involved simultaneously in incorporating the cargo and deforming the donor membrane into the budding vesicle (Cai et al., 2007). After budding, the vesicles are transported to their destination donor compartments by molecular motors such as dynein, kinesin, and myosin along cytoskeletal tracks (Hammer and Wu, 2002; Matanis et al., 2002; Short et al., 2002). Once the vesicle reaches the acceptor organelle, tethering of the vesicle to the acceptor organelle occurs by the joint action of tether complexes and Rab-GTPases (Sztul and Lupashin, 2006; Whyte and Munro, 2002). The final step is fusion, which involves the soluble NSF attachment protein receptor (SNAREs), where NSF stands for *N*-ethyl-maleimide-sensitive fusion protein (Numrich and Ungermann, 2013).

4.1 Regulation by Rab GTPases

The Rab family of small Ras-like GTPases constitutes a critical group of endocytic regulators. In mammalian cells, over 60 different members of the Rab family-function as multifaceted regulators of distinct trafficking pathways. Rab-GTP-binding proteins function as molecular switches, which are either in the guanosine triphosphate

Figure1.2 Schematic representation of the steps of vesicle transport.

a. Coat proteins are recruited to the cytoplasmic face of the donor membrane and induce the formation of a vesicle. The coat recruits SNAREs and transmembrane receptors bound to their cargo. **b.** After uncoating, motor protein can be recruited to enable the vesicle to travel along microtubules or actin filaments. **c.** Once at its destination, the vesicle becomes tethered to the acceptor membrane, probably by long coiled-coil proteins or multimeric tethering complexes. **d.** The SNAREs on the vesicle and acceptor membrane form a complex that drives membrane fusion and hence delivery of the contents of the vesicle (Image used with permission from Behnia and Munro, 2005).

Figure 1.2

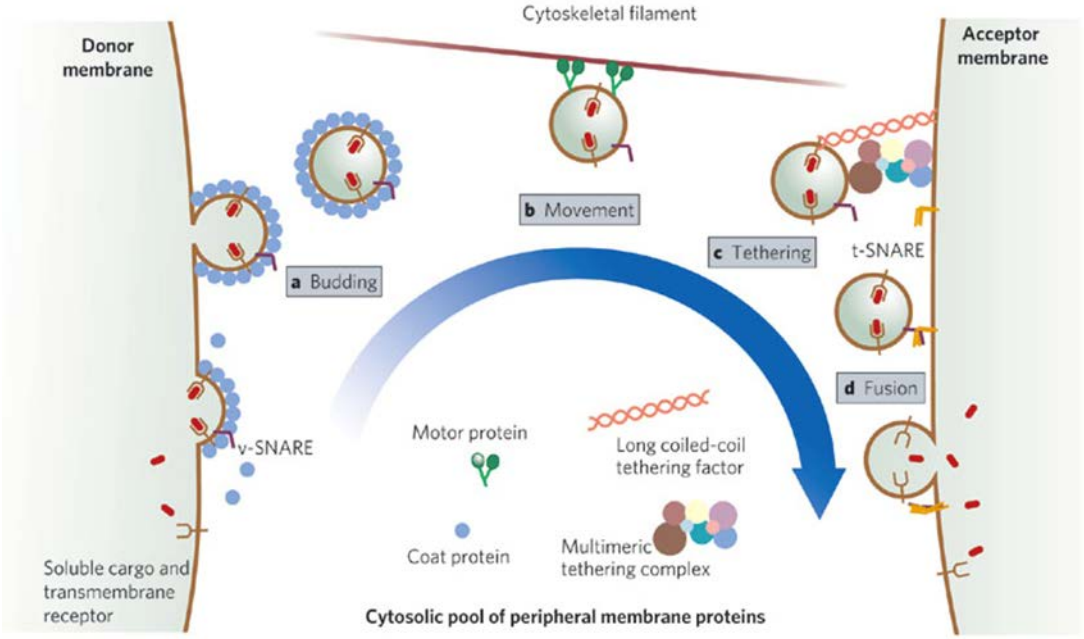
Cytoskeletal filament
Donor membrane
Acceptor membrane
b Movement
c Tethering
t-SNARE
a Budding
d Fusion
v-SNARE
Motor protein
Long coiled-coil tethering factor
Coat protein
Multimeric tethering complex
Soluble cargo and transmembrane receptor
Cytosolic pool of peripheral membrane proteins

(GTP)-bound “active” form or the guanosine diphosphate (GDP)-bound “inactive” form (Zerial and McBride, 2001; Grosshans et al., 2006). As shown in Fig 1.3, the membrane association/dissociation of Rabs is intimately associated with the nucleotide/hydrolysis cycle (“active” and “inactive” forms) and is regulated by specific cofactors. Exchange of GDP with GTP is catalyzed by guanyl nucleotide exchange factors (GEFs), which facilitate the release of GDP by inducing a conformational change in the Rab proteins (Delparto et al., 2004). In the GTP-bound state, Rabs are stably associated with the membrane via the membrane affinity endowed by the prenyl anchor. The prenyl anchor is generated by the attachment of geranyl-geranyl groups to one or two cysteine residues in the C-terminal cysteine-alanine-alanine-X stands for any amino acid (CAAX) motif (Colicelli 2004; Lueng et al, 2006). GDP-dissociation inhibitor (GDI) maintains the GDP-bound Rab in a soluble state by masking the C-terminal prenyl anchor. In order to recruit Rab proteins to the membrane, the GDI has to be released by GDI displacement factor (GDF). However, recent reports suggest that GEF may be sufficient to remove the GDI, as well as function as a GDF (Itzen and Goody, 2011).

Different GTP-bound Rabs serve as distinct membrane scaffolds to coordinate three major steps: vesicle budding, cytoskeletal transport, targeted docking and fusion. Accordingly, Rabs sequentially interact with specific types of effector molecules, including sorting adaptors, tethering factors, kinases, phosphatases and motor proteins, to regulate each step in a spatiotemporal manner (Grosshans et al., 2006; Stein et al., 2003). Therefore, Rabs act as membrane domain organizers that can locally change the environment of the membrane (Miaczynska and Zerial, 2002). Once the individual transport step catalyzed by a particular Rab is completed, the specific GAPs accelerate GTP hydrolysis, converting the Rab protein to inactive GDP-bound state. The GDP-bound Rabs can be extracted from the membrane by the effector GDI and recycled back to the cytosol (Goody et al., 2005 and Grosshans et al., 2006)(Fig 1.3).

4.1.1 Rab5 and the early endosome

Rab5 is the best-characterized and most extensively studied Rab of the early endocytic pathway (Zerial and McBride, 2001; Grosshans et al., 2006). Rab5 is the most prominent identity marker and a regulator of the EE. Rab5 regulates the entry of cargo from the PM to the EE, generates PI(3)P lipid, which is enriched on EE membrane (Christoforidis et al., 1999; Murray et al., 2002), catalyzes homotypic fusion (Gorvel et al., 1991), and facilitates the motility of EE on actin and microtubular tracks (Nielsen et al., 1999; Pal et al., 2006). Rab5 is activated on the EE membrane by the recruitment of its effector, Rabex-5 (Horiuchi et al., 1997). Another Rab5 effector, Rabaptin-5, further promotes the GEF activity of Rabex-5, and these both together with Rab5 form a complex known as the “Rab5 domain” (Stenmark et al., 2009). This complex is required to establish a feedback loop for maintaining and stabilizing Rab5-GTP on the EE membrane (Lippe et al., 2001). These transient but high levels of Rab5-GTP are sufficient to recruit effector proteins to the EE, where they can carry out their specialized functions in trafficking and sorting (Grosshans et al., 2006). Additionally, this complex also triggers the rapid recruitment of other Rab5 effectors, PI(3)P-kinase/hVPS34/p150 (VPS34), and forms a complex. This complex generates PI(3)P, the most abundant phosphoinositide in the EE membrane. The concomitant presence of Rab-GTP and PI(3)P acts as a signal to recruit a spectrum of effector proteins such as EEA1 (Lawe et al., 2000, 2002; Pfeffer, 2001) and Rabenosyn-5 (Nielsen et al., 2000).

EEA1 and Rabenosyn-5 bind to the PI(3)P-enriched membrane through their FYVE (named after 4 cysteine-rich proteins-Fab1, YOTB, Vac1, and EEA1) zinc finger domains (Nielsen et al., 2000) (Lawe et al., 2000; Nielsen et al., 2000; Stenmark and Aasland, 1999). EEA1 interacts with SNARE proteins Syntaxin 13 (McBride et al., 1999)

Figure 1.3. The Rab switch and its circuitry.

Conversion of the GDP-bound Rab into the GTP-bound form occurs through the exchange of GDP for GTP, which is catalysed by a guanine nucleotide exchange factor (GEF) that leads to a conformational change. The GTP-bound 'active' conformation is recognized by multiple effector proteins and is converted back to the GDP-bound 'inactive' form through hydrolysis of GTP, which is stimulated by a GTPase-activating protein (GAP) and releases an inorganic phosphate (Pi). A Rab escort protein (REP) recognizes the newly synthesized Rab, in the GDP-bound form. The REP presents the Rab to a geranylgeranyl transferase (GGT), which geranylgeranylates the Rab on one or two carboxy-terminal Cys residues. The geranylgeranylated, GDP-bound Rab is recognized by Rab GDP dissociation inhibitor (GDI), which regulates the membrane cycle of the Rab. Targeting of the Rab–GDI complex to specific membranes is mediated by interaction with a membrane-bound GDI displacement factor (GDF) (Image used with permission from Stenmark et al., 2009).

Figure 1.3

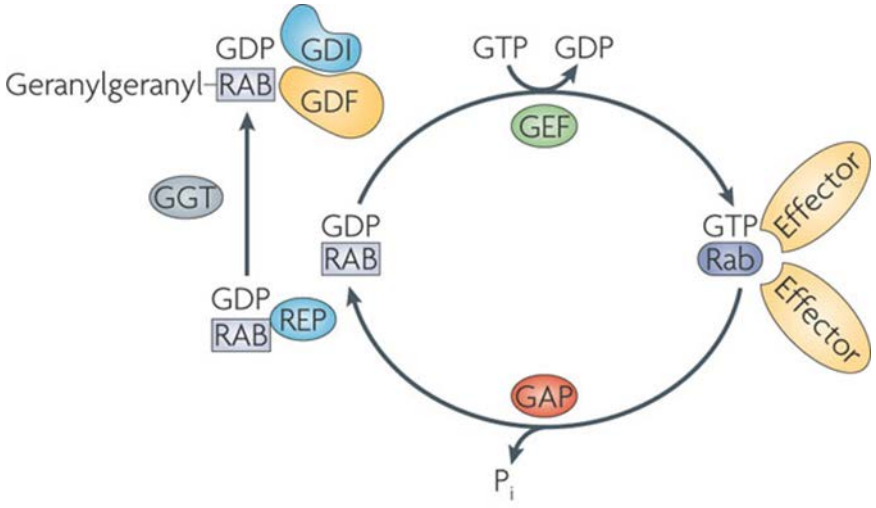

Nature Reviews | Molecular Cell Biology

and Syntaxin 6 (Simonsen et al., 1999), which regulate vesicular fusion at the EE. EEA1 also facilitates the fusion of transport vesicles with recycling endosomes (REs) and the Golgi, respectively.

Rabenosyn-5 is regarded as a dual Rab5 and Rab4 effector, as it can bind to both of these Rabs in their active states. Rabenosyn-5 also interacts with EHD1 and EHD3. EHD1 regulates recycling of cargo from the perinuclear ERC back to the PM (Caplan et al., 2002; Naslavsky et al., 2004) and EHD3 is involved in the transport of cargo from EE to the ERC (Naslavsky et al., 2009). Thus, Rabenosyn-5 might serve as the Rab5 effector that is the link between sorting events at the EE and the recycling of cargo back to the PM either directly from EE (fast recycling) or via the ERC (slow recycling).

Rabankyrin-5, another Rab5 effector is required for macropinocytosis and EE fusion (Schnatwinkel et al., 2004). Our studies have identified a novel role of Rabankyrin-5 in the regulation of retromer localization, which is contingent upon its specific interaction with EHD1 (Zhang et al., 2012).

4.1.2 Rab7 and the maturation of late endosomes

Rab7 is the best-known regulator and organelle identifier of late endosomes (LE). Although Rab7 localizes to both the EE and the LE/MVB, it regulates the late steps of endocytic trafficking and lysosomal degradation (Wichhmann et al., 1992). The prerequisites for the generation of a new LE are: the generation of a Rab7 domain, and the removal of Rab5 (Rink et al., 2005; Vonderheit and Helenius, 2005). The current model, which is known as the “Cascade Model” is used to describe the Rab5-to-Rab7 switch. The level of Rab5 on the EE membrane is not constant but fluctuates dynamically. As the EEs grow in size due to frequent homotypic fusion events and accumulation of cargo destined for degradation, the surface density of Rab5 increases

until it reaches its maximum concentration (Rink *et al.,* 2005; Lakadamyali *et al.*, 2006). At this stage, a further increase in Rab5 levels triggers rapid recruitment of Rab7 on the endosomal membrane via class C core vacuole/endosome tethering (CORVET)/ homotypic fusion and protein sorting (HOPS) complexes. Once Rab7 reaches a threshold level, it starts to repress Rab5. Mon1-Ccz1, an evolutionarily preserved protein complex, physically interacts as a stable pair and facilitates the Rab5-Rab7 exchange by simultaneously displacing Rabex-5 and activating a GEF of Rab7 (Wang et al., 2002; Kucharczyk et al., 2009; Kinchen and Ravichandran, 2010). VPS39, a HOPS complex subunit acts as a GEF for Rab7. Additionally, Mon1/Ccz1 complex binds to Rab7 on the membrane and controls the localization of Rab7 on LE and subsequent activation (Rink et al., 2005; Hutanglang and Novick, 2011). Rab7-GTP also recruits its own effectors, such as, Rab7-interacting lysosomal protein (RILP), which interacts with Rab7 on LEs and lysosomes (Cantalupo et al., 2001). RILP then connects dynein-dynactin motor complexes to Rab7-containing LEs and lysosomes (Jordens et al., 2001). Dynein transports LE to the minus end of microtubules by the motor complexes towards the lysosomes (Johansson et al., 2007).

4.1.3 Rabs in Fast Recycling

Rab4 is required for the fast recycling of Tf and glycophospholipids from the EE to the PM (Sonnichsen et al., 2000; Maxfield and MacGraw, 2004). Rab4 regulates fast recycling through interaction with various effector proteins, including Rabenosyn-5 and Rabapatin-5/Rabex-5 complex (Vitale et al., 1998; de Renzis et al., 2002; Mattera and Bonifacino, 2008). Recent studies have identified that Rab35 localizes to the PM as well as to the EE, and is an important regulator of rapid recycling (Sato et al., 2008). Rab35 also associates with Arf6 and EHD1-positive TREs carrying cargo back to the PM. The GAP for Rab35 is TBC domain member 10C (TBC1D10C) (Walseng et al., 2008).

Furthermore, Rab35 recruits the EHD1 binding protein MICAL-L1 to the Arf6 positive recycling tubules (Rahajeng et al., 2012). Moreover, Rab35 recruits multiple Rabs, Rab8, Rab13 and Rab36 at the recycling tubules through MICAL-L1 during nerve growth factor (NGF)-induced neurite outgrowth (Kobayashi et al., 2014).

4.1.4 Rab11 and Slow Recycling

Slow recycling occurs through the ERC and is facilitated by the recycling endosomes (REs) that originate from the ERC (Grant and Donaldson, 2009; Stenmark, 2009; van Ijzendoorn, 2006). Rab11 is the signature marker for the REs that originate from the ERC. The Rab11-decorated REs selectively transport CME cargos from the ERC to the PM and are distinct from the TREs that preferentially transport CIE cargoes from the ERC to the PM. The Rab11-family interacting proteins (Rab11-FIPs) constitute an evolutionarily conserved family of proteins (Hales et al., 2002; Prekeris et al., 2001). There are several members in this family including FIP1, FIP2, FIP3 (Hales et al., 2001), FIP4 (Wallace et al., 2002a), FIP5 (Prekeris et al., 2000), RCP (Wallace et al., 2002b; Lindsay et al., 2002), Rabphilin-11/Rab11BP (Mammoto et al., 1999; Zeng et al., 1999). Each of the FIPs is characterized by the presence of a highly conserved coiled-coiled alpha-helical Rab11-binding domain at the C-terminus (Horgan and McCaffrey, 2009).

Rab11-FIP5 mediates transport from EEs to REs through binding with Kif3B, a component of the kinesin II motor protein (Schonteich et al., 2008). We have recently demonstrated in our studies, another Rab11 effector, Rab11-FIP2, which facilitates the recycling of receptors through its specific interaction with EHD1 and EHD3 by its NPF motifs (Naslavsky et al., 2009). Thus, Rab11-FIP2 serves as a link between EHDs and Rab11. Furthermore, Rab11-FIP2 forms a ternary trafficking complex with Rab11, and the motor protein myosin Vb for the regulation of the recycling process (Hales et al., 2001; Hales et al., 2002).

4.2 Arf GTPases

The Arf family of proteins, like the Rabs, belongs to the Ras superfamily of small GTPases (Jackson and Cassanova, 2000). The Arf proteins cycle between their active GTP-bound states and inactive GDP-bound states like other GTPases. Exchange of GDP for GTP is catalyzed by GEFs, and GTP hydrolysis to GDP is mediated by GAPs. Several specific Arf GAPs and GEFs have been identified. The membrane tethering of Arf proteins is facilitated by myristoylation at the N-terminus (Jackson and Cassanova, 2000; Randazzo and Hirsch, 2004).

In mammals, there are six members of the Arf family, which are divided into three classes (Kahn et al., 2006). Class I Arf proteins (Arf1, Arf2, and Arf3) share 96% sequence homology (Bonifacino and Glick, 2004). There are two Class II Arf proteins Arf4 and Arf5; Arf5 has been implicated in early Golgi transport and in recruiting coat components to *trans*-Golgi membrane (Claude et al., 1999; Takatsu et al., 2002). Class III has a single member known as Arf6 that regulates endosomal trafficking and structural organization of the cell surface (D'Souza Schorey et al., 1995; Grant and Donaldson, 2009).

Arf1 and Arf6 are the most studied mammalian Arf proteins whose primary localization in cells is at the Golgi and PM respectively. In cells, Arf1 reversibly associates with Golgi membranes during its activated state, Arf1-GTP. Arf1-GTP recruits coat protein complex I (COPI) on to pre-and *cis*-Golgi structures through the recruitment of heterotetrameric complex (AP1, AP3, and AP4) and monomeric Golgi-localized γ-ear-containing ARF-binding protein (GGA) on to TGN and endosomal membranes (Bonifacino and Glick, 2004).

On the other hand, Arf6 is mainly localized at the PM and to some extent on the endosomal membranes (Donaldson, 2003). Arf6 primarily functions in CIE-mediated

internalization and recycling. Arf6 promotes the recycling of MHCI molecules back to the PM (Naslavsky et al., 2003). Moreover, Arf6 forms a ternary complex with Rab11, Rab11-FIP3, and Rab11-FIP4 (Fielding et al., 2005), which regulates the recycling of β1-integrin (Powelka et al., 2004). Arf6 regulates recycling at the molecular level by activating phospholipase D2 (PLD2) that generates phosphatidic acid (PA) and diacylglycerol (DAG), and PIP5K that generates PIP2 (Jonavic et al., 2006; Brown et al., 2001). Furthermore, the Arf6 GTPase regulates EHD1-containing TRE. Indeed, the cycling of Arf6 between its GTP-and GDP-bound forms impacts the localization of EHD1 on the tubular membranes (Caplan et al., 2002). Co-expression of the GTP-locked Arf6-Q67L mutant with Myc-EHD1 led to altered EHD1 localization, loss of EHD1-associated tubular structures and recruitment of EHD1 to enlarged Arf6 endosomes. Furthermore, overexpression of Arf6-GEF, EFA6, or the Arf6-GAP, ACAP1 in HeLa cells, leads to loss of EHD1 from the tubular membranes (Caplan et al., 2002). In addition, our recent studies have demonstrated that PA is an essential component of TREs (Giridharan et al., 2013). Moreover, PIP2 is primarily localized to the PM, where it mediates vesicular fusion and recruits Arp2/Arp3-actin polymerization machinery (Santy and Cassanova, 2001; Vitale et al., 2002). Hence, Arf6 mediates the recycling process by regulating the lipid dynamics of the membranes involved in recycling and the PM.

4.3 SNAREs

SNAREs are a highly conserved family of membrane proteins primarily regulating vesicular fusion events in membrane trafficking pathways (Bennett et al., 1995; Sollner, 1995). The hallmark of SNARE proteins is the presence of a heptad SNARE motif: an evolutionarily conserved domain of 60-70 amino acids arranged to form a coiled-coiled region (Fasshauer, 2003). A SNARE on the transport vesicle (v-SNARE) pairs with its cognate SNARE-binding partner (t-SNARE) with the acceptor

membrane, which drives fusion and delivery of cargo (Chen and Scheller, 2001). The interaction of cognate v-and t-SNAREs leads to the formation of a *trans*-SNARE complex or SNAREpin, in which four SNARE motifs assemble as a twisted parallel four-helix bundle. The formation of a SNAREpin is not only important for the specificity of the initial interaction but also for bringing opposing membranes together and eventually membrane fusion. The energy released during the formation of SNAREpin drives the fusion of lipid bilayers (Lin and Scheller, 1997). After the fusion process is complete, the remaining part of the SNARE complex on the fused membranes is called the *cis*-SNARE complex. This complex undergoes recycling upon disassembly catalyzed by AAA ATPase NSF and its cofactor soluble NSF attachment protein (SNAP) (Sollner et al., 1993; Mayer et al., 1996; Hanson and Whiteheart, 2005).

The structural studies of SNAREs have revealed that the helical core contains three highly conserved glutamine (Q) residues and one highly conserved arginine (R) residue. Consequently, the SNARE proteins are classified as Qa-, Qb-, Qc- and R-SNAREs. Four SNAREs, with one member each of Qa-, Qb-, Qc- and R-SNARE subfamilies form a functional SNARE complex that drives membrane fusion (Fasshauer et al., 1998; Bock et al., 2001). The Rab5 effector protein EEA1 can recruit Syntaxin13 and Syntaxin6 on the EE membrane (McBride et al., 1999; Simonsen et al., 1999). Syntaxin13-Vps10p tail interactor 1 and (Vti1a)-Syntaxin6-VAMP4 are the key SNARE complexes involved in the homotypic fusion of EEs (Brandhorst et al., 2006; Zwilling et al., 2007). The SNARE complex Syntaxin 13-SNAP23/25-VAMP2/3 has been implicated in the trafficking of cargo from RE to the PM (Kubo et al., 2015). The Syntaxin16-Vti1a-Syntaxin 6-VAMP3/4 SNARE complex functions between EE and the TGN, whereas the Syntaxin 16-Vti1a-Syntaxin 10-VAMP3 complex operates between LE and the TGN (Ganley et al., 2008). The lysosomal degradation pathway involves Syntaxin4-SNAP23-VAMP7 for the fusion of the LE and lysosomes to the PM (Williams et al., 2014).

5. C-terminal Eps15 Homology Domain containing proteins (EHDs)

A novel group of endosomal scaffolding proteins, the EHDs, regulates specific steps of endocytic trafficking pathway. Mammalian cells express four EHD protein paralogs, EHD1, EHD2, EHD3, EHD4 having a high level of amino acid sequence similarity and showing about 70-86% identity (Naslavsky and Caplan, 2005). The genomes of many invertebrate organisms, including *Caenorhabditis elegans (C. elegans)* and *Drosophila melanogaster*, contain a single EHD family gene, most closely resembling EHD1/EHD3. *C. elegans* homolog of EHD1, receptor mediated endocytosis-1(RME-1), displays 67% identity with EHD1 and is a component of the recycling machinery regulating the return of yolk receptors back to the PM (Grant et al., 2001). *Drosophila has a* putative achaete-scute target 1 (PAST1) protein that is evolutionarily closest to EHD2 displaying 70% homology and is involved in regulating endocytosis. The flies lacking PAST1 are infertile and die prematurely (Olswang-Kutz et al., 2009). Recent studies have further highlighted the role of PAST1 in the development of the neuro-muscular junction and differentiation of rod and cone cells of the fly eye ommatidia (Koles et al., 2015; Dorot et al., 2017).

5.1 Domain Architecture, Structure and Organization of EHD Proteins

The four EHD protein (EHD1-4) paralogs have conserved domain architecture. The structural studies by McMahon's group, which solved the first crystal structure of mouse full-length EHD2 protein have been instrumental in our understanding of the domain architecture and structure of EHD proteins (Daumke et al., 2007). The domain architecture of EHD proteins consists of a nucleotide binding domain (G-domain) enclosed between helical domains at the N-terminus, followed by a linker region, and a

C-terminal Eps15 homology (EH) domain (Fig. 1.4A) (Grant and Caplan, 2008; Naslavsky and Caplan, 2011) (Fig 1.5).

One of the trademark characteristics of EHD proteins is their distribution to the cytosolic face of long tubular endosomal membranes. Electron microscopy studies have determined that the tubular structures containing EHD1 are 200 nm wide and up to 10 μm long (Caplan et al., 2002). Consistent with the high degree of homology between EHD proteins, all four paralogs are capable of localizing to tubular membranes when overexpressed. However, the extent of tubulation varies between different paralogs (Blume et al., 2007; George et al., 2007). Both EHD1 and EHD3 localize primarily to tubular membranes, which emanate from the perinuclear ERC and from the peripheral SE, while EHD2 and EHD4 are mostly present on vesicular membranes with very few tubules (Caplan et al., 2002; Naslavsky et al., 2006; Sharma et al., 2008). Since EHD proteins lack a transmembrane domain, the recruitment of EHD proteins is dependent upon EH domain lipid-binding ability. The positively charged lysine 483, which is very well conserved, has been hypothesized to mediate the EH-domain/lipid-binding. Indeed, charge reversal mutation of this lysine to glutamate (K483E) completely abrogates the tubular localization of the mutant EHD1, resulting in redistribution to endosomal vesicles, a phenotype similar to the truncation of the entire EH-domain (Naslavsky et al., 2007). Sequence alignment analysis led to the prediction that EHD proteins have a putative phosphate binding (P)-loop motif in the G domain, an ATP/GTP-binding site found in GTPases such as Dynamin and Ras.

Figure 1.4 Domain architecture of EHD proteins, structure of EHD2 and, solution structure of EH domain of EHD1

(A) Domain architecture of EHD proteins consists of a N-terminal and central α-helices together form a single helical domain that mediates lipid binding (Daumke, et al. 2007), a dynamin-like G-domain binds ATP and serves as a platform for homo-dimerization and a C-terminal EH-domain exhibits preferential binding to NPF motifs. **(B)** The crystal structure of full-length mouse EHD2. EHD2 exists as a homo-dimer and the EH-domains of two monomers cross over to align themselves with the N-terminus of the opposing monomer (see the ribbon structure in red denoting a monomer). The primary lipid-binding site is on the opposite face from the EH-domains (Image used with permission from Daumke, et al. 2007). **(C)** Solution structure of EH domain of EHD1, stereoview of the ribbon diagram of the lowest energy EHD1 EH domain structure showing the location of the calcium binding site.

Figure 1.4

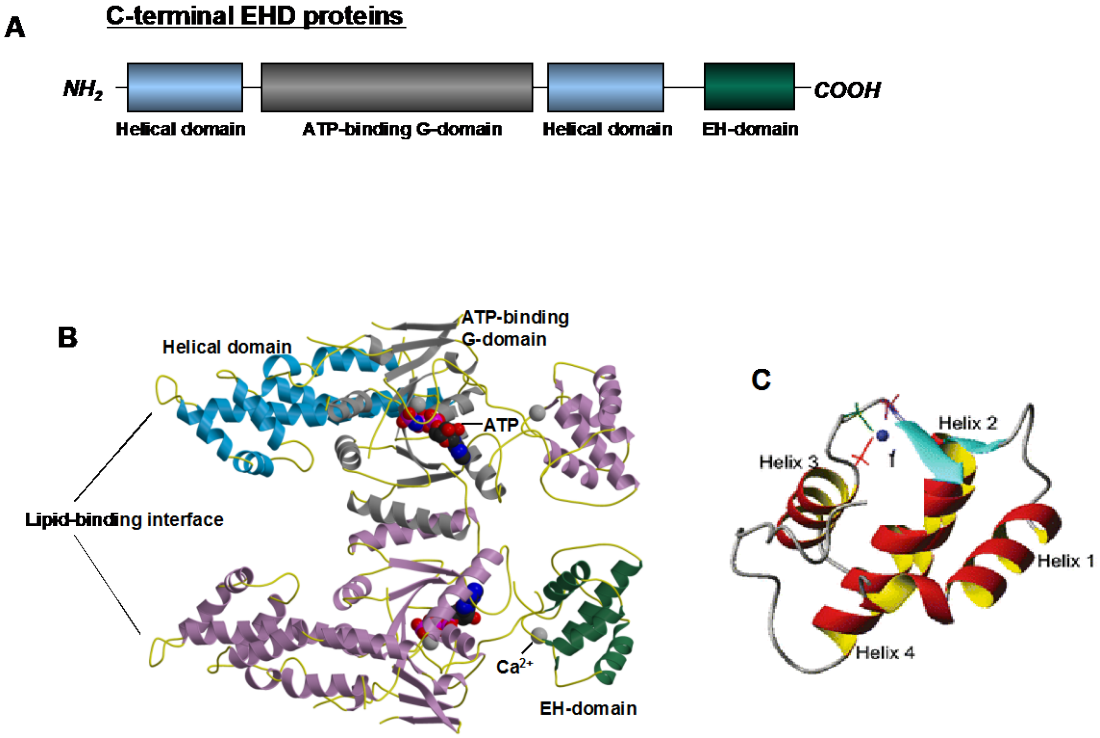
A
C-terminal EHD proteins
NH2
COOH
Helical domain
ATP-binding G-domain
Helical domain
EH-domain
B
Helical domain
ATP-binding
G-domain
ATP
Lipid-binding interface
Ca2+
EH-domain
C
Helix 2
Helix 3
Helix 1
Helix 4

When the crystal structure of EHD2 was solved in the presence of the non-hydrolysable ATP analog adenylyl imidodiphosphate (AMPPNP), it was confirmed that EHDs bind to ATP instead of GTP (Lee et al., 2005; Daumke et al., 2007). Indeed, the Km value also depicts the stronger preference of EHDs for ATP compared to GTP (Km of 80 μM for ATP vs. no detectable Km for GTP-binding) (Daumke et al., 2007). The functional importance of the nucleotide binding was demonstrated by endocytic assays in *C. elegans* oocytes that displayed impaired yolk receptor recycling in the G65R mutant. RME-1 nucleotide binding ability affects its oligomerization ability and endosomal binding (Grant et al., 2001). Additionally, the equivalent mutation in mammalian EHD1 of the critical glycine residue in the nucleotide-binding domain to arginine (G65R) rendered the protein cytosolic, suggesting that membrane binding is contingent upon nucleotide binding status of the EHDs (Caplan et al., 2002). Further support for the interaction with membranes upon binding with the nucleotide, came from fluorescence recovery after photobleaching (FRAP) studies, which displayed recovery of EHD1 on tubular membranes within a few minutes upon photobleaching (Caplan et al., 2002). The ability of EHD proteins to undergo nucleotide hydrolysis and membrane fission has also been demonstrated in recent studies (Lee et al., 2005; Naslavsky et al., 2007).

Even though EHD proteins bind ATP and not GTP, there are similarities with the Dynamin superfamily GTPases. Similar to Dynamin, EHD2 has the ability to tubulate negatively charged liposomes *in vitro*, forming spiral ring-like oligomers around lipid tubules. ATP hydrolysis was also observed with purified mouse EHD2 and was stimulated up to ten-fold in the presence of lipids (Daumke et al., 2007; Pant et al., 2009). However, the rate of nucleotide hydrolysis of EHD2 is 600-fold slower as compared to that of Dynamin. This slow rate of ATP hydrolysis facilitates conformational changes leading to membrane destabilization and tubulation or release of vesicular

structures. Furthermore, another unique capability of EHD proteins to undergo homo-dimerization and hetero-dimerization is invaluable for the trafficking process. The two helical regions fold to form a coiled-coiled region that mediates lipid binding and facilitates homo-and hetero-oligomerization of EHDs (Daumke et al., 2007). All the EHD family members are capable of hetero-dimerization except EHD2. Moreover, binding of the EHD proteins to the NPF-containing binding partners is also facilitated by oligomerization in some cases (Naslavsky et al., 2006).

5.2 EH Domain

The EH domain present at the C-terminus is the hallmark of EHD proteins, since this domain is generally present at the N-terminus of other proteins (Paoulazi et al., 1998). The EH domain was first identified as three copies of ≈100 residues repeat regions at the N-terminus of the epidermal growth factor receptor tyrosine kinase substrate, Eps15 (Fazoli et al., 1993; Wong et al., 1995). EH domains are well conserved evolutionarily in species as diverse as yeast and humans. Accumulating evidence supports a high level of structural homology of EH domains as well. Each domain contains two calcium-binding helix-loop-helix motifs (EF-hands) connected by a short antiparallel β-sheet in between the loops, canonically only the second loop can bind to calcium (Ca^{2+}). However, the functional importance of the EH domain as a protein interaction module was discovered when innovative nuclear magnetic resonance (NMR) studies demonstrated that the EH domain of Eps15R has the ability to interact with proteins that contain the tripeptide, NPF motif (Salcini et al., 1997 and De Beer et al., 1998). The NPF residues attain a conformation of a type I β turn for binding and access a conserved hydrophobic pocket that is deeply buried within the EH domain. This allows close contact between the asparagine and a conserved tryptophan in the pocket and provides stability of interaction (Kieken et al., 2007). It is not surprising that mutating

this tryptophan in EHD proteins (W485 in the case of EHD1) abrogates the binding with the NPF-containing binding partners (Naslavsky et al., 2004).

In collaboration with Dr. Sorgen's group, we solved the NMR solution structure of the EH domain of EHD1 (Fig 1.4 C). As compared to the EH domains of Eps15 proteins, the EH domain of EHD proteins has a highly positively charged surface area (Kieken et al., 2007). Hence, the positively charged surface of the EH domain of EHD protein predisposes the EHDs to preferentially bind with the proteins containing an NPF motif followed by acidic residues (Kieken et al., 2010, Henry et al., 2010). Moreover, the NMR solution structure was solved in the presence of bound MICAL-L1 peptide (NPFEEEEED). The sequence of MICAL-L1 peptide provided advanced insight on the stability of binding of the EH domain-NPF, which can be attributed to the fact that the first two glutamate residues of the peptide are located close to the lysine residues of the EH domain, thus favoring the formation of salt bridges (Kieken et al., 2010).

5.3 Interaction Partners of EHD proteins

About 30 different direct and indirect interaction partners of EHD proteins have been reported. In most cases, the mode of interaction of the binding partners with the EHDs is through the EH domain that preferentially binds to NPF-containing proteins followed by acidic residues. Rabenosyn-5 (Naslavsky et al., 2004), Rab11-FIP2 (Naslavsky et al., 2006), Syndapin2 (Braun et al., 2005; Xu et al., 2004), and synaptosome-associated protein 29 (SNAP29) (Xu et al., 2004) are examples of interaction partners utilizing this mechanism of interaction with EHDs. Previously, using mass spectrometry (MS) studies, we identified a novel binding partner of EHD1, known as MICAL-L1 (Sharma et al., 2009). A common feature between Rabenosyn-5, Rab11-FIP2, Syndapin2 and MICAL-L1 is that they all contain multiple NPF motifs (human Rabenosyn-5 has five NPF motifs, mammalian Rab11-FIP2 has three NPF motifs,

Syndapin2 has three NPF motifs and MICAL-L1 has two NPF motifs). We also identified a novel interaction partner Rabankyrin-5 for EHD1 (Zhang et al., 2012).

Despite the high level of identity between the EHDs, the EHD proteins display different selectivity for binding to NPF-containing proteins. MICAL-L1 binds to EHD1 and EHD3 but not to EHD2 and EHD4 (Sharma et al., 2009). Rabankyrin-5 binds only to EHD1 and not to EHD2-4 (Zhang et al., 2012). Although the individual EHD proteins interact with unique subsets of binding partners, EHDs can also bind to the same partner in some cases. For instance, Syndapin2 is a protein with three different NPF motifs and all four EHDs interact with Syndapin2 (Braun et al., 2005). Hence, Syndapin2 serves as a unique model to identify the different amino acid residues surrounding its three different NPF motif responsible for the binding selectivity of each EHD protein. Strikingly, one intriguing factor governing differential binding to the NPF-containing binding partners is the oligomerization state of the protein. For instance, oligomerization of EHD1 and EHD3 is required for binding to Rab11-FIP2, but not for Rabenosyn-5 (Naslavsky et al., 2006). More details of binding partner selectivity of EHD1 and EHD3 will be discussed later, in Chapter IV.

Rabenosyn-5, Rab11-FIP2, Rabankyrin-5 and MICAL-L1 are all Rab effectors and through EH domain-NPF interactions, EHD1 cross-talks with various Rabs. Thus, Rabs and EHDs provide a network for endocytic regulation that is bridged by “Rab effectors” (Naslavsky and Caplan, 2011; Zhang et al., 2012). SNAP29 forms a complex with clathrin, AP-2, and EHD1, indicating its involvement in the endocytic machinery (Rapaport et al., 2010). A current model holds that EHD1 is recruited to TRE membranes by a complex formed by the stable interaction of MICAL-L1 and Syndapin2 to perform fission of TREs and give rise to newly formed vesicles (Giridharan et al., 2013). We have further demonstrated that Rabankyrin-5 and EHD1 play an important role in regulating localization of the retromer complex (Zhang et al., 2012).

The atomic and molecular mechanisms underlying this differential EHD partner binding are not understood. We propose two models describing the binding partners to understand the nuances of binding with the EHD proteins.

In the "*Downstream" Number Model,* we propose that a number of sequential acidic residues are needed after the phenylalanine (F) of the NPF motif. Rabankyrin-5 has a motif composed of negatively charged residues at the +1 and +2 positions (NPFED) but binds to EHD1 and not EHD3 (Schnatwinkel et al., 2004; Zhang et al., 2012). On the other hand, MICAL-L1 has 6 negatively charged residues immediately following its phenylalanine (NPFEEEEED), and it interacts robustly with both EHD1 and EHD3.

In the "*Upstream" Residue Model,* we postulate that the residues just prior to the NPF motif might dictate the selectivity of binding. MICAL-L1 has KPY residues immediately upstream to the NPF motif that might allow more promiscuous binding than the QSV upstream to the Rabankyrin-5 NPF motif (Schnatwinkel et al., 2004).

We have further discussed these models in Chapter IV for understanding the fine-tuning of partner binding with EHD proteins. Moreover, the differences in the EH domain could also be responsible for differential binding. Other interaction motifs have also been observed, aside from the typical NPF-EH interface. One such atypical interaction motif is the YPXL motif found in the RME-1 interaction partner, is the *C. elegans* protein ALX-1/Alix, Alix the V domain (the structure of the residues spanning 360-702 amino acids of Alix has the shape of the letter "V") of which binds to YPXL motif in the extreme C-terminus of RME-1 (Lee et al., 2007; Shi et al., 2007).

5.4 Distinct features of EHD proteins

Despite having such high level of identity, EHD proteins have unique subcellular localizations and regulate distinct steps of trafficking. EHD1 is localized mainly at the

tubular components of the endosomal recycling compartment (ERC), punctate membranes and cytoplasm. The primary function of EHD1 is to carry the receptors from ERC back to the PM (Grant et al., 2001; Caplan et al., 2002). EHD2 is recruited to the PM by PIP2 and where it interacts with molecular components of caveolae and regulates caveolar mobility (Daumke et al., 2007; Stoeber et al., 2012; Simone et al., 2013). EHD3 facilitates the trafficking of receptors from EE to the ERC and the Golgi (Galperin et al., 2002; Nasvalsky et al., 2006). EHD4 localizes to the Rab5 and EEA1 positive EEs and regulates the trafficking of receptors from EE to the ERC with EHD3 and primarily to the lysosomes for degradation (Sharma et al., 2008) (Fig 1.5). EHD4 has also been implicated in regulating nerve growth factor receptor (TrkA) internalization and L1/neuron-glia cell adhesion molecule (NgCAM) trafficking in neuronal cells (Shao et al., 2002; Yap et al., 2010). Given that EHD proteins have an indispensable role in the regulation of trafficking process, it is not surprising that aberrant function or expression of EHD proteins would lead to a host of diseases (Table 1).

6. EHD1

EHD1 is the best-characterized and most extensively studied member of the EHD protein family. The primary role of EHD1 is to promote the recycling of receptors from the ERC back to the PM (Caplan et al., 2002). EHD1 regulates the recycling of an extensive array of receptors that have been internalized by both CME and CIE. Some of the examples of receptors recycled by EHD1 are transferrin receptor (TfR) (Caplan et al., 2002), major histocompatibility complex I (MHCI) (Jovic et al., 2009), glucose transporter type 4 (GLUT4) receptor (Guilherme et al., 2004), and 2-amino-3 (3-hydroxy-5-methyl-isoxazol-4-yl) propanoic acid (AMPA) receptors (Park et al., 2004).

Figure 1.5 Endocytic transport and regulatory proteins.

EHD family members regulate endocytic trafficking at different steps. EHD1 regulates trafficking at the endocytic recycling compartment and also localizes to the retromer tubules during retrograde transport to the *trans*-Golgi network. Rab5 regulates the of entry cargo from plasma membrane to the early endosome. Rab4 and Rab11 regulate fast recycling and slow EHD2 regulates caveolin assembly and trafficking to the early endosome; whereas EHD3 regulates the transport from the Early Endosome to the Endocytic Recycling Compartment and to the *trans*-Golgi network; EHD4 and Rab7 regulate the movement from early endosome to the late endosome and lysosomes.

Figure 1.5

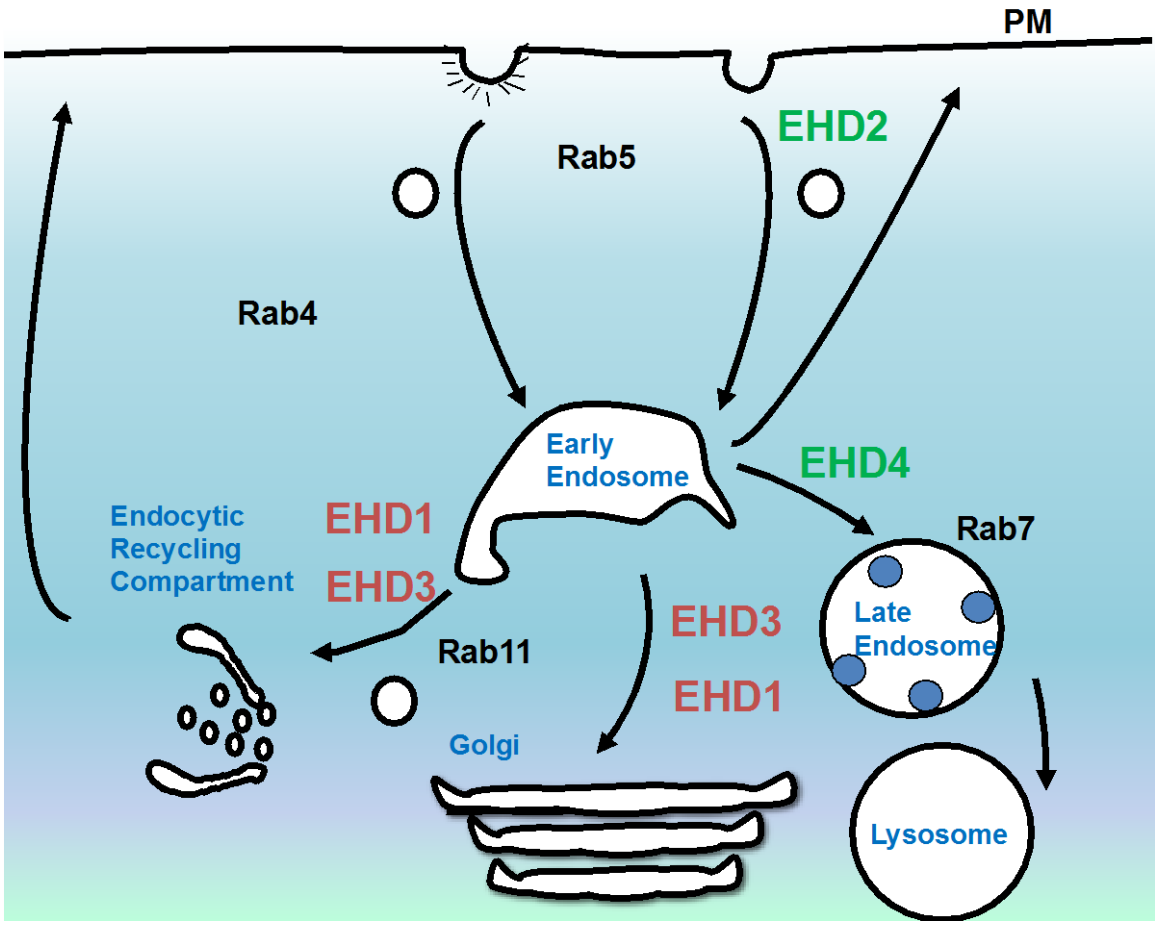
PM
Rab5
EHD2
Rab4
Early
Endosome
EHD4
Rab7
Endocytic
Recycling
Compartment
EHD1
EHD3
Rab11
EHD3
EHD1
Late
Endosome
Golgi
Lysosome

EHD1 localizes to a distinct array of tubular and vesicular membranes (Caplan et al., 2002). The EH domain of EHD1 interacts with lipids and localizes EHD1 to the tubules. Indeed, mutating lysine (K) at position 483 (present within the EH domain) affects the binding of EHD1 to lipids and abrogates its tubular localization, thereby rendering the protein cytosolic (Naslavsky et al., 2007a). Recent studies have demonstrated that the loss of tubular localization leads to accumulation of cargo in the ERC. Thus, the function of EHD1 is contingent upon localization to tubular endosomes. Recent studies from our lab have highlighted the role of EHD1 in release of cargo-containing vesicles from the TREs by the process of vesiculation.

6.1 EHD1 as a vesiculator

Vesiculation is the process of generation and release of vesicles from the tubular endosomes. This process requires the recruitment of an array of proteins that orchestrate the inward bending of the PM to form a deeply invaginated budding vesicle and subsequently promote its fission (Ferguson and DeCamilli, 2012). One of the most extensively studied proteins that directly catalyze the process of fission of vesicles is the GTPase Dynamin. Accumulating evidence has suggested that GTP-bound Dynamin assembles as helical polymers around the necks of invaginated membrane and upon GTP hydrolysis, Dynamin polymer constricts and releases the budding endocytic vesicle from the PM (Takei et al., 1995; Hinshaw and Schmid, 1995)

EHD proteins are thought to share common features with Dynamin. Indeed, EHD2 forms spiral-like oligomers around the negatively charged liposomes and stimulates ATP hydrolysis upon lipid binding, consequently tubulating the liposomes *in vitro* (Daumke et al., 2007; Pant et al., 2009). This led to an initial conclusion that EHD proteins can tubulate membranes. However, our studies in cells seem to suggest that EHD proteins are not capable of generating tubules. Our initial evidence came from the

observation that EHD1 localizes to pre-existing tubular membranes (Jovic et al., 2009). Furthermore, identification of MICAL-L1 as not only a novel direct interaction partner of EHD1 but also as a protein that co-localizes with EHD1 on the TREs, has augmented our understanding of TREs (Sharma et al., 2009). Interestingly, MICAL-L1 functions as a membrane hub and is capable of interaction with a battery of proteins that have an impact on TRE membrane shaping. MICAL-L1 is capable of direct interaction with Syndapin2, which can induce membrane curvature and also directly interact with EHD1 (Braun et al., 2005). We also identified phosphatidic acid (PA) as a lipid indispensable for the generation of TREs. Both MICAL-L1 and Syndapin2 preferentially bind to membranes having a high concentration of PA. Subsequently, the MICAL-L1-PRD (2 of the 14 PRDs) interacts with the SH3 domain of Syndapin2, and this stable interaction leads to the generation of TREs. Upon completion of TRE generation, EHD1 is recruited to the TRE membranes and it leads to the fission of vesicles containing cargo from the TREs by the process of vesiculation (Giridharan et al., 2013). Evidence for this model came from the knockdown of EHD1 in HeLa cells, which led to the generation of long, more elaborate and extensive TREs in the cells in the absence of EHD1. Furthermore, the addition of purified EHD1 to a novel semi-intact cell system in the presence of ATP fostered the release of vesicles from TREs, reinforcing the notion of EHD1 as a vesiculator (Cai et al., 2013). EHD4 also behaves as a vesiculator like EHD1 in a semi-intact cell system. In agreement with our notion of EHD1 as a vesiculator, studies in *Lampetra fluviatilis* have also demonstrated that the EHD ortholog, l-EHD1, is present on presynaptic sites and co-operates with Dynamin2, to promote the release of synaptic vesicles (Jakobsson et al., 2011).

Furthermore, we have previously shown that the lipid modifier cytosolic phospholipase A2α (cPLA2α) cooperates with EHD1 in the vesiculation of GPI-AP-containing endosomes, using endogenous CD59 as a cargo for GPI-APs. We

hypothesize that cPLA2α might act by locally modifying lipids and ultimately promoting the membrane curvature, to generate a template for EHD1 to cleave vesicles (Cai et al., 2012). Furthermore, we also discovered that TRE vesiculation is supported by a synergistic role of GRAF1 and EHD1 (Cai, Xie et al. 2014). Chapter IV of this dissertation describes the studies which have been performed to elucidate the molecular and atomic basis of EHD1 function as a vesiculator.

7. EHD2

EHD2 is the most diverse member of the EHD family in terms of sequence homology that is (>70%) and function. EHD2 is recruited to the PM by the lipid PIP2 (Simone et al., 2013). At the PM, EHD2 localizes to small cave-like structures known as caveolae. The structure of caveolae comprises the integral membrane caveolin proteins and cavin proteins coat it. A recent model by Stoeber et al., 2016 proposes that caveolin and cavin proteins form a well-defined decahedron, a structural unit of the caveolae, which provides stability and membrane confinement (Stoeber et al., 2016). In addition, Syndapin2 is recruited to caveolae and functions in shaping the caveolae. Through its NPF motif Syndapin2 binds to the EH domain of EHD2 (Braun et al, 2005); however, it is not responsible for recruiting EHD2 to the caveolae. ATP and the unstructured loop containing the sequence KPFRKLNPF are required for recruiting EHD2 to the caveolae. EHD2 primarily functions in restricting the mobility of caveolae (Stober et al., 2012; Moren et al., 2012). EHD2 is also present in the actin-rich regions of the PM and is connected to the cytoskeleton. EHD2 is connected to the actin cytoskeleton by the EHD2 binding protein 1 (EHBP1) (Guilherme et al., 2004). Further, it has been hypothesized that EHD2 behaves as a vesiculator in the caveolae (similar to the role of EHD1 in TREs and Dynamin in CME) and gives rise to caveolar vesicles. Hence, EHD2

regulates caveolar mobility by interaction with the actin cytoskeleton and possibly by releasing caveolar vesicles (Stoeber et al., 2012).

7.1 Structure of EHD2

EHD2 crystallizes as a dimer; the dimerization is mediated by a highly conserved hydrophobic interface. The crystal structure was solved as a dimer in the presence of AMPPNP (Fig 1.4 B). The two G-domains along with the helical domains adopt a compact scissor-shaped orientation, such that the C-termini of the two monomers cross each other, orienting the EH domains on top of or on the same axis as the G-domains of opposing monomers (Daumke et al., 2007). The stretch of polybasic residues close to the helical tip is involved in lipid binding. EH domains were proposed to mediate homo-oligomerization by binding to intrinsic NPF motifs in adjacent EHD2 dimers (Daumke et al, 2007). This internal NPF is a part of a partially conserved unstructured loop with the sequence KPFRKLNPF (Daumke et al., 2007).

Recent studies focusing on the structural analysis of EHD2 have highlighted the role of N-terminus of EHD2 in governing the conformation of EHD2 and subsequently targeting EHD2 to the caveolae. The N-terminus of EHD2 is a switch region and it exists in two states, dependent upon the localization of EHD2. When EHD2 is in solution, it exists in a highly ordered state that is stabilized by the interaction of its N-terminus with the G domain specifically the KPFRKLNPF motif. This state is called the “auto-inhibited” state. However, in the presence of membrane, there is a flexible state of the N-terminus also known as the “open conformation”. The N-terminal residues are buried in a hydrophobic pocket of the G domain in the crystal structure. In the presence of lipid membranes, N-terminal residues relocate and insert into the lipid bilayer; hence, the “open conformation” is a prerequisite for the membrane insertion of EHD2 and conformational change in helical domains. Upon insertion of the N-terminus of EHD2 into

the membrane, the KPFRKLNPF loop is free and can interact with the EH domain of the neighboring dimer, facilitating oligomerization (Shah et al., 2014; Alves Melo et al., 2017). Furthermore, another recent study has firmly established that ATP binding is indispensable for partial insertion of the N-terminus of EHD2 into the membrane enabling G-domain-mediated oligomerization. Upon completion of this step, ATP hydrolysis occurs and the EHD2 oligomers are disassembled, released and subsequently EHD2 detaches from the membrane (Hornecke et al., 2017).

7.1.1 Homo-and Hetero-oligomerization of EHDs

C-terminal EHD proteins have a unique ability to homo- and hetero-oligomerize. Initial evidence of EHD1 existing in a large oligomeric complex and not as monomers in HeLa cells came from the sedimentation velocity analysis of EHD1 (Caplan et al., 2002). In addition, hetero-oligomerization of EHD1 and EHD3 was demonstrated by yeast two-hybrid analysis and overexpression studies (Galperin et al., 2002). A previous study from our group has demonstrated the hetero-oligomerization of EHD1 and EHD3 with EHD4 in physiological conditions (Sharma et al., 2008). Interestingly, EHD2 is the only EHD protein that is not capable of hetero-oligomerization with the other three paralogs (George et al., 2007; Sharma et al., 2008). The coiled-coiled region in EHDs was predicted to be the region of dimerization and oligomerization (Lee et al., 2005). Interestingly, we were able to identify a conserved valine in EHD1, EHD2, and EHD3 in the coiled-coiled region using Paircoil-coil prediction program (http://paircoil.lcs.mit.edu/cgi-bin/paircoil) that is critical for mediating dimerization. Mutation of this valine residue (at 203 positions in EHD1 and EHD3, and 297 positions in EHD2) to a proline residue prevents dimerization and renders the protein insoluble (Naslavsky et al., 2006; Bahl et al., 2015).

7.1.2 Role of KPFRKLNPF loop in EHD2 oligomerization

The crystal structure of EHD2 had shed new light on the putative region involved in oligomerization. The crystal structure of EHD2 was solved as a dimer and it led to the identification of a partially conserved unstructured loop KPFRKLNPF in the G-domain. The unstructured loop has an intrinsic NPF motif, which mediates the oligomerization of EHD2 dimers by interacting with the EH domain of the neighboring EHD2 dimer (Daumke et al., 2007; Shah et al., 2014). This serves as a unique case of EH-NPF interaction involved in mediating self-interaction, in addition, to the well-established role of EH domain of EHDs in mediating interaction with NPF containing binding partners. Structural data also demonstrate that EHD2 forms dimers through the previously proposed G-domain hydrophobic interface (Daumke et al., 2007), but the conserved KPFRKLNPF loop in the G domain plays a role in oligomerization (Moren et al, 2012). Recent studies have also demonstrated the role of the KPF motif on caveolar targeting; however, its exact function remains elusive. The current model holds that the assembly of EHD2 into ring-like structures creates the scaffold that generates and/or stabilizes at the membrane. As discussed in the previous section, oligomerization of EHD2 was significantly enhanced in the presence of ATP, suggesting that the membrane-inserted open conformation of EHD2 provides an optimized template for oligomerization, and the KPFRKLNPF loop is available for EH-binding (Hornecke et al., 2017). Studies described in Chapter III have defined the precise role of the KPFRKLNPF loop in homo-oligomerization, localization to PM and binding to the interaction partners. We have also delineated the function of the single RPF motif of EHD1 in homo and hetero-oligomerization, localization on the TREs and binding to interaction partners.

8. EHD3

EHD3 shares the highest level of homology with EHD1, about 86% identity at the amino acid level (Galperin et al., 2002). EHD3 is involved in the regulation of transport from the EE to the ERC and the absence of EHD3 leads to failure of transport of cargo to ERC (Naslavsky et al., 2006). Moreover, EHD3 is involved in retrograde transport from the EE to the TGN and maintenance of Golgi morphology (Naslavsky et al., 2009). Thus, it is obvious that absence of EHD3 leads to trapping of cargo in the EE, a characteristic phenotype of EHD3 knock-down (KD) (Naslavsky et al., 2006). EHD3 is capable of heterodimerizing with EHD1 and colocalizes with EHD1 on the tubulo-vesicular endosomes (Galperin et al., 2002). Similar to EHD1, EHD3 binds to Rab effectors, such as Rab11-FIP2, Rabenosyn-5, and MICAL-L1 (Naslavsky et al., 2004; Naslavsky et al., 2006; Sharma et al., 2009).

The knockout mouse of EHD1 did not show a discernable phenotype and we hypothesized that EHD3, being so similar to EHD1, would be responsible for compensation of the protein (Rapaport et al., 2006). However, an additional mouse model revealed that EHD1 is required for normal spermatogenesis and fertility of male mice (Rainey et al., 2010). These differences in the phenotypes of two mouse models might be subject to a different strain of the background mouse used for the crosses.

Since EHD3 has such a high level of homology with EHD1, one would expect EHD1 and EHD3 to have a similar function. However, our knockdown studies demonstrated that loss of EHD3 has an opposing effect on TREs, namely the loss of TRE in cells as compared with EHD1. This finding was further corroborated by our semi-intact cell system, wherein upon addition of purified EHD3, rapid induction of tubules was observed (Cai et al., 2014). The *in vitro* experiments using purified liposomes also demonstrated that EHD3 is required for membrane tubulation. However, liposomes come with a caveat that they have an innate propensity towards tubulation (Henmi et al.,

2016). Although, our findings suggest that EHD3 is involved in tubulation, its precise role is unclear.

Regardless of the disparate functions of EHD3 and EHD1, EHD3 does display functional redundancy in some aspects of cellular regulation. For instance, EHD1 and EHD3 are both required for the formation of ciliary vesicles (Lu et al., 2015).

8.1 Curvature and tubule generation

The generation of a tubule from a flat lipid bilayer requires the dynamic interplay of proteins and lipids that sense and stabilize the local regions of membrane curvature (McMahon and Gallop, 2006). The phospholipid bilayer can be deformed causing positive or negative membrane curvature. There are five main categories: 1) changes in lipid composition 2) influence of integral membrane proteins that have intrinsic curvature or have curvature upon oligomerization 3) changes in cytoskeletal polymerization and pulling of tubules by motor proteins 4) direct and indirect scaffolding of the bilayer and 5) active amphipathic helix insertion into one leaflet of the bilayer (McMahon and Gallop, 2005).

One important class of membrane curvature sensor and generating proteins is the BAR-domain containing protein. The BAR domain bears a dimeric, crescent-shaped membrane binding region that senses curved membranes and generates a positive curvature upon binding (Peter et al., 2004). Based on sequence homology and structural analysis, BAR domain-containing proteins are classified into several types: classical BAR, N-BAR, BAR-PH, PX-BAR, F-BAR and I-BAR (Frost et al., 2009; Suetsugu et al., 2010). The BAR domain includes elongated homo-dimers of 6-alpha-helical coiled coils and is often referred to as a crescent-shaped or banana–shaped structure (Frost et al., 2008; Peter et al., 2004).

Recently, we have linked one of the three isoforms of Syndapin, Syndapin2, to TRE biogenesis (Braun, et al., 2005; Giridharan et al., 2013). Syndapin2 also contains a C-terminal SH3 domain (Kessels et al., 2004) along with three NPF motifs (Braun et al., 2005), which serve as protein binding modules. Some of the Syndapin2 SH3 domain-interacting proteins are: dynamin, synaptojanin, synapsin, Rac1 and neural Wiskott-Aldrich syndrome protein (N-WASP) and MICAL-L1 (de Kreuk et al., 2011; Kessels and Qualmann, 2004; Giridharan et al., 2013). Syndapin2 interaction with the EH domain of EHD1 is mediated by its NPF motifs (Braun et al., 2005). The current proposed model for the generation of TREs suggests that local high concentration of PA is a prerequisite for the generation of tubules. Localized high concentration of PA leads to the formation of microdomains and supports slight positive curvature (Faraudo and Travesse, 2007). The F-BAR domain of Syndapin2 binds to the slightly curved surface and preferentially recruits other TRE generation proteins MICAL-L1 and EHD3 (See Figure 1.5 for the proposed model depicting the function of Syndapin2 in TRE biogenesis). Once TRE biogenesis is completed, EHD1 is recruited to release cargo-containing vesicles by the process of vesiculation. This biogenesis process is vital for cargo sorting into the recycling pathways because depletion of MICAL-L1 and EHD1 results in significant accumulation of cargo in the ERC (Giridharan et al., 2013). The function of EHD3 in the process of TRE generation remains unclear. We hypothesize that there are two alternate possibilities: 1) EHD3 can induce tubulation (the prerequisite for tubulation is the ability to sense and generate curved membranes, for instance, functioning similar to BAR domains) or 2) EHD3 stabilizes the newly synthesized MICAL-L1 and Syndapin2-decorated TRE, according to our current understanding of TRE biogenesis (Giridharan et al., 2013). Studies described in chapter IV of this dissertation test the two alternatives to delineate the precise role of EHD3 in the process of TRE generation.

Figure1.6 Model for biogenesis of tubular recycling endosomes.

(A) Phosphatidic acid is generated or enriched on membranes. **(B)** MICAL-L1 (via its CC domain) and Syndapin2 (via its F-BAR domain) are recruited to PA-enriched membranes. **(C)** The MICAL-L1 PXXP motifs interact with the SH3 domain of Syndapin2 to stabilize both proteins on the membranes **(D)** Next, facilitate the generation of tubular endosomes by Syndapin2. **(E)** Syndapin2 and MICAL-L1 bind to the EH domain of EHD1 via their NPF motifs and recruit EHD1 to these tubular membranes, potentially facilitating vesiculation (Image used with permission from Giridharan et al., 2013).

Figure 1.6

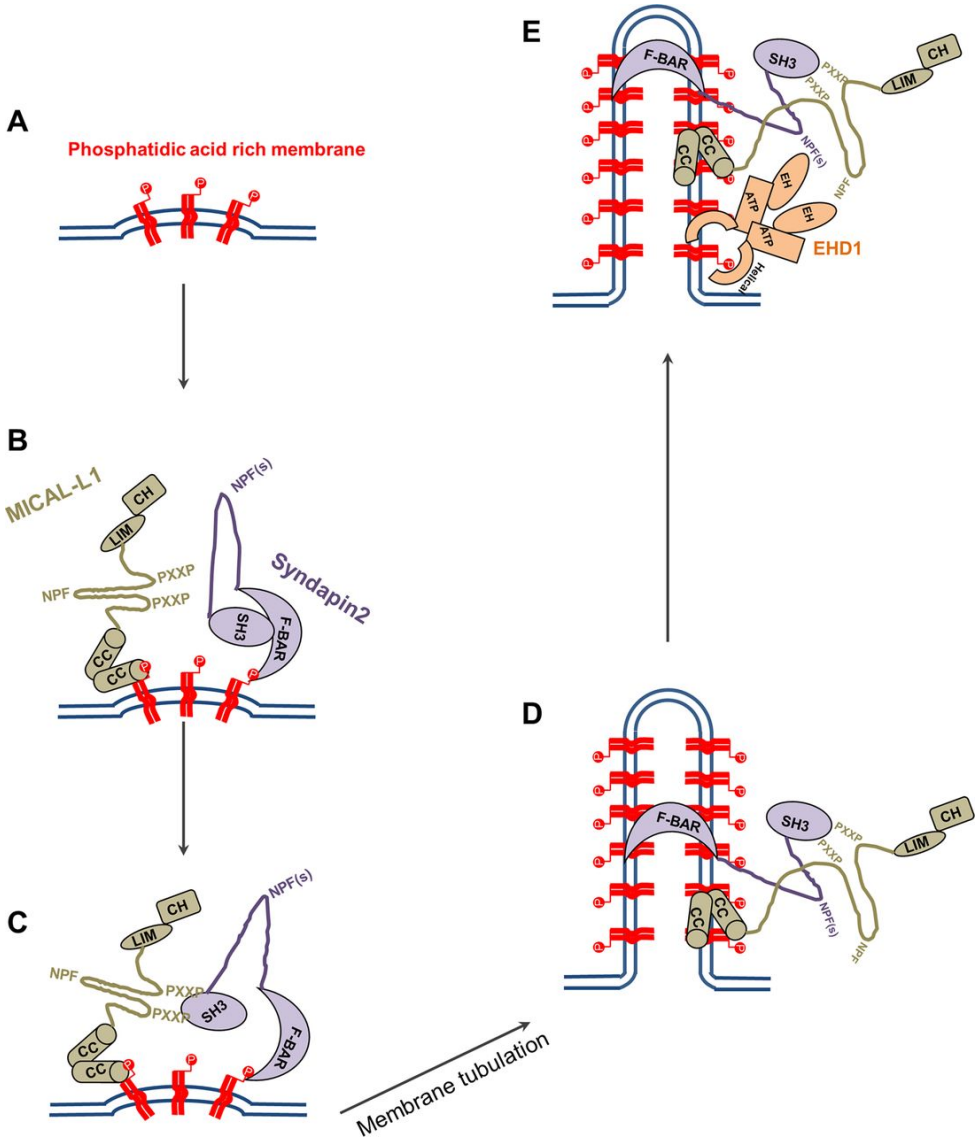
A
Phosphatidic acid rich membrane
B
MICAL-L1
CH
LIM
NPF
PXXP
PXXP
NPF(s)
Syndapin2
SH3
F-BAR
CC
C
D
E
EH
ATP
EHD1
Helical
Membrane tubulation

9. Conclusion

In recent years, there has been an intense interest in the EHD protein family and many studies have focused on EHD proteins. Major advances have been made towards gaining insight into structure-function relationship of EHD2. A partially conserved unstructured loop, KPFRKLNPF loop in the G-domain, which is primarily responsible for oligomerization and targeting of EHD2 to caveolae has been characterized. Strikingly, EHD2 is the only family member that has 2 proline-phenyalanine (PF) (KPF and NPF) motifs in this loop and with an internal NPF motif. However, the exact role of the 2PF motifs in the unstructured loop remains unknown. In this dissertation, we focus on delineating the precise role of 2PF motifs in oligomerization, targeting to the PM and binding to the interaction partners.

EHD1 and EHD3 have the highest level of homology amongst the members of the EHD family. Despite hetero-dimerizing and co-localizing at TRE membranes, surprisingly, EHD1 and EHD3 have distinct, even opposing functions in the TRE biogenesis/stabilization and vesiculation. EHD1 is involved in the release of vesicles by the process of vesiculation and EHD3 has been implicated in the tubulation and/or stabilization of TREs. In this dissertation, we set out to determine the precise mechanistic role of EHD3 in TRE generation and/or stabilization. Furthermore, we aimed to elucidate the molecular and atomic basis of the differential function of two such similar proteins likely evolved through gene duplication and divergent evolution.

Table 1: Relationship between EHD proteins and disease

EHD protein	Disease	Abberant Phenotype	Reference
EHD1 and EHD3	Alzheimer's Disease	Loss of EHD1or EHD3	Buggia-Prévot et al., 2013
EHD1	Non-small lung cancer	Overexpression	Meng et al., 2016
EHD1	Breast Cancer	Overexpression	Tong et al., 2017
EHD1	Sickle Cell Anemia	4.9 fold increased expression	Ammann et al., 2009
EHD2	Breast Cancer	Overexpression	Yang et al., 2015
EHD3	Gliomas	Overexpression	Chukkapalli et al., 2014
EHD3	Small-cell lung carcinoma	Overexpression	Taniwaki et al., 2006
EHD4	Systemic onset juvenile idiopathic arthritis	Overexpression	Allantaz et al., 2007

CHAPTER II

Materials and Methods

10 Materials and Methods

10.1 Recombinant DNA Constructs

The following constructs were used for studies conducted in chapter III and chapter IV. Cloning of EHD1, EHD2, EHD3, EHD4, MICAL-L1, Rabankyrin-5, Syndapin2 into yeast two-hybrid vectors pGBKT7 and pGADT7, glutathione-S-transferase (GST)-EH1 and GST-EH3 vectors as well as cloning of green fluorescent protein (GFP)-Myc–EHD1, GFP-Myc-EHD2, GFP-Myc-EHD3 in expression vectors and their SiRNA-resistant versions have been described previously (Caplan et al., 2002; Sharma et al., 2009; Giridharan et al., 2013; Zhang et al., 2013). The SiRNA-resistant-GFP-Myc-EHD3/EH1 chimera was generated, by cloning amino acid residues 1-434 of EHD3 and 435-450 of EHD1 in eGFP-C3 vector. Two-hybrid control vectors (Gal4ad-SV40 large T-antigen and Gal4bd-p53) were purchased from (BD Biosciences Clontech, Palo Alto, CA). The following constructs were generated for the studies described in chapter III using QuikChange site-directed mutagenesis kit (Stratagene, La Jolla, CA): in the pGADT7 vector (yeast-two hybrid vector), in the GFP-Myc-EHD1 and in the GFP-Myc-EHD2 vectors (mammalian expression vectors); pGADT7 EHD2 and GFP-Myc-EHD2 (NPF-to-NAF), pGADT7 EHD2 and GFP-Myc-EHD2 (NPF-to-NPA), pGADT7 EHD2 and GFP-Myc-EHD2 (NPF-to-APA), pGADT7 EHD2 and GFP-Myc-EHD2 (KPF-to-KAF), pGADT7 EHD2 and GFP-Myc-EHD2 (KPF-to-APA), GFP-Myc-EHD2 (NPF-to-NPY), GFP-Myc-EHD2 (NPF-to-NFP), pGADT7 EHD1(RPF-to-APA), pGADT7 EHD1(NAF-to-NPF), pGADT7 EHD1(RPF-to-APA+NAF-to-NPF) and GFP-Myc-EHD1 (RPF-to-APA).

The following mutations were introduced by site-directed mutagenesis for studies described in chapter IV: pGADT7 EHD3 (AHLL523PHLV), pGADT7 EHD3 (D459N), pGADT7 EHD3 (M447T), pGADT7 EHD3 (KVAE523RHE), pGADT7 EHD3 (N519A), pGDAT7 EHD3 (NE519AD), pGADT7 EHD1 (AD519NE), pGBKT7 MICAL-L1

(NPFDEEEEE to NPFDEEEEA), pGBKT7 MICAL-L1 (NPFDEEEEE to NPFDEEEAA), pGBKT7 MICAL-L1 (NPFDEEEEE to NPFDEEAAA), pGBKT7 MICAL-L1 (NPFDEEEEE to NPFDEAAAA), pGBKT7 MICAL-L1 (NPFDEEEEE to NPFDAAAAA), pGBKT7 MICAL-L1 (NPFDEEEEE to NPFAAAAAA), pGADT7 Rabankyrin-5 (NPFEDV to NPFEDE), pGADT7 Rabankyrin-5 (NPFEDV to NPFEDEE), pGADT7 Rabankyrin-5 (NPFEDV to NPFEDEEE), pGADT7 Rabankyrin-5 (QSV to KPY), pGADT7 Rabankyrin-5 (QSV to KSV), pGADT7 Rabankyrin-5 (QSV to QPV), pGADT7 Rabankyrin-5 (QSV to QSY) and GST-EH3 (NE519AD).

10.2 Antibodies and Reagents

The primary antibodies used in the studies described in Chapter III and IV were: the affinity-purified rabbit polyclonal antibodies directed against the C-terminus of human EHD1 (DLPPHLVPPSKRRHE), EHD2 (VERGPDEAMEDGEEGSDDEA) (Anaspec, Fremont, CA) have been described previously (Naslavsky et al., 2004). Mouse polyclonal anti–MICAL-L1 (Novus Biologicals, Littleton, CO), rabbit polyclonal anti-Syndapin2 used for immunofluroscence (IF) (Abgent, San Diego, CA) and for western blot (WB) (ProteinTech, Chicago, IL), goat anti-GST conjugated to horseradish peroxidase (HRP) (GE life sciences, Piscataway, NJ), mouse anti-Rabankyrin-5 (Novus Biologicals, Littleton, CO), rabbit anti-HA (Signalway Antibody, Pearland, TX), rabbit anti-HA (Bethyl, Montgomery, TX), and rabbit anti-caveolin1 (Cell Signaling Technology, Danvers, MA). The following secondary antibodies were used in studies described in Chapter III and Chapter IV: Alexa-Fluor-568-conjugated goat anti-mouse, Alexa-Fluor-488-conjugated goat anti-mouse, Alexa-Fluor-568-conjugated goat anti-rabbit antibodies, and Alexa-Fluor 568–labeled transferrin (Tf-568) (Life Technologies, Carlsbard, CA). Goat anti-mouse HRP was obtained from (Jackson ImmunoResearch Laboratories, West Grove, PA). Donkey anti-rabbit HRP was obtained from (GE Life

Sciences, Piscataway, NJ). CAY 10593 and CAY 10594 were purchased from (Cayman Chemical Company, Ann Arbor, MI).

10.3 Cell culture, transfections and SiRNA treatment

The HeLa cervical cancer cell line (ATCC-CCL2; Manassas, VA) was maintained in high-glucose Dulbecco's modified Eagle medium (DMEM) supplemented with 10% (v/v) fetal bovine serum (FBS) (Sigma-Aldrich, St.-Louis, MO), 200 U/ml penicillin, 200 µg/ml streptomycin. On-Target-plus SMART pool SiRNA for EHD3, MICAL-L1, Syndapin2, and SiRNA duplexes for EHD1 (base pairs gaaagagatgcccaatgtc) and synthesized by Dharmacon, Lafayette, CO were transfected using Lipofectamine RNAiMax (Life Technologies, Carlsbad, CA) to perform knockdown studies as previously described (Naslavsky et al., 2006 and Sharma et al., 2009) for 48 hour (h) or 72 h depending on the efficiency of the SiRNA duplexes. For transfection, HeLa cells, plated on 6-well plates, were transfected using 6 µl X-tremeGENE 9 (Roche Life Sciences, Indianapolis, IN) or 6 µl Lipofectamine 2000 (Life Technologies, Carlsbad, CA) with 2 µg of DNA for 16-18 h at 37°C according to manufacturer's protocol.

10.4 Protein Purification

The EH domains of EHD1, EHD3 and EHDNE519AD mutant were cloned into bacterial expression vector pGEX-6p-2 and transformed into BL-21 cells. A single colony from the transformed cells was cultured overnight in 50 ml LB medium containing 10% glucose. The next day, 20 ml of the culture was transferred to 2 L Super Broth medium and grown at 37°C. When the optical density (O.D.) reached 0.6-0.7, the cells were induced with 0.2 mM isopropyl β-D-1-thiogalactopyranoside (IPTG) and transferred to an 18°C incubator shaker for 3 h. Cells were then pelleted and lysed using Emulsiflex-C3

homogenizer (Avestin, Ottawa, Canada). The EH1, EH3 and EH3 (NE519AD) proteins were purified from the lysate using the gluthathione-agarose resin.

10.5 Immunoblotting

For immunoblotting experiments described in both Chapter III and Chapter IV, HeLa cells were harvested and lysed on ice for 30 minutes (min) in lysis buffer containing 50 mM tris(hydroxymethyl)aminomethane(Tris), pH 7.4, 150 mM NaCl, 1% Triton-X, 1.8 mg/ml iodoacetamide, and protease inhibitor mixture (Roche Life Sciences, Indianapolis, IN). Total protein levels in the lysate were calculated by BioRad protein assay reagent (Bio-Rad Laboratories, Hercules, CA) and normalized for equal protein loading on gels. Protein samples were separated on 8%, 10% or 13% sodium dodecyl sulphate (SDS)- polyacrylamide gel electrophoresis (PAGE) depending on the molecular weight of the protein of interest. The separated proteins were transferred to nitrocellulose membrane and detected by immunoblotting with appropriate antibodies.

10.6 GST pull-down and co-immunoprecipitation

For the co-immunoprecipitation experiments between EHD2 and Syndapin2, HeLa cells were transiently transfected with either GFP-Myc-EHD2, or GFP-Myc-EHD2 mutants (NPF-to-NAF, NPF-to-APA, KPF-to-KAF, KPF-to-APA), lysed 24 h later in a buffer containing 50 mM Tris-HCl (pH 7.4), 150 mM NaCl, 1% Triton-X, 1:1000 of 1 mg/ml protease inhibitor cocktail (Calbiochem, San Diego, CA) and subjected to immunoprecipitation with antibodies against Syndapin2. Separated proteins were transferred on to nitrocellulose membrane and then immunoblotted with anti-EHD2 antibodies. Input lane contains 5% of the total lysate immunoprecipitated.

In order to address the binding of EH domains of EHD1, EHD3, and EHD3 NE519AD proteins with Rabankyrin-5, in chapter IV, we performed GST pull-down

experiments: 50 µg of purified GST-fusion proteins EH1, EH3 or EH3 (NE519AD) were incubated with GST beads, in buffer containing 20 mM Tris and 300 mM NaCl containing 0.1% Triton-X-100, leupeptin and incubated for 4 h as previously done (Giridharan et al., 2013). GST beads were then washed 4X in 20 mM Tris and 300 mM NaCl containing 0.1% Triton-X-100 and leupeptin. HeLa cells were transiently transfected with HA-Rabankyrin-5 for 24 h and lysed in buffer containing 50 mM Tris-HCl, pH 7.4, 150 mM NaCl, 0.5% Triton-X-100, 1.8 mg/ml iodoacetamide and protease inhibitor cocktail. GST beads were then incubated with the HeLa lysate overnight, washed 4X in 20 mM Tris and 300 mM NaCl containing 0.1% Triton-X-100 and leupeptin, eluted with 4X sample buffer, and analyzed by immunoblotting with the anti-HA antibody.

10.7 Yeast Two Hybrid

The yeast two-hybrid assay was utilizing the *Saccharomyces cerevisiae (S. cerevisiae)* strain, AH109 (BD Biosciences Clontech, Palo Alto, CA) maintained on yeast extract, peptone and dextrose (YPD) agar plates. A loop full of yeast was grown overnight at 30°C with shaking at 250 rpm in liquid YPD medium. The transformation was done by the lithium acetate procedure as described in the instructions for the MATCHMAKER two-hybrid kit (BD Biosciences Clontech, Palo Alto, CA). For colony growth assays AH109 co-transformants were streaked on plates lacking leucine and tryptophan. Co-transformants were allowed to grow at 30°C, usually for three days, or until the colonies were large enough for further assays. An average of three to four colonies were selected and suspended in water, equilibrated to the same optical density at 600 nm, and replated on plates lacking leucine and tryptophan (+HIS, -2 plates), as well as plates also lacking histidine (-HIS, -3 plates). The interaction between p53 and SV40 was used as positive control.

10.8 Transferrin uptake and recycling assays

The rate of recycling of transferrin (TfR) was measured for experiments described in Chapter III and Chapter IV. HeLa cells were plated on 35-mm plates containing five coverslips each. Cells were approximately 75% confluent by the time of experiment. The cells were starved in DMEM containing 0.5% bovine serum albumin (BSA) for 1 h. After starvation, the cells were “pulsed” with 1 µg/ml of Tf-568 for 15 min and chased for 15 min in complete media, to allow the Tf-568 to be recycled. The coverslips were then fixed in 4% (v/v) paraformaldehyde in PBS and imaged by confocal microscopy.

10.9 CAY inhibitor washout assay

HeLa cells were grown on coverslips in 6-well plates and were subjected to SiRNA treatment using SiRNA duplexes against Syndapin2, EHD1 and EHD3. After 48 h, the cells were subjected to100 µM PLD inhibitors (CAY10593 and CAY10594) for 30 min at 37°C. The cells were then washed 3X with complete medium and allowed to recover after the washout of the inhibitors for 20 min, 1 h, 4 h, and 6 h. The coverslips were fixed in 4% (v/v) paraformaldehyde in PBS and stained with anti-MICAL-L1 antibodies for the assessment of TRE.

10.10 Isothermal Titration Calorimetry (ITC)

Heat produced by the binding of MICAL-L1 peptide with the EH domains of EHD1 and EHD3 was measured by ITC using the MicroCal iTC200 isothermal titration calorimeter (Malvern, Worcestershire, UK). All proteins were equilibrated in 1X phosphate-buffered saline (PBS) at pH 7.4 by overnight dialysis. ITC binding isotherms were collected at 25°C by injecting 20 x 2 µL of peptide (930 µM) into a solution of each of the EH domains (90 µM), representing a 1:10 molar ratio. The heat from each

injection was measured by integrating the area of the injection peak, corrected for the background heat produced by the dilution of the peptide into the buffer, and plotted as a function of the EH domain/MICAL-L1 peptide molar ratio. Dissociation constant (K_D) values were calculated by fitting the titration curves according to a single binding site mode with Origin 7 software with ITC add-ons supplied by Malvern.

10.11 Confocal microscopy imaging

HeLa cells were grown on cover slips and fixed with 4% (v/v) paraformaldehyde in PBS. The fixed cells were then incubated with primary antibodies prepared in staining solution (0.2% (w/v) saponin and 0.5% (w/v) bovine serum albumin (BSA) in PBS) for 1 h at room temperature. After washing in PBS, the cells were incubated with the appropriate fluorochrome-conjugated secondary antibody mixture in staining solution for 30 min at room temperature. Images were acquired with a Zeiss LSM 5 Pascal confocal microscope (Carl Zeiss, Thornwood, NY) using a 63 X 1.4 numerical aperture (NA) objective with appropriate filters.

10.12 Structured illumination microscopy (SIM) imaging

SIM images were collected on samples obtained as described above with a Zeiss ELYRA PS.1 illumination system (Carl Zeiss, Thornwood, NY) using a 63 X objective lens with a NA of 1.4 at room temperature as we have done previously (Reinecke et al., 2014; Xie et al., 2015). Three orientation angles of the excitation grid were acquired for each z-plane, with z-spacing of 110 nm between planes. SIM processing was performed using the SIM module of the ZEN BLACK software (Carl Zeiss, Thornwood, NY). The processed SIM images were then exported in TIFF format.

10.13 Quantification of MICAL-L1-containing tubular recycling endosomes

Tubular recycling endosomes (TREs) were quantified as described previously (Cai et al., 2013). Briefly, using NIH ImageJ software, threshold was adjusted to reduce the background in the image. The particle size was set between 5 μm^2 and 150 μm^2. All MICAL-L1-containing particles (tubules and vesicles) in this range were counted. Ten fields of images from each treatment were analyzed for statistical analysis.

10.14 Statistical analysis

The data sets (n=100 unless otherwise indicated) presented were collected from three independent experiments and were analyzed by one-way ANOVA, with one star for $p < 0.01$, and three stars for $p < 0.05$. The *p*-values are shown for each experiment.

10.15 Sequence homology and Identity Analysis

Sequence homology and identity between EHD1, EHD2, EHD3, MILCAL-L1, Rabankyrin-5 and their respective mutants generated by site-directed mutagenesis, was analyzed using AlignX program of Vector NTI. Vector NTI performs multiple sequence alignments using a modified Clustal W algorithm.

CHAPTER III

Role of the EHD2 Unstructured Loop in Dimerization, Protein Binding and Subcellular Localization

The following chapter has been published in PLoS One. 2015 Apr 15;10(4):e0123710

11 Introduction

The C-terminal Eps15 homology domain-containing (EHD) proteins coordinate various endocytic membrane regulatory events in mammalian cells (Naslavsky and Caplan, 2011). All four EHDs (EHD1-4) share a common domain architecture that includes three characteristic domains: 1) a Dynamin-like-G-domain that binds and catalyzes hydrolysis of ATP (Caplan et al., 2002; Naslavsky et al., 2006; Lee et al., 2005; Daumke et al., 2007; Simone et al., 2014), 2) a coiled-coiled domain n formed by two helical regions that facilitates EHD oligomerization and lipid binding, 3) a C-terminal Eps15 Homology (EH) domain with a positively charged electrostatic surface that preferentially binds to proteins containing an asparagine-proline-phenylalanine (NPF) motif followed by acidic residues (Kieken et al., 2007; Kieken et al., 2009; Kieken et al, 2010; Henry et al., 2010), that is a hallmark of these proteins. The most diverse EHD both in terms of sequence homology and function is EHD2 (Marg et al., 2012). A series of recent studies has established the involvement of EHD2 in regulating a variety of important functions that include sarcolemmal repair (Marg et al., 2007), myogenesis (Posey et al., 2011; Doherty et al., 2008), and control of Rac1 and the actin cytoskeleton (Stoeber et al., 2012; Benjamin et al., 2011; Park et al., 2004; Guilherme et al., 2004). Unlike EHD2, EHD1, EHD3 and EHD4, all of which play roles in regulating endocytic transport from sorting and recycling endosomes (Naslavsky and Caplan, 2011; Grant and Caplan, 2008; Naslavsky and Caplan, 2005). However, EHD2 is recruited to the cytoplasmic interface of the plasma membrane (PM) by phosphatidylinositol 4,5 bisphosphate (PIP2) (Simone et al., 2013) where it interacts with caveolin and regulates caveolar mobility (Benjamin et al., 2011; Hansen et al., 2011; Moren et al., 2012).

EHD2 was the first family member whose crystal structure was solved and the structure indicates that this protein contains a partially conserved region with two proline-phenylalanine (2 PF) motifs KPFRKLNPF in an unstructured flexible loop near the G-

domain (Daumke et al., 2007) (Fig 3.1A). This unstructured KPFRKLNPF region was proposed to link EHD2 dimer pairs through interactions with neighboring EH domains (Daumke et al., 2007). This is a unique situation where the NPF motif is intrinsic and the NPF-EH interaction facilitates the self-interaction of the protein. Recent studies have firmly established that N-terminus plays an indispensable role in targeting of EHD2 to the membrane (Shah et al., 2014), and provide support for the notion that both PF motifs play an important role in EHD2 localization and function (Moren et al., 2012). However, the degree to which both of these closely situated PF motifs impact EHD2 function, and particularly how each motif affects dimerization and interactions with binding partners remains obscure. The function of the PF motifs in the unstructured loop in EHD proteins is further complicated because while EHD2 has two PF motifs in its KPFRKLNPF sequence, the other three EHD paralogs all contain only one PF motif (Fig 3.1B); either a KPF or RPF motif at the N-terminal side of the unstructured loop. Indeed, both EHD1 and EHD3 have a NAF motif (instead of NPF), whereas EHD4 has a SRF motif. In this study, we sought out to determine the significance of the two proline-phenylalanine (2PF): KPF and NPF motifs of EHD2 for their ability to dimerize, interact with protein partners and localize to caveolae. To test the role of the NPF motif, we generated an EHD2 NPF-to-NAF mutant to mimic the homologous sequences of EHD1 and EHD3. While the EHD2 NPF-to-NAF mutant lost its dimerization potential and protein binding ability, this motif had little impact on its localization within the cell. On the other hand, mutation of the NPF motif to APA had little or no impact on dimerization or partner binding, but shunted EHD2 localization away from the PM primarily to the nucleus. We further examined EHD1 as a representative of the other three more closely related EHDs; we found that a single RPF motif of EHD1 is essential for (i) its dimerization, (ii) interaction with protein partners, and (iii) its localization to tubular recycling endosomes.

Overall, our data suggests that the phenylalanine residue in the NPF motif is

crucial for EHD2 localization to the PM, whereas the proline residue is essential for EHD2 dimerization and binding. These studies support the recently proposed model suggesting that the EHD2 N-terminal region regulates the availability of the unstructured loop for interactions with neighboring EHD2 dimers, thus promoting oligomerization.

12 Results

12.1 Alteration of the EHD2 NPF motif to NAF impairs dimerization and binding with interaction partners, but does not affect EHD2 localization

EHD2 is the only member of EHD protein family that homo-dimerizes but does not hetero-dimerize (Simone et al., 2013). This homo-dimerization potential may be required for interaction with NPF-containing protein binding partners. Accordingly, our goal was to first determine the requirement of the EHD2 NPF motif for homo-dimerization (Fig 3.1A and 3.1B). By selective two-hybrid binding assay, we demonstrated that while wild-type EHD2 proteins homo-dimerize, they were not capable of interacting with wild-type EHD1, EHD3 or EHD4 (Fig 3.2A). On the other hand, when the EHD2 NPF motif was perturbed by introduction of a point mutation to convert to a NAF, the homo-dimerization was no longer observed. EHD2 binds to specific subsets of NPF-containing protein partners through its EH domain. Indeed, wild-type EHD2 interacted with Syndapin2, but not MICAL-L1, even though both proteins contain NPF motifs followed by acidic clusters (Fig 3.2B). *In vivo*, co-immunoprecipitation analysis between EHD2 and Syndapin2 further confirmed the interaction (Fig 3.4A and Table 3.1). However, the EHD2 NPF-to-NAF mutant lost its ability to interact with Syndapin2, suggesting that the EHD2 NPF motif is required for both homo-dimerization and for protein partner binding. Despite these data in yeast two-hybrid binding studies, the NAF mutant retained its ability to bind to Syndapin2 by co-immunoprecipitation, suggesting

the involvement of bridging proteins in the cells (Fig 3.4A and Table 3.1). In our previous studies, we demonstrated that interaction of EHD2 with PIP2 is responsible for recruitment of EHD2 to the PM and is independent of interaction with other binding partners through its EH domain (Simone et al., 2013). Recent findings by Moren et al. showed that EHD2 caveolar localization was independent of its protein-binding EH domain, which supports our conclusions (Moren et al., 2012). Furthermore, using selective yeast two-hybrid studies we have demonstrated that the EH domain is not required for EHD2 (or EHD1) homo-dimerization (Fig 3.2A-3.2C). Accordingly, we wanted to test the impact of EHD2 NPF-to-NAF modification on the localization of protein to the PM. Confocal microscopy demonstrated that both wild type and EHD2 NPF-to-NAF primarily displayed PM localization (Fig 3.3C and 3.3D). We further analyzed both the wild-type and EHD2 NPF-to-NAF mutant using Structured Illumination Microscopy (SIM) and also observed both the wild-type and EHD2 NPF-to-NAF mutant partially co-localized to structures positive for caveolin-1 (Fig3.3E-3.3H); (see insets, asterisks indicate transfected cells). These data support the notion that the EHD2 NPF motif plays an essential role in EHD2 dimerization and binding to NPF-containing interaction partners. However, normal localization of EHD2 to the PM and colocalization of EHD2 with caveolae are not contingent upon the homo-dimerization ability of EHD2.

12.2 Modification of the EHD2 NPF motif to APA induces loss of PM localization, but does not affect homo-dimerization and interactions with binding partners.

Recent studies by Moren et al. demonstrated that upon mutating the coding sequence of phenylalanine 128 of the EHD2 NPF motif (see Fig 3.1A) to that of alanine (NPF-to-NPA), there is no significant effect on the subcellular localization of EHD2 (Moren et al., 2012). In order to recapitulate the homologous sequence found in both EHD1 and EHD3, we decided to initially disrupt the NPF motif by substituting the proline

for alanine (NPF-to-NAF). Furthermore, we aimed at delineating the functional role of EHD2 when the proline residue of its NPF motif is left intact. To this aim, we assessed homo-dimerization of EHD2 NPF-to-APA mutants as well as its interaction with Syndapin2 (Fig 3.5A and 3.5B). Surprisingly, unlike the EHD2 NPF-to-NAF mutant, the NPF-to-APA mutants retained both homo-dimerization and binding to Syndapin2. On the other hand, despite normal dimerization and binding, EHD2 NPF-to-APA displayed a dramatic relocation to the nucleus (Fig 3.5D). Previous studies have demonstrated EHD2 has a bipartite nuclear localization sequence and many cells display a portion of their EHD2 in the nucleus (Fig 3.5C) (Pekar et al., 2012). Interestingly, the NPF-to-APA mutant displayed primarily nuclear localization (Fig 3.5D). Accordingly, despite the yeast two-hybrid binding data, we were unable to detect EHD2 NPF-to-APA interactions with Syndapin2 by co-immunoprecipitation, likely due to the mislocalization of the mutant exclusively to the nucleus (Fig 3.4A and Table 3.1). However, Moren et al. used a subtler EHD2 NPF-to-NPA mutant (rather than NPF-to-APA) and did not report such relocation to the nucleus (Moren et al., 2012). Consequently, we resolved to compare the functional role of EHD2 NPF-to-APA mutant to EHD2 NPF-to-NPA. As demonstrated in (Fig 3.6A and 3.6B), similar to the APA mutant, EHD2 NPF-to-NPA continued to homo-dimerize and interact with Syndapin2. Furthermore, the subcellular distribution of EHD2 NPF-to-NPA was also similar to that of EHD2 NPF-to-APA, with most of the mutant localizing to the nucleus and diminished localization at the PM (compare Fig 3.6C and 3.6D). Taken together, these results suggested that the NPF phenylalanine residue contributes to the localization of EHD2 at the PM, either by preserving EHD2 at the PM, or by possibly preventing it from transporting to or exporting out of the nucleus. However we cannot entirely reconcile the differences we observed in EHD2 NPF-to-NPA localization (largely nuclear) compared to those of Moren et al. (Fig 3.6B; GFP-EHD2 F128A) (Moren et al., 2012), where EHD2 continued to localize at the caveolae on the

PM and a small fraction was localized to the nucleus (data not shown).

12.3 The phenylalanine residue of NPF motif plays a key role in the PM localization of EHD2.

We then proceeded to analyze the precise role of phenylalanine 128. To this end, we engineered an EHD2 NPF-to-NPY mutant. The rationale behind this mutant protein was that tyrosine is structurally the closest residue to phenylalanine, with the only difference being the additional hydroxyl group on the aromatic ring. Interestingly, the EHD2 NPF-to-NPY mutant displayed an intermediate cellular distribution (compare Fig 3.7A with 3.7C and 3.7D). Although PM association was not abrogated, a significant portion of the EHD2 NPF-to-NPY EHD2 mutant was observed in the nucleus. However, the NPF-to-NPY mutant continued to homo-dimerize with wild-type EHD2 and maintains binding with Syndapin2 (Fig 3.4A and Table 3.1). We further posited that the spatial localization of phenylalanine 128 is essential for its function in facilitating EHD2 localization, primarily to the PM. Accordingly, we engineered EHD2 NPF-to-NFP by swapping the proline and phenylalanine residues at positions 127 and 128. Although some EHD2 was clearly localized to the PM, the majority of this NFP had a subcellular localization in the nucleus (Fig 3.7F). Furthermore, the NPF-to-NFP mutant failed to either homo-dimerize or interact with Syndapin2 (Fig 3.4A and Table 3.1). These data firmly establish that the position of phenylalanine at residue 128 within the unstructured loop is highly significant and is crucial for the localization to the PM.

12.4 Disruption of the EHD2 KPF motif induces relocalization of EHD2 to the nucleus, but does not alter its oligomerization and partner binding ability.

Previous studies by Moren et al. have implicated the role of the KPF motif in the unstructured loop of EHD2 (Fig 3.3A and 3.3B) in caveolar binding and stable

association of EHD2 with the membrane (Moren et al., 2012). However, the impact of the KPF motif on EHD2 homo-dimerization and interactions with binding partners has not been studied. Hence, we turned our attention to the KPF motif of EHD2 and accordingly, we generated EHD2 KPF-to-APA or KPF-to-KAF mutants. EHD2 KPF-to-APA or KPF-to-KAF mutants had no effect on dimerization or binding to Syndapin2 (Fig 3.9A–3.9D) by yeast two-hybrid binding assays. Both KPF mutants reduced the level of EHD2 on the PM and increased the level of nuclear-localized EHD2 compared to wild-type EHD2 (Fig 3.9E–3.9G). Furthermore, the co-immunoprecipitation experiments did not detect binding between the mutants and Syndapin2, possibly because the mutants are localized primarily to the nucleus (as opposed to the normal PM localization). Overall, these studies help elucidate the complicated functional role for the unstructured loop and its two PF motifs, which is in agreement with both the initial structural model (Daumke et al., 2007; Moren et al., 2012) and the revised model (Shah et al., 2014) proposed for dimer pair PF-EH domain interactions and EHD2 oligomerization (see model for further elaboration Fig 3.12).

12.5 A single EHD1 PF motif (RPF) controls its homo- and hetero-dimerization, binding to interaction partners, and localization to Tubular Recycling Endosomes (TRE).

Given that EHD1 contains a single PF motif, namely the RPF motif that aligns with the EHD2 KPF motif (see Fig 3.1B), we evaluated the role of this motif on EHD1 dimerization and partner binding. The ability to homo-and heterodimerize was lost in the EHD1 RPF-to-APA mutant (Fig 3.10A). Furthermore, EHD1 RPF-to-APA had abrogated binding to MICAL-L1, and decreased binding to Syndapin2 (Fig 3.10B). Moreover, the typical subcellular localization of EHD1 to an array of tubular and vesicular recycling endosomes (Fig 3.10C) was lost and the EHD1 RPF-to-APA mutant was mislocalized to

the cytoplasm (Fig 3.10D). These data suggest that the single RPF motif in EHD1 is necessary and sufficient to successfully carry out functions that the dual NPF and KPF motifs present in EHD2 execute.

12.6 The NAF motif of EHD1 is dispensable for homo- or hetero-oligomerization, and for its association with binding partners.

Additionally, since EHD1 has a “non-functional” NAF motif aligned with the NPF motif of EHD2 (depicted in Fig 3.1B) we hypothesized that the EHD1 NAF motif would still function if its lone existing PF motif (RPF) was impaired. To begin with, we engineered EHD1 NAF-to-NPF mutants as a control and showed that as expected, homo- and hetero-dimerization along with MICAL-L1 and Syndapin2 binding remained stable (Fig 3.11A and 3.11B). Next, we generated double mutants where the EHD1 RPF motif was disrupted (RPF-to-APA) and the NAF motif was ‘corrected’ to NPF. Compared to the EHD1 RPF-to-APA single mutants, which lost all of their dimerization and protein interactions, the additional NAF-to-NPF mutation partially rescued homo- dimerization (Fig 3.11C) and binding to MICAL-L1 (Fig 3.11D).

12.7 The EHD1 RPF motif is essential for receptor recycling.

To evaluate the functional role of the EHD1 RPF motif, we utilized a siRNA approach combined with rescue by transient transfection. As demonstrated, EHD1-siRNA treatment was successful in depleting more than 90% of EHD1 from HeLa cells (Fig 3.12C). HeLa cells on coverslips were either mock-treated or treated with EHD1-siRNA and subjected to “pulse-chase” experiments with fluorochrome-labeled transferrin (Tf-568). After the pulse with Tf-568, both mock- and EHD1-siRNA treated cells exhibited a similar subcellular distribution of internalized Tf-568 (Fig 3.12C). However, after a 20 min chase, mock-treated cells had recycled most of their internalized Tf-568

back to the PM, whereas EHD1 depleted cells exhibited significant accumulation of Tf in the ERC (compare Fig 3.12B with control Fig 3.12A). This accumulation was ‘rescued’ in EHD1-depleted cells where a siRNA-resistant form of the wild-type EHD1 (siEHD1) had been transfected (Fig 3.12D and 3.12E; see yellow borders for transfected cells). However, when an EHD1 RPF-to-APA mutant (that is mislocalized to the cytoplasm) was reintroduced into EHD1-depleted cells, the Tf and its receptor remained accumulated in the perinuclear region of the cell (Fig 3.12F and 3.12G; see yellow borders for transfected cells). Quantification of these data (from 3 independent experiments) demonstrated that wild-type EHD1 rescued the recycling defect in > 85% of the EHD1-depleted cells whereas the RPF-to-APA mutant displayed less than 15% rescue (Fig 3.12H).

13 Discussion

Despite being the first EHD protein whose crystal structure was solved (Daumke et al., 2007), and important structural characterizations of its interaction with membranes (Shah et al., 2014) and its recruitment by PI(4,5)P2 to the PM (Simone et al., 2013), nonetheless many of the mechanistic aspects by which EHD2 functions have remained obscure. In this study we have identified intriguing differences in the function of the proline and phenylalanine residues of the NPF motif that is found within the KPFRKLNPF region of the unstructured loop present in the G-domain of EHD2 (Fig 3.1A). Our data suggest that the phenylalanine is crucial for localization of EHD2 to the PM. Indeed, mutation of this residue leads to the translocation and accumulation of EHD2 in the nucleus. On the other hand, mutation of the proline residue of this same NPF motif not only leads to loss of homo-oligomerization and presumed loss of oligomerization, but also loss of protein partner binding without impacting localization to the PM. Given the elegant structural studies that propose the PF-EH domain interactions

for EHD2 oligomerization (Shah et al., 2014), how does our data contribute to the current model? Shah and colleagues recently proposed that upon membrane sensing, the EHD2 N-terminus disrupts its interaction with the unstructured loop in the G-domain and moves away (illustrated in Fig 3.11A–3.11B), rendering the KPFRKLNPF unstructured loop in a conformation that is competent for interactions with EH domains of nearby EHD2 dimer pairs, thus promoting oligomerization and caveolar localization (Fig 3.11C) (Shah et al., 2014).

Based on this model, we hypothesize that the N-terminus of the EHD2-NPF-to-NPA mutant (Fig 3.11D), even in the presence of the membrane, may not completely detach from the G-domain regions flanking the unstructured loop and thus fail to insert properly into the PM. We rationalize that under conditions where membrane binding is partially impaired, the string of lysine residues in the EHD2 helical domain, which perform the dual function of being membrane contact sites (Daumke et al., 2007) and a bipartite nuclear localization sequence (Pekar et al., 2012), are now free to act in the latter capacity and facilitate the transport of EHD2 to the nucleus. The support for this notion also comes from previous studies that have described the role of EHD2 as a transcriptional repressor (Pekar et a., 2012). On the other hand, we predict that with the EHD2 NPF-to-NAF mutant, the EHD2 N-terminus is nonetheless freed from the G-domain to interact with the PM. However, despite its correct localization to the PM, the NAF motif abrogates EH binding and consequently the dimerization and oligomerization potential is impaired. Overall, our study provides support and additional novel details that further clarify the complex structural model of EHD2 localization, membrane binding, protein binding, dimerization, oligomerization, and function.

Figure 3.1. EHD protein domain architecture and sequence homology.

(A) The Eps15 Homology Domain (EHD) proteins have a conserved domain architecture comprised of four domains: two helical domains, a G-domain, and a C-terminal EH domain. The G domain of EHD2 contains an unstructured loop containing the following amino acid sequence, KPFRKLNPF, which is required for oligomerization. **(B)** The four EHD isoforms share 67–86% residue identity. The amino acid sequence alignment of the unstructured loop for all four EHDs (see green frame) shows that only EHD2 has two successive PF motifs: NPF and KPF, whereas the other EHD proteins have only one PF motif.

Figure 3.1

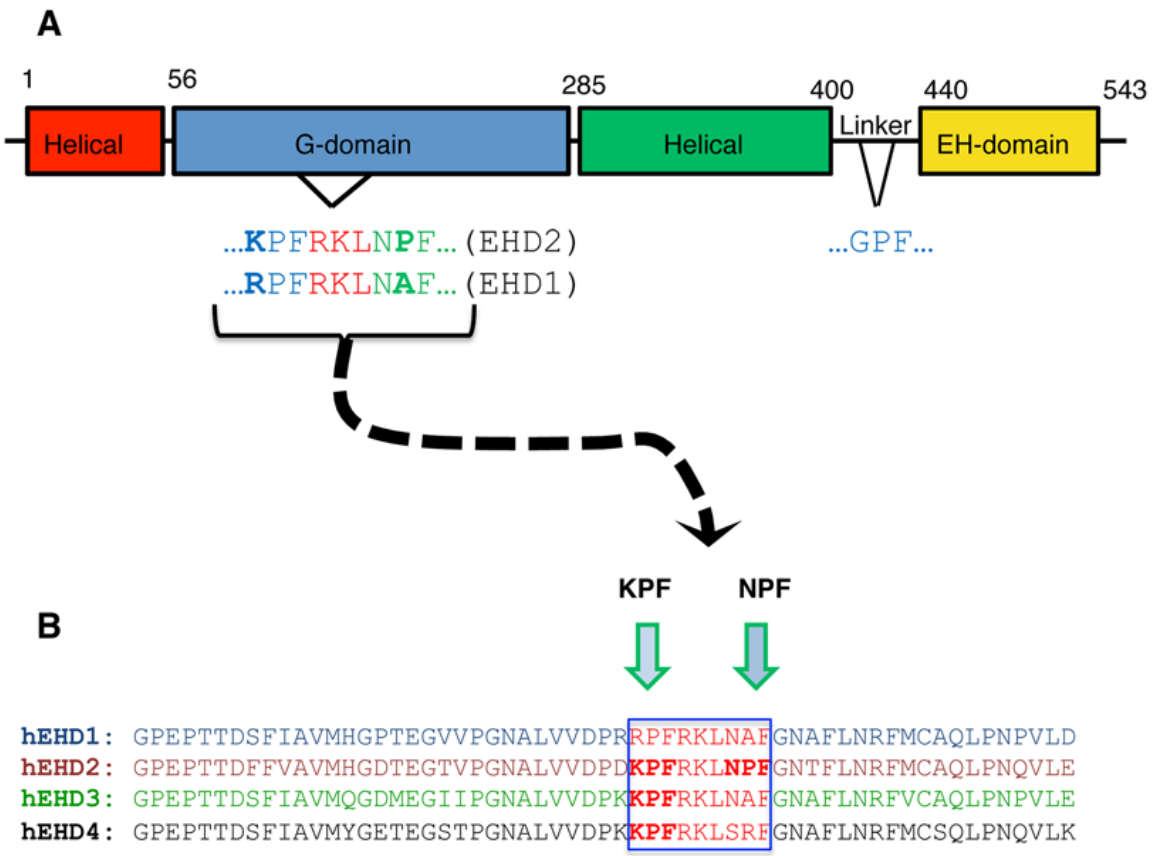
A
1
56
285
400
440
543
Helical
G-domain
Helical
Linker
EH-domain
...KPFRKLNPF... (EHD2)
...RPFRKLNAF... (EHD1)
...GPF...
KPF
NPF
B
hEHD1: GPEPTTDSFIAVMHGPTEGVVPGNALVVDPRRPFRKLNAFGNAFLNRFMCAQLPNPVLD
hEHD2: GPEPTTDFFVAVMHGDTEGTVPGNALVVDPDKPFRKLNPFGNTFLNRFMCAQLPNQVLE
hEHD3: GPEPTTDSFIAVMQGDMEGIIPGNALVVDPKKPFRKLNAFGNAFLNRFVCAQLPNPVLE
hEHD4: GPEPTTDSFIAVMYGETEGSTPGNALVVDPKKPFRKLSRFGNAFLNRFMCSQLPNQVLK

Figure 3.2 EHD dimerization requires an intact α-helical region, but not the presence of EH domains.

(A) Schematic diagram of EHD2 domain organization. **(B–C)** Yeast were co-transformed with Gal4bd fusion constructs: Gal4bd-p53 (control), EHD2 (wt), EHD2 (ΔEH) along with Gal4ad-SV40 (control), EHD2 (wt), EHD2 (ΔEH), EHD1 (wt), EHD1 (ΔEH), and EHD1. All co-transformants were plated on non-selective (+HIS) and selective (-HIS) media.

Figure 3.2

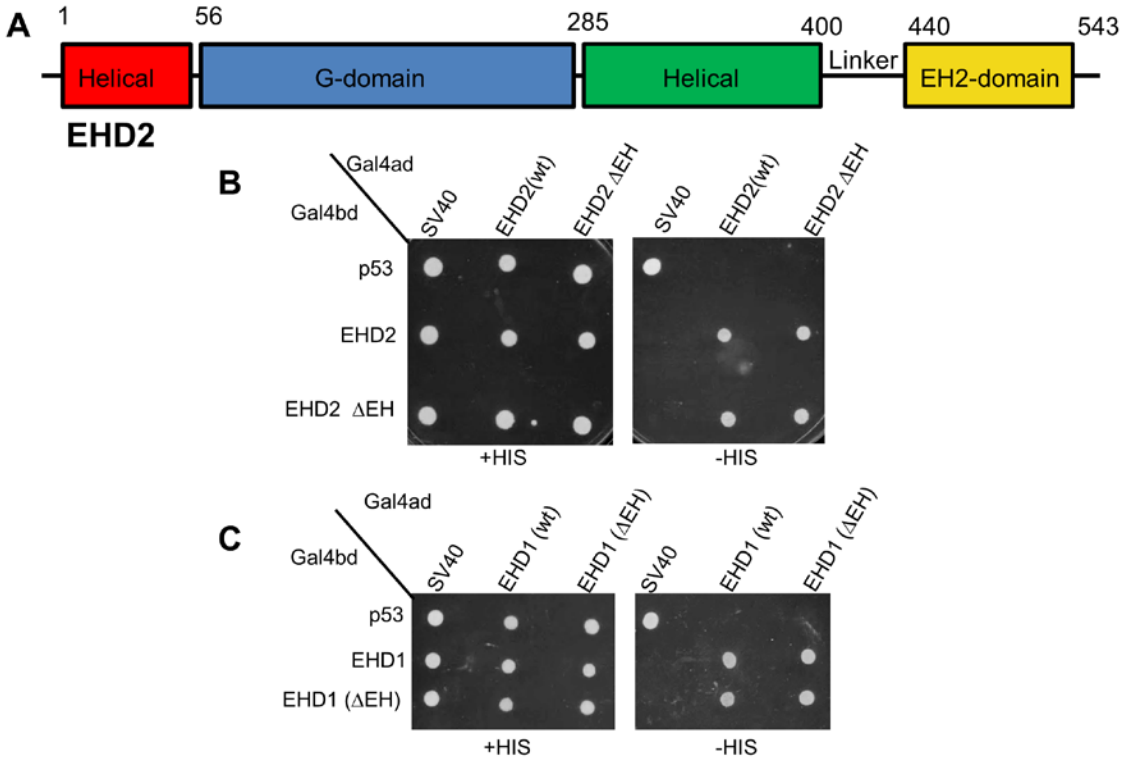
A
1
56
285
400
440
543
Helical
G-domain
Helical
Linker
EH2-domain
EHD2
B
Gal4ad
Gal4bd
SV40
EHD2(wt)
EHD2 ΔEH
SV40
EHD2(wt)
EHD2 ΔEH
p53
EHD2
EHD2 ΔEH
+HIS
-HIS
C
Gal4ad
Gal4bd
SV40
EHD1 (wt)
EHD1 (ΔEH)
SV40
EHD1 (wt)
EHD1 (ΔEH)
p53
EHD1
EHD1 (ΔEH)
+HIS
-HIS

Figure 3.3. Modification of the EHD2 NPF motif to NAF impairs dimerization and binding with interaction partners, but does not affect EHD2 localization.

(A) *S. cerevisae* yeast were co-transformed with the following Gal4 binding domain (Gal4bd) fusion constructs (see Materials and Methods): p53 (control), -Syndapin-2 and -MICAL-L1. Gal4 activating domain (Gal4ad) fusion constructs were either-SV40 (control), -EHD2 (wt) or -EHD2 (NPF-to-NAF). Cotransformants were plated on non-selective (+HIS) and selective (-HIS) agar plates. **(B)** As in (A), co-transformation was with Gal4bd-p53 (control), -EHD2 (wt), -EHD1 (wt), -EHD3 (wt), and -EHD4 (wt) and with Gal4ad-SV40 (control), -EHD2 (wt) and -EHD2 (NPF-to-NAF). (C–H) HeLa cells were grown on coverslips, transfected with GFP-myc-EHD2 (wt) (C, E, G) or with GFP-myc-EHD2 (NAF-to-NPF) (D, F, H) and fixed. **(C–D)** are transfected cells imaged by confocal microscopy, whereas **(E–H)** does Structured Illumination Microscopy (SIM) obtain micrographs. Asterisks indicate transfected cells. Bar;10 μm.

Figure 3.3

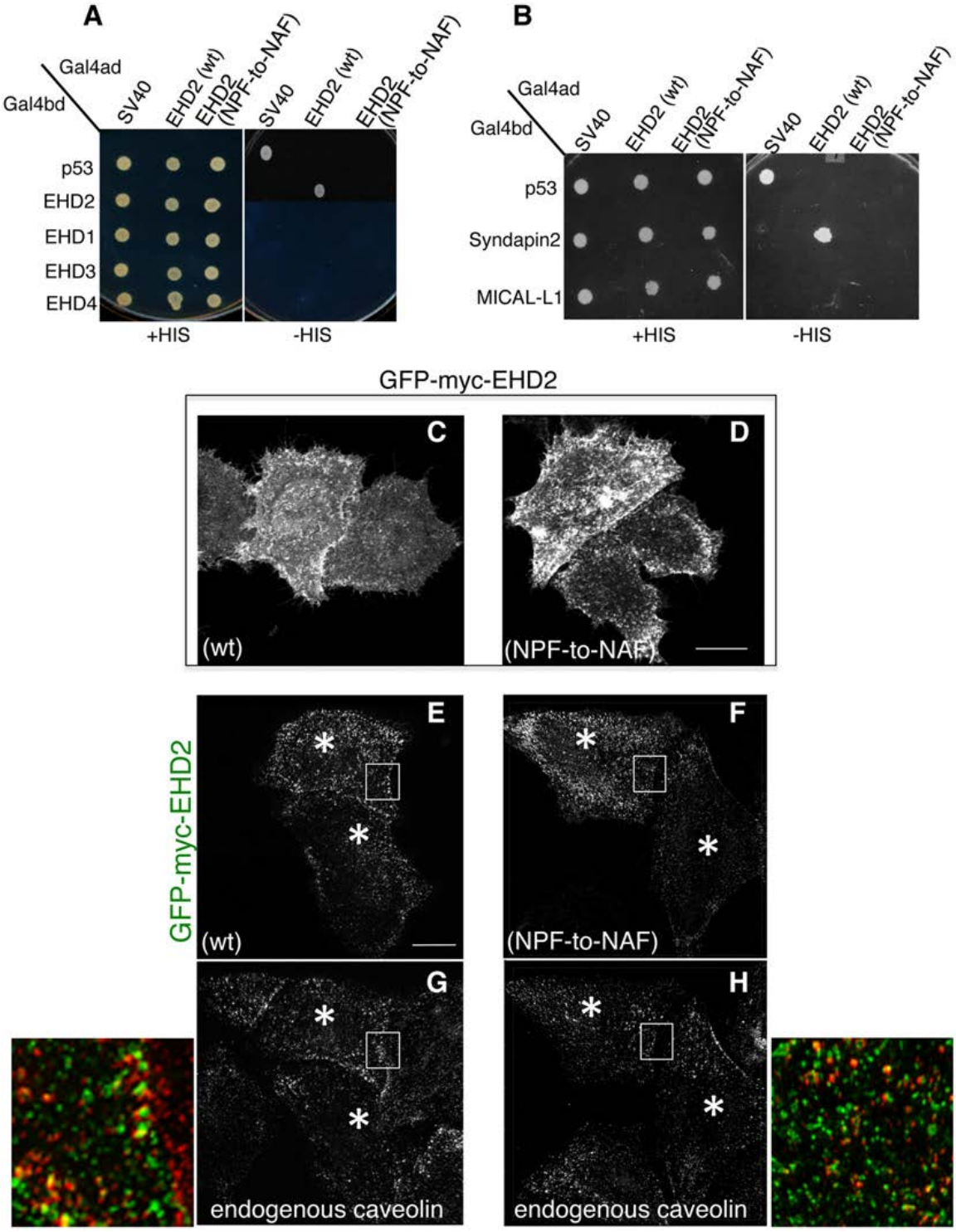
A
Gal4ad
Gal4bd
SV40
EHD2 (wt)
EHD2 (NPF-to-NAF)
p53
EHD2
EHD1
EHD3
EHD4
+HIS
-HIS
B
Gal4ad
Gal4bd
SV40
EHD2 (wt)
EHD2 (NPF-to-NAF)
p53
Syndapin2
MICAL-L1
+HIS
-HIS
GFP-myc-EHD2
C
D
(wt)
(NPF-to-NAF)
GFP-myc-EHD2
E
F
(wt)
(NPF-to-NAF)
G
H
endogenous caveolin
endogenous caveolin

Figure 3.4 Co-immunoprecipitation of EHD2 and mutant EHD2 proteins with Syndapin2.

(A and B) HeLa cells were transfected with either GFP-Myc-EHD2, or GFP-Myc-EHD2 mutants (NPF-to-NAF, NPF-to-APA, KPF-to-KAF, KPF-to-APA), lysed 24 h later and subjected to immunoprecipitation with antibodies against Syndapin2. Separated proteins were transferred onto nitrocellulose and then immunoblotted with anti-EHD2 antibodies. Input contains 5% of the total lysate immunoprecipitated.

Figure 3.4

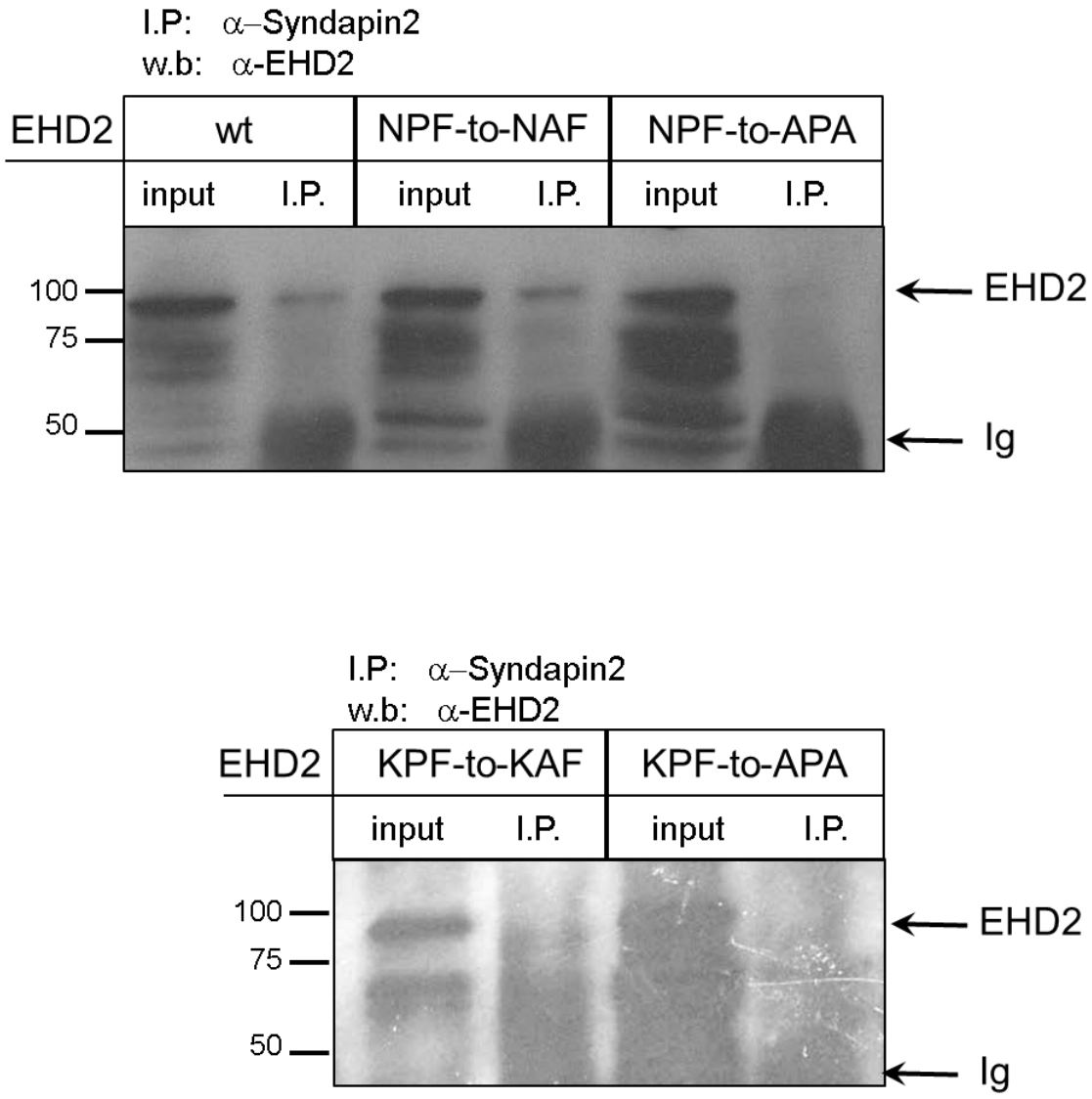
I.P: α–Syndapin2
w.b: α-EHD2
EHD2
wt
NPF-to-NAF
NPF-to-APA
input
I.P.
input
I.P.
input
I.P.
100
75
50
EHD2
Ig
I.P: α–Syndapin2
w.b: α-EHD2
EHD2
KPF-to-KAF
KPF-to-APA
input
I.P.
input
I.P.
100
75
50
EHD2
Ig

Figure 3.5. Modification of the EHD2 NPF motif to APA induces loss of plasma membrane localization, but does not affect interactions with binding partners.

(A) *S. cerevisae* yeast were co-transformed with thefollowing Gal4bd fusion constructs: Gal4bd-p53 (control), -Syndapin-2 and -MICAL-L1 along with Gal4ad fusion constructs Gal4ad-SV40 (control), -EHD2 (wt.) and -EHD2 (NPF-to-APA). **(B)** As in (A) cotransformationwas with Gal4bd fusion constructs: Gal4bd-p53 (control), -EHD2 (wt) along with Gal4ad fusion constructs: Gal4ad-SV40 (control), -EHD2 (wt) and -EHD2 (NPF-to-APA). Co-transformants from A-B were plated on non-selective (+HIS) and selective (-HIS) agar plates. **(C–D)** HeLa cells were grown on coverslips, transfected with GFP-myc-EHD2 (C) or GFP-myc-EHD2 NPF-to-APA (D). Bar; 10 μm.

Figure 3.5

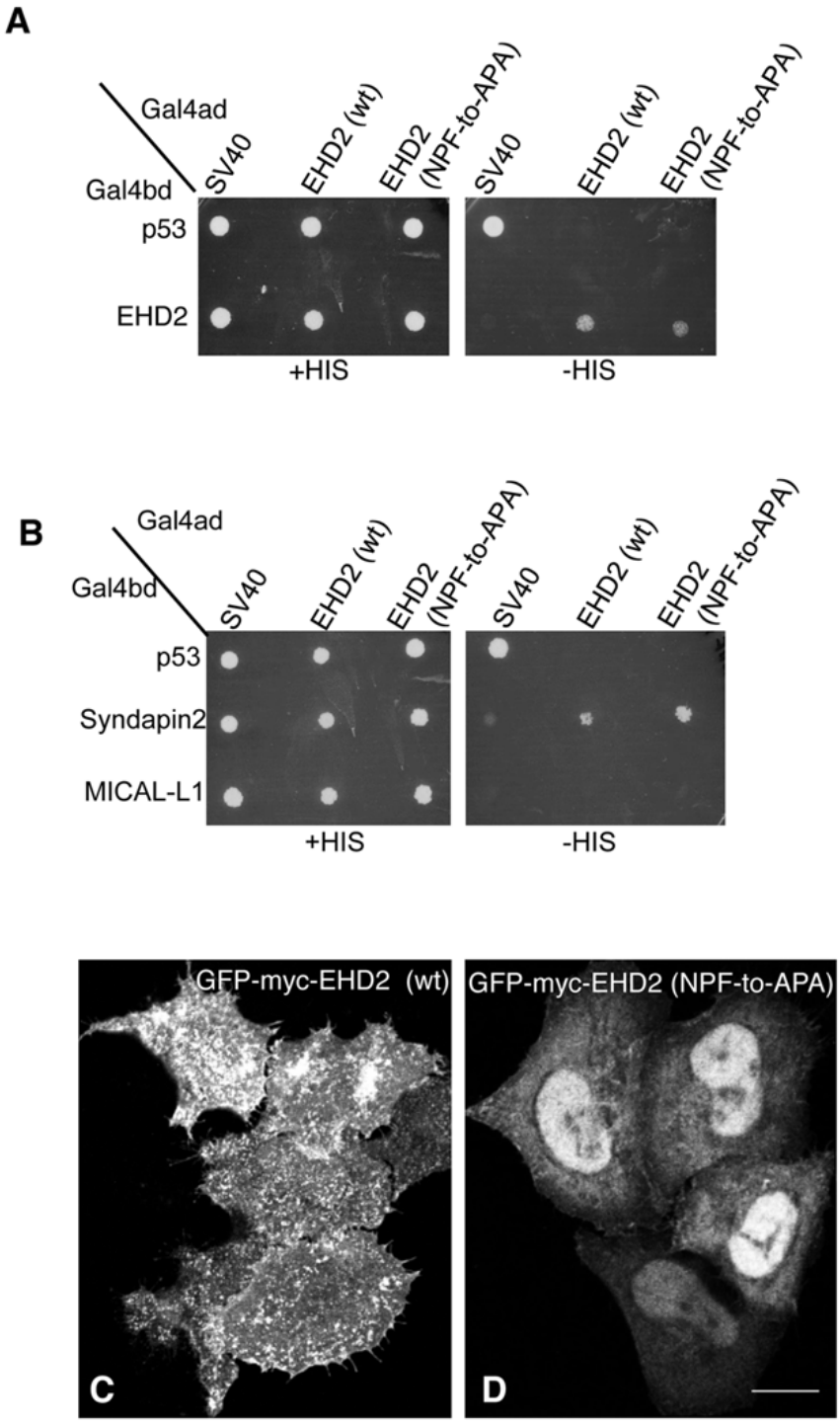
A
Gal4ad
Gal4bd
SV40
EHD2 (wt)
EHD2 (NPF-to-APA)
SV40
EHD2 (wt)
EHD2 (NPF-to-APA)
p53
EHD2
+HIS
-HIS
B
Gal4ad
Gal4bd
SV40
EHD2 (wt)
EHD2 (NPF-to-APA)
SV40
EHD2 (wt)
EHD2 (NPF-to-APA)
p53
Syndapin2
MICAL-L1
+HIS
-HIS
GFP-myc-EHD2 (wt)
GFP-myc-EHD2 (NPF-to-APA)
C
D

Figure 3.6. The NPF phenylalanine residue is responsible for the plasma membrane localization of EHD2.

(A) *S. cerevisae* yeast were co-transformed with the following Gal4bd fusion constructs: Gal4bd-p53 (control), -Syndapin-2 and -MICAL-L1 along with Gal4ad fusion constructs: Gal4ad-SV40 (control), -EHD2 (wt) and -EHD2 (NPF-to-NPA)**. (B)** As in (A)**,** yeast were co-transformed with the Gal4bd fusion constructs: Gal4bd-p53 (control), -EHD2 (wt) alongwith Gal4ad fusion constructs: Gal4ad-SV40 (control), -EHD2 (wt.) and -EHD2 (NPF-to-NPA). Co-transformants were plated on non-selective (+HIS) andselective (-HIS) agar plates. **(C–I)** HeLa cells were grown on coverslips and transfected with: (C) GFP-myc-EHD2 (wt), (D) GFP-myc-EHD2 (NPF-to-NPA), **(E)** GFP-myc-EHD2 (NPF-to-NPY), **(F)** GFP-myc-EHD2 (NPF-to-NPA), **(G)** GFP-myc-EHD2 (NPF-to-NFP). Bar;10 µm.

Figure 3.6

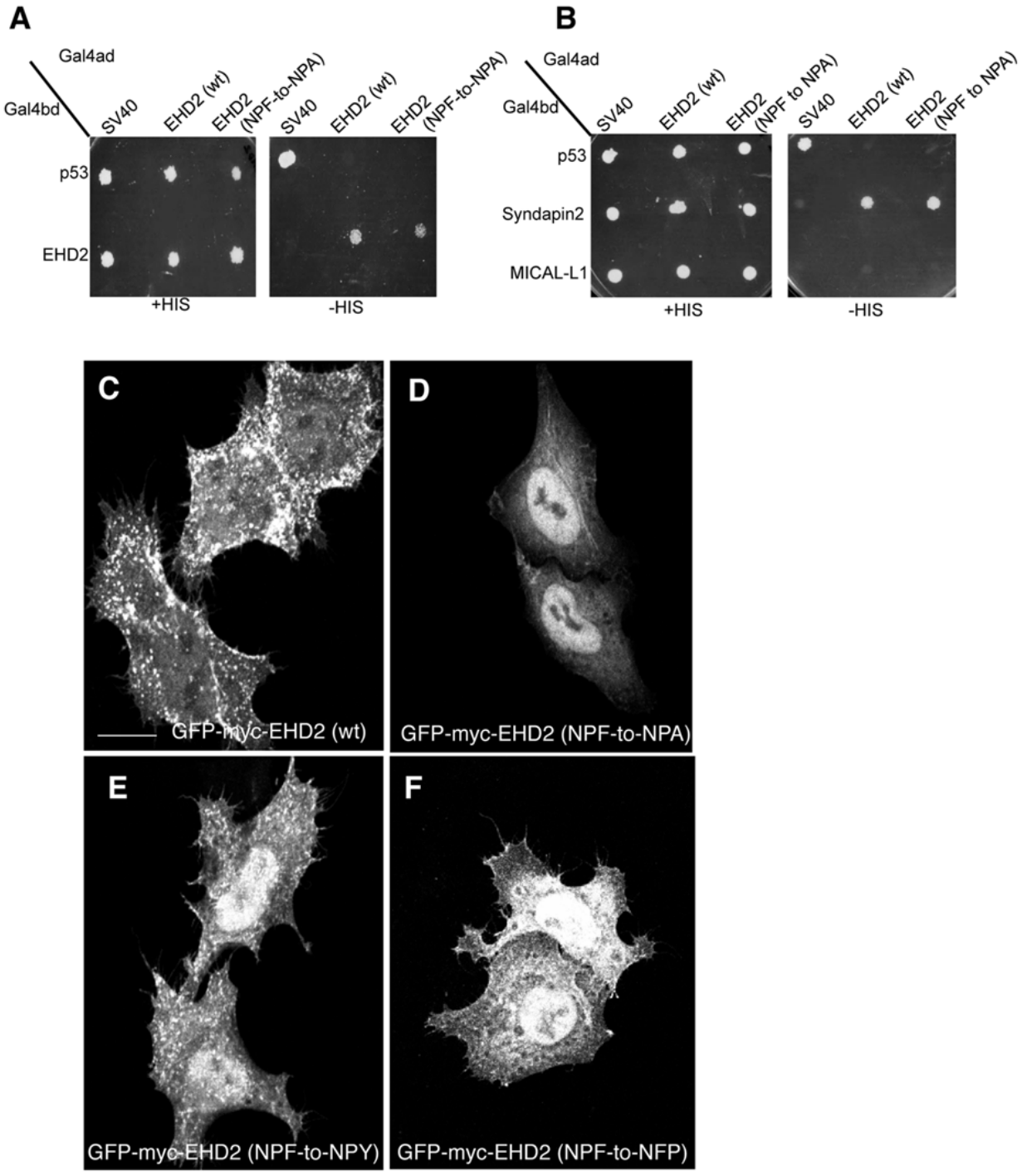
A
Gal4ad
Gal4bd
SV40
EHD2 (wt)
EHD2 (NPF-to-NPA)
SV40
EHD2 (wt)
EHD2 (NPF-to-NPA)
p53
EHD2
+HIS
-HIS
B
Gal4ad
Gal4bd
SV40
EHD2 (wt)
EHD2 (NPF to NPA)
SV40
EHD2 (wt)
EHD2 (NPF to NPA)
p53
Syndapin2
MICAL-L1
+HIS
-HIS
C
GFP-myc-EHD2 (wt)
D
GFP-myc-EHD2 (NPF-to-NPA)
E
GFP-myc-EHD2 (NPF-to-NPY)
F
GFP-myc-EHD2 (NPF-to-NFP)

Figure 3.7. Wild-type and EHD2 NPF-to-NPY homo-dimerize and interact with Syndapin2, whereas EHD2 NPF-to-NFP does not.

(A and B) *S. cerevisae* yeast were co-transformed with the following Gal4bd fusion constructs: Gal4bd-p53 (control), -EHD2 (wt), -MICAL-L1, and -Syndapin-2 along with Gal4ad-SV40 (control), -EHD2 (wt), -EHD2 NPY, and EHD2 NFP. Co-transformants in were plated on non-selective (+HIS) and selective (-HIS) agar plates.

Figure 3.7

A

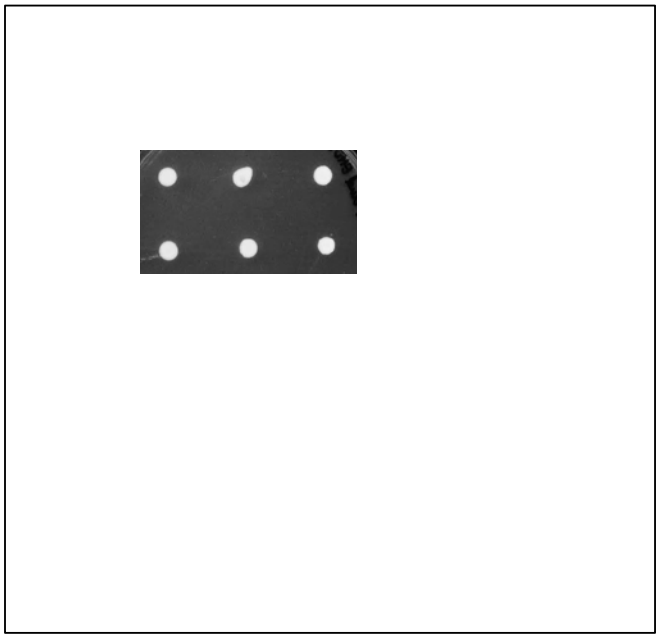

B

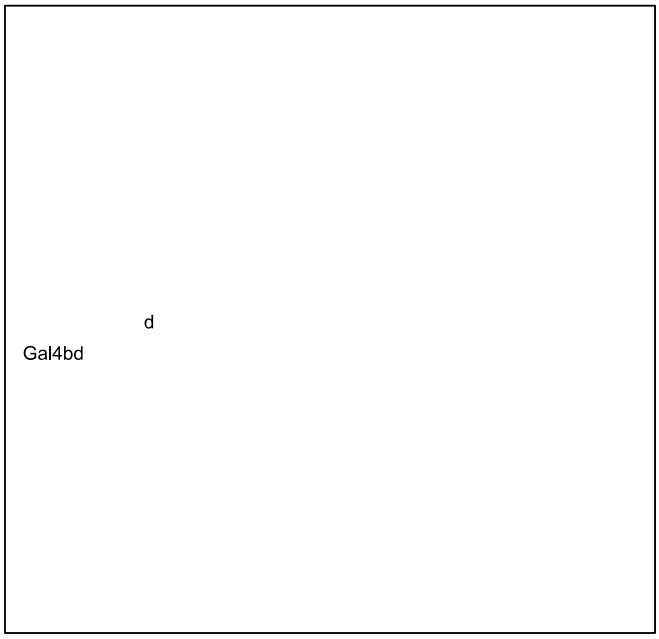

Figure 3.8. Disruption of the EHD2 KPF motif induces relocalization of EHD2 to the nucleus, but does not alter its binding ability.

(A–D) *S.cerevisae* yeast were co-transformed with the following Gal4bd fusion constructs: Gal4bd-p53 (control), -Syndapin-2 and -MICAL-L1 along with Gal4ad fusion constructs: Gal4ad-SV40 (control), -EHD2 (wt), -EHD2 (KPF-to-APA) and—EHD2 (KPF-to-KAF). Co-transformants were plated on non-selective (+HIS) and selective (-HIS) media. **(E–H)** HeLa cells were grown on coverslips, transfected with GFP-myc-EHD2 (wt) **(E),** GFP-myc-EHD2 (KPF-to-APA) **(F),** or GFP-myc-EHD2 (KPF-to-KAF) **(G)** and analyzed by confocal microscopy. Bar;10 μm.

Figure 3.8

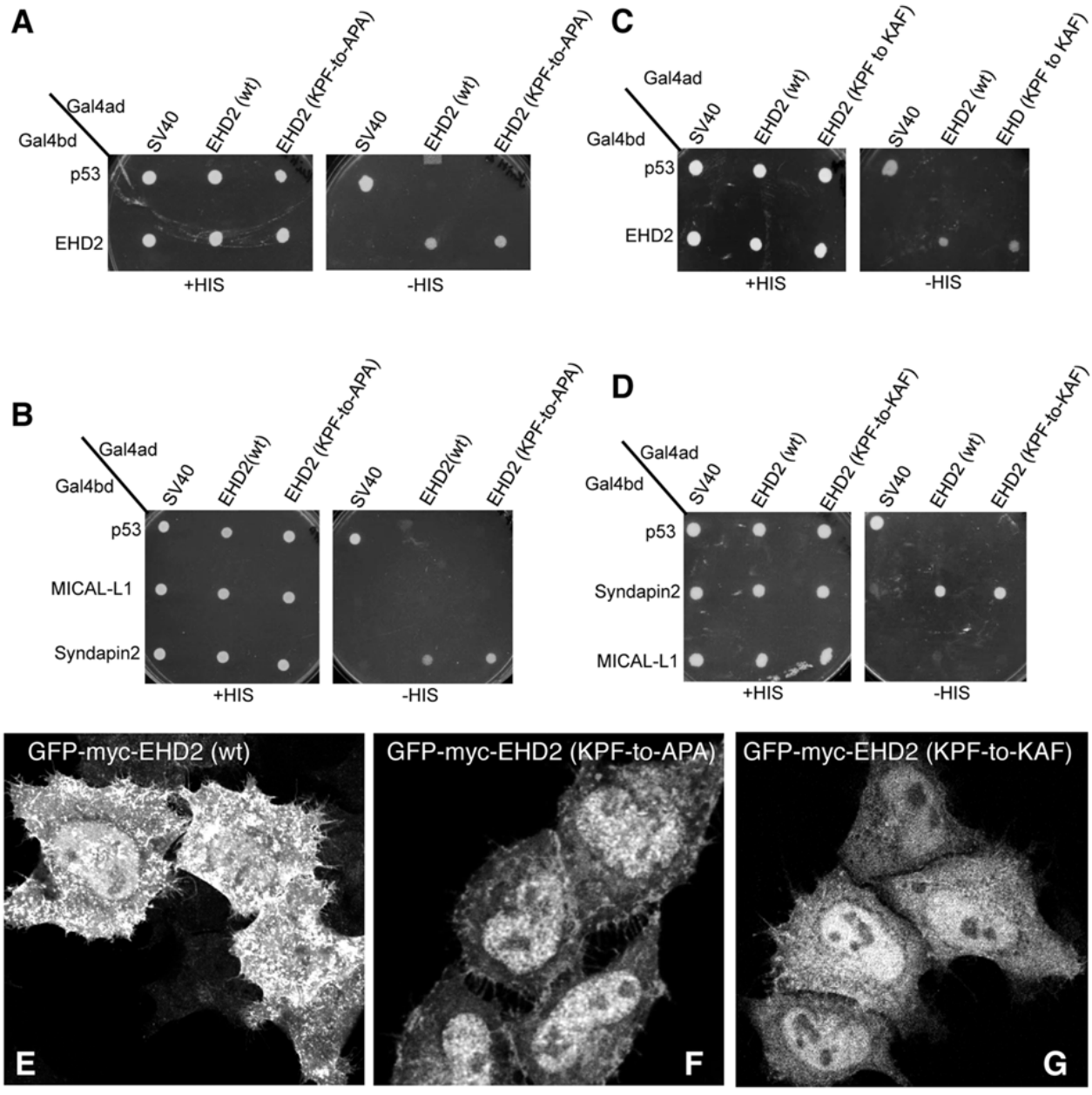
A
Gal4ad
Gal4bd
SV40
EHD2 (wt)
EHD2 (KPF-to-APA)
p53
EHD2
+HIS
-HIS
C
EHD2 (KPF to KAF)
EHD (KPF to KAF)
B
EHD2(wt)
MICAL-L1
Syndapin2
D
GFP-myc-EHD2 (wt)
GFP-myc-EHD2 (KPF-to-APA)
GFP-myc-EHD2 (KPF-to-KAF)
E
F
G

Figure 3.9. A single EHD1 PF motif (RPF) controls its homo- and hetero-dimerization, binding to interaction partners, and localization to Tubular Recycling Endosomes (TRE).

(A) *S. cerevisae* yeast were co-transformed with Gal4bd fusion constructs: Gal4bd-p53 (control), -Syndapin-2 and-MICAL-L1 along with Gal4ad-SV40 (control), -EHD1 (wt.) and -EHD1 (RPF-to-APA). **(B)** As in (A)**,** yeast were co-transformed with Gal4bd-p53 (control),-EHD1 (wt), -EHD3 (wt), -EHD4 (wt), along with Gal4ad-SV40 (control), -EHD1 (wt) and EHD1 (RPF-to-APA). Co-transformants from A-B were plated on non-selective (+HIS) and selective (-HIS) agar plates. **(C–D)** HeLa cells were grown on coverslips, transfected with GFP-myc-EHD1 (wt) **(C),** GFP-myc-EHD1 (RPF-to-APA) (D, arrows point to TRE). Bar; 10 µm.

Figure 3.9

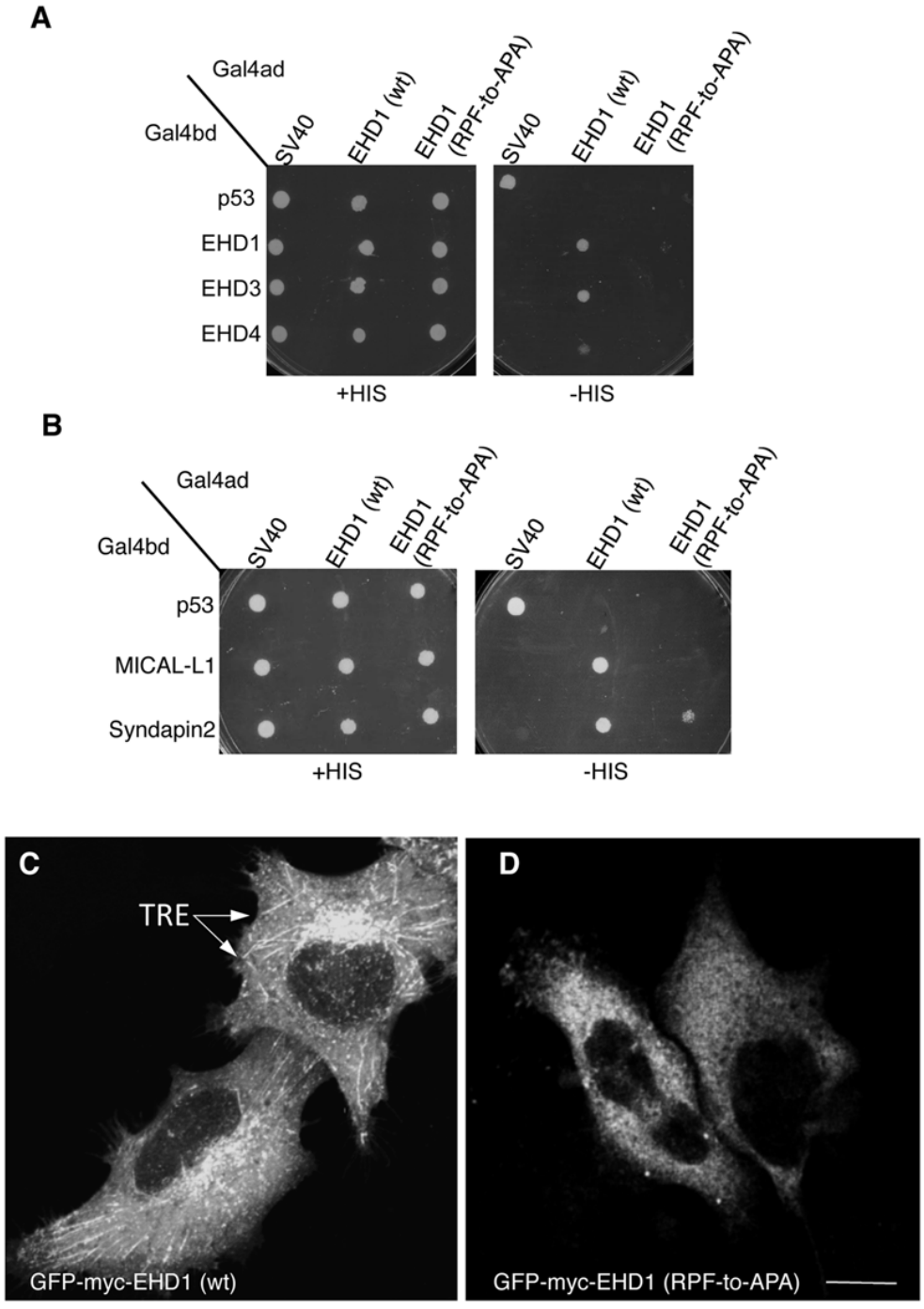
A
Gal4ad
Gal4bd
SV40
EHD1 (wt)
EHD1 (RPF-to-APA)
SV40
EHD1 (wt)
EHD1 (RPF-to-APA)
p53
EHD1
EHD3
EHD4
+HIS
-HIS
B
Gal4ad
Gal4bd
SV40
EHD1 (wt)
EHD1 (RPF-to-APA)
SV40
EHD1 (wt)
EHD1 (RPF-to-APA)
p53
MICAL-L1
Syndapin2
+HIS
-HIS
C
TRE
GFP-myc-EHD1 (wt)
D
GFP-myc-EHD1 (RPF-to-APA)

Figure 3.10. The NAF motif of EHD1 is dispensable for homo- or hetero oligomerization, and for its association with binding partners.

(A) *S. cerevisae* yeast were co-transformed with the following Gal4bd fusion constructs: Gal4bd-p53 (control), -MICAL-L1, and -Syndapin-2 along with Gal4ad-SV40 (control), -EHD1 (wt.) and -EHD1 (NAF to NPF). **(B)** As in **(A),** yeast were co-transformed withGal4bd-p53 (control), -EHD1 (wt), -EHD2 (wt), -EHD3 (wt) and -EHD4 (wt), along with Gal4ad-SV40 (control), -EHD1 (wt) and -EHD1 (NAF-to-NPF). **(C)** As in (A), yeast were co-transformed with Gal4bd-p53 (control), -EHD1 (wt), -EHD3 (wt), and -EHD4 (wt), along with Gal4ad-SV40 (control), -EHD1 (wt) and -EHD1 (NAF-to-NPF). **(D)** Yeast were co-transformed with Gal4bd-p53 (control), -Syndapin-2, and -MICAL-L1, along with Gal4ad-SV40 (control), EHD1 (wt) and EHD1 (NAF-to-NPF). Co-transformants in A-D were plated on non-selective (+HIS) and selective (-HIS) agar plates.

Figure 3.10

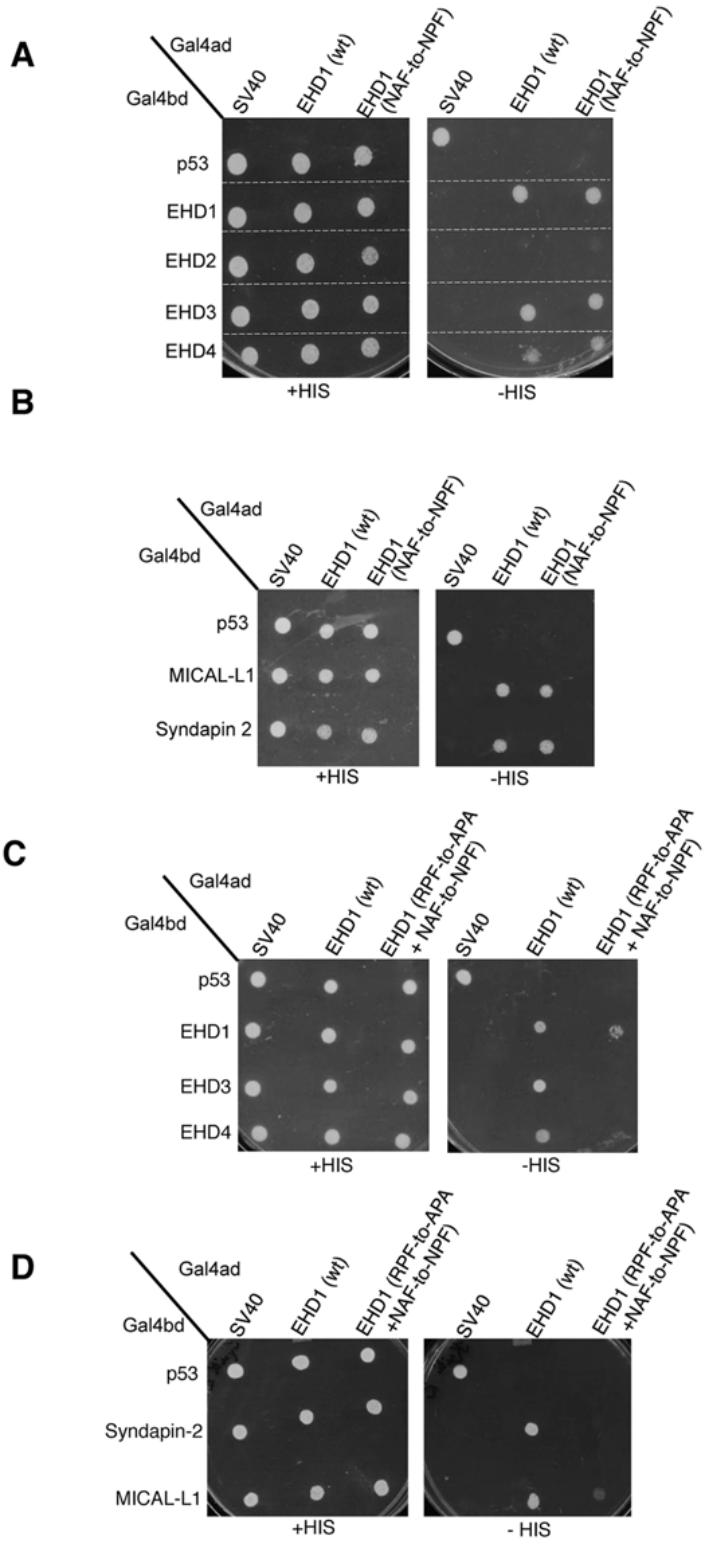
A
Gal4ad
Gal4bd
SV40
EHD1 (wt)
EHD1 (NAF-to-NPF)
p53
EHD1
EHD2
EHD3
EHD4
+HIS
-HIS
B
MICAL-L1
Syndapin 2
C
EHD1 (RPF-to-APA + NAF-to-NPF)
D
Syndapin-2
- HIS

Figure 3.11. The EHD1 RPF motif is essential for receptor recycling.

(A–B) HeLa cells grown on coverslips were mock-treated **(A)** or treated with EHD1-siRNA **(B–F).** For A–B, After a 30 min. serum-starvation, cells were allowed to uptake Tf-568 for 15 min., and then chased in complete media for 15 min. to permit Tf- 568 recycling to the PM. **(C)** Immunoblot analysis of Mock- or EHD1-siRNA-treated cells depicting levels of actin (control) or EHD1. **(D–G)** During the EHD1-siRNA treatment, cells were transfected with the siRNA-resistant EHD1 constructs: siRNA-res-GFP-myc-EHD1 (wt) in **(D),** and siRNA-res-GFP-myc- EHD1 (RPF-to-APA) in **(F).** Following serum-starvation, Tf-568 was internalized for 15 min , and chased in complete media for 15 min. Note the typical concentration of Tf in the ERC in untransfected cells treated with EHD1-siRNA. **(H)** Quantitative analysis of 100 cells from 3 independent experiments as in **(E and G).** Cells that recycled Tf-568 (“empty of Tf”) were scored and calculated as % of total cell number, and portrayed with standard error bars. Stars represent significance of $p < 0.01$ (one star) or $p < 0.05$ (three stars) for one-way ANOVA tests. Bar; 10 μm.

Figure 3.11

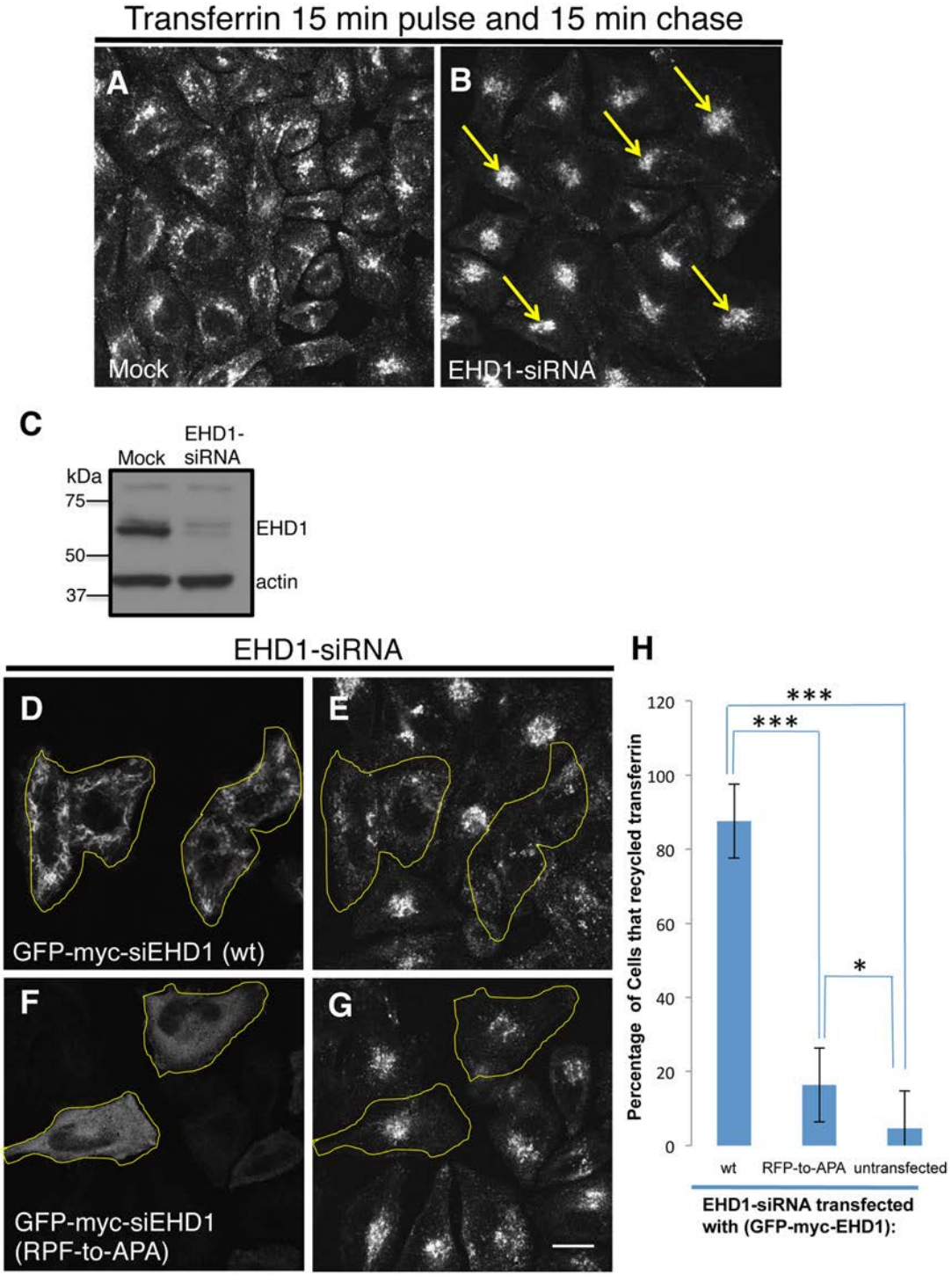
Transferrin 15 min pulse and 15 min chase
A
Mock
B
EHD1-siRNA
C
Mock
EHD1-siRNA
kDa
75
50
37
EHD1
actin
EHD1-siRNA
D
GFP-myc-siEHD1 (wt)
E
F
GFP-myc-siEHD1 (RPF-to-APA)
G
H
***
***
*
Percentage of Cells that recycled transferrin
120
100
80
60
40
20
0
wt
RFP-to-APA
untransfected
EHD1-siRNA transfected with (GFP-myc-EHD1):

Figure 3.12. Model for the role of the EHD2 unstructured KPFRKLNPF motif in subcellular localization.

(A) In the absence of PIP2-containing membrane, the N-termini interact with regions flanking the unstructured loops (U.L.) of EHD2 dimer pairs. **(B)** PIP2-binding by the N-terminus facilitates a-8 helical binding to the membrane and frees the U.L. **(C)** the U.L. NPF motif is now capable of interacting with an EH domain of a neighboring EHD2 dimer pair, inducing oligomerization. **(D)** For EHD2 NPF-to-NPA mutants, we hypothesize that the N-terminus may not insert into membranes, thus preventing the U.L. from oligomerizing and maintaining the lysine residues on α-8 helix free to serve as a nuclear localization sequence.

Figure 3.12

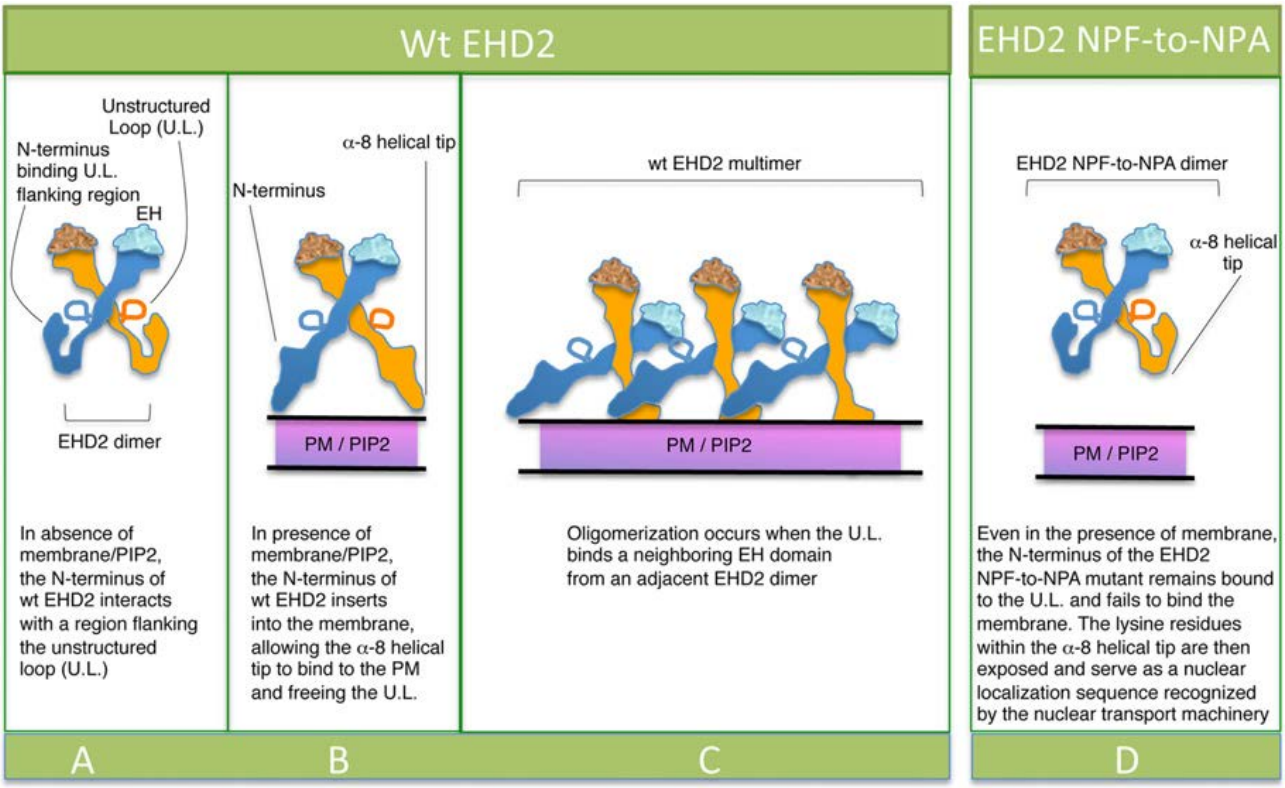
Wt EHD2
EHD2 NPF-to-NPA
Unstructured Loop (U.L.)
N-terminus binding U.L. flanking region
EH
EHD2 dimer
α-8 helical tip
N-terminus
PM / PIP2
wt EHD2 multimer
PM / PIP2
EHD2 NPF-to-NPA dimer
α-8 helical tip
PM / PIP2
In absence of membrane/PIP2, the N-terminus of wt EHD2 interacts with a region flanking the unstructured loop (U.L.)
In presence of membrane/PIP2, the N-terminus of wt EHD2 inserts into the membrane, allowing the α-8 helical tip to bind to the PM and freeing the U.L.
Oligomerization occurs when the U.L. binds a neighboring EH domain from an adjacent EHD2 dimer
Even in the presence of membrane, the N-terminus of the EHD2 NPF-to-NPA mutant remains bound to the U.L. and fails to bind the membrane. The lysine residues within the α-8 helical tip are then exposed and serve as a nuclear localization sequence recognized by the nuclear transport machinery
A
B
C
D

Table 3.1 Comparison of wild-type EHD2 and mutants in homo-dimerization, Syndapin2-binding and sub-cellular localization.

EHD2	Binding to Syndapin2 by 2 Hybrid	Binding to Syndapin2 by I.P.	Localization by (I.F)
KPF RKL NPF	+	+	PM
K**A**F	+	-	nuclear
AP**A**	+	-	nuclear
N**A**F	-	+	PM
AP**A**	+	-	nuclear
NP**Y**	+	N.D.	PM / nuclear
N**FP**	-	N.D.	nuclear

Chapter IV

EHD3 Protein Is Required for Tubular Recycling Endosome Stabilization, and an Asparagine-Glutamic Acid Residue Pair within Its Eps15 Homology (EH) Domain Dictates Its Selective Binding to NPF Peptides

The following chapter has been published in JBC. 2016 Jun 24; 291(26):13465-78

14 Introduction

Endocytic trafficking entails internalization, sorting, degradation, and recycling of macromolecules in mammalian cells (Conner and Schmid, 2003). These processes are not only essential for the maintenance of cellular homeostasis, but also key for the regulation of a variety of cellular events, including nutrient uptake, cell adhesion, cell migration, cell polarity, cytokinesis, and signal transduction. In this process, receptors encounter ligands, the ligand-receptor complexes are internalized and enter peripheral sorting endosomes (SE). While some receptors are fated for degradation, others are sent back to plasma membrane to partake in subsequent rounds of internalization (Jovic et al., 2009). The latter process is known as endocytic recycling, which can occur through distinct routes (Grant and Donaldson, 2009). Recycling of receptors can occur either directly from the SE known as fast recycling, or indirectly in a process known as slow recycling (Hao and Maxfield, 2011). For slow recycling process, receptors are first trafficked to a transitory perinuclear organelle adjacent to the microtubule-organizing center (MTOC), known as the endocytic recycling compartment (ERC) (Maxfield and McGraw, 2004).

The ERC maintains cargo segregation, acquired upon exit from the SE, and serves as a focal point for vesicular transport to the plasma membrane (Xie et al., 2016). The Rab family of small GTP-binding family proteins has been characterized as a key group of endocytic regulatory proteins. Rabs interact with specific effectors to promote SNARE-based membrane fusion. Although each pathway requires a multitude of regulatory proteins, Rab4 and Rab11 are among the best-characterized Rabs involved in fast and slow recycling, respectively (van der Sluijs et al., 1992; Ullrich et al., 1996). The ERC is comprised of an array of dynamic, densely situated yet largely independent, tubular and vesicular recycling endosomes (Jovic et al., 2009). Efficient recycling via the ERC relies on the integrity of an elaborate network of elongated, non-symmetrical

endosomes known as tubular recycling endosomes (TRE) (Jovic et al., 2009). Furthermore, TREs are defined as tubular endosomes with lengths of up to 10 µm and diameters of up to 200 nm. Some of the TRE also originate from the SE and carry cargo towards the ERC (Xie et al., 2015). Current models hold that fission of TRE containing receptors facilitates the formation of vesicle carriers that carry receptors to be recycled back to the plasma membrane (Cai et al., 2012; Cai et al., 2013; Cai et al., 2014; Daumke et al., 2007).

Because of the significance of TRE in membrane recycling, a growing number of studies have addressed a family of proteins known as the C-terminal Eps15 homology domain (EHD1–4) proteins that have been implicated in TRE generation and fission and control membrane recycling (Naslavsky and Caplan, 2011). EHD1–4 are hetero/ homodimeric ATPases that oligomerize and influence endocytic trafficking by promoting the bending and/or fission of endosomes. Despite their high level of amino acid identity (70–86%), the EHD proteins display unique subcellular localizations and regulate distinct steps of endocytic trafficking. EHD3 and EHD1 are the most closely related members of the EHD protein family. While EHD1 induces the vesiculation of TRE, EHD3 supports the process of membrane tubulation (Cai et al., 2013). The hallmark of EHDs is their C-terminal Eps15 Homology (EH) domain (Grant and Caplan, 2008; Naslavsky and Caplan, 2005). These EH domains contain a positively charged electrostatic surface that preferentially binds to proteins containing NPF motifs followed by acidic residues (Kieken et al., 2007; Kieken et al., 2009; Kieken et al., 2010). Over the last decade, we have identified a variety of important EHD interaction partners, including molecules interacting with CasL-like1 (MICAL-L1) and Syndapin2 (Giridharan et al., 2013; Sharma et al., 2009). Both MICAL-L1 and Syndapin2 are essential for TRE biogenesis, and impaired recruitment of either protein to membranes causes a failure of TRE biogenesis and impaired recycling (Giridharan et al., 2013; Sharma et al., 2009). Indeed, TRE

biogenesis involves the recruitment of MICAL-L1 and Syndapin2 to membranes that have a high local concentration of phosphatidic acid, a lipid essential for TRE biogenesis (Giridharan et al., 2013; Sharma et al., 2009). MICAL-L1 and Syndapin2 stably interact with each other via the Syndapin2 Src homology 3 (SH3) domain and proline rich domain (PRD) of MICAL-L1. The MICAL-L1-Syndapin2 interaction leads to membrane bending and tubulation. EHD3 is subsequently recruited to these membranes through the interaction of its EH domain with the NPF motifs of MICAL-L1 and/or Syndapin2. A recent model holds that EHD1, thereafter, joins this complex on TRE, where it binds to both MICAL-L1 and Syndapin2, possibly replacing EHD3 within the complex to perform fission and give rise to newly formed vesicles (Cai et al., 2013). Given the 86% amino acid identity between EHD1 and EHD3, and their disparate cellular functions, these findings frame new questions of outstanding biological significance. What is the mechanism by which two such remarkably similar proteins play opposing roles in the generation and vesiculation of TRE? What is the specific role of EHD3 in the process of TRE biogenesis? Does EHD3 directly promote membrane bending as proposed or via its interaction with Syndapin2 (Daumke et al., 2013)? Or does EHD3 play a role in stabilization of MICAL-L1-Syndapin2 complexes on the TRE membranes? Here we demonstrate that EHD3 is dispensable for TRE biogenesis but that it serves to stabilize these membrane structures after their generation. Moreover, we characterize the molecular and atomic bases for the differential interactions of EHD1 and EHD3 with binding partners, providing new insights into their differential roles in vesiculation and tubulation, respectively.

15 Results

15.1 TRE can undergo biogenesis in the absence of EHD3.

We have previously delineated the model required for TRE biogenesis (Giridharan et al., 2013) and our previous studies have lent support for the disparate functions of EHD3 and EHD1 in the tubulation and vesiculation of TRE, respectively (Cai et al., 2013). Furthermore, our prior studies have established a strong consensus for the function of EHD1 as membrane vesiculator (Cai et al., 2012; Cai et al., 2013; Cai et al., 2014; Jakobsson et al., 2011), recruited by MICAL-L1 and Syndapin2, with the latter proteins directly implicated in TRE biogenesis (Giridharan et al., 2013). Although, both MICAL-L1 and Syndapin2 interact directly with EHD3, the mechanistic role of EHD3 in the process of TRE biogenesis is not well understood (Cai et al., 2013; Naslavsky and Caplan, 2011). Because chronic depletion of EHD3 leads to a loss of MICAL-L1 and Syndapin2 containing TRE, we hypothesized two potential distinct roles for EHD3 in TRE biogenesis: 1) EHD3 is directly required for membrane bending and TRE generation (together with Syndapin2 and MICAL-L1), or 2) EHD3 is not required for TRE biogenesis but instead serves to stabilize TRE when they have been generated. To address the definite functional role of EHD3 in TRE biogenesis, we took advantage of our recent observation that, upon treatment of cells with 100 μM phospholipase D (PLD), inhibitors CAY 10593 and CAY 10594 (that inhibit the two mammalian PLD isoforms PLD1 and PLD2, respectively) for 30 minutes (min) at 37°C, TRE were depleted (Giridharan et al., 2013). Remarkably, upon washout of the inhibitors, we observed a rapid, synchronized de-novo regeneration of TRE (“burst”), providing us with a system to temporally monitor the role of EHD3 in acute TRE biogenesis. However, it was not feasible to repeat these findings using a different PLD inhibitor, 5-fluoro-2-indolyl des-chlorohalopemide (FIPI) because previous studies indicated that washout of this PLD inhibitor led to only 29% recovery of PLD activity 1 h after removal (Su et al., 2009). As depicted in Fig 4.1, 75% of mock-treated cells contained some visible MICAL-L1 decorated TRE (Mock; the pretreatment, mean tubule area is quantified in Fig. 4.2 B).

We have demonstrated in our previous studies that upon PLD inhibitor treatment, TRE were almost entirely depleted from cells. Interestingly, we made an important discovery that within a 20 min washout of the inhibitor, there was a dramatic recovery of TRE levels that returned to (and exceeded) baseline levels (Fig. 4.1, Mock; quantified in Fig. 4.2B). In comparison, as anticipated, upon Syndapin2 knockdown (efficiency of knockdown calculated at 90%, Fig. 1B), no TRE were observed either at pretreatment, after inhibitor treatment, or even following washout (20 min to 1 h). Therefore, this further validated the essential role of Syndapin2 in TRE biogenesis (Fig. 4.1,Syndapin2-KD; quantified in Fig. 4.2B). On the other hand, although no TRE were observed upon chronic EHD3 knockdown (efficiency of knockdown calculated at ≈85%, Fig. 4.1B), or following PLD inhibitor treatment, a dramatic recovery of TRE was documented following inhibitor washout (20 min to 1 h). This indicated that TRE can be generated even in the absence of EHD3 (Figs. 4.1 and 4.2, EHD3-KD; quantified in Fig 4.2B). Upon EHD1 knockdown in pretreated cells (efficiency of knockdown calculated at 90%, Fig. 4.1B), we observed increased TRE, consistent with its role in TRE vesiculation (Fig. 4.1, EHD1-KD; quantified in Fig. 4.2B). As expected, PLD inhibitors depleted cellular TRE in EHD1 knockdown cells, but upon inhibitor washout, TRE levels were recovered (Fig. 4.1), (EHD1-KD; quantified in Fig. 4.2B). Collectively, these data suggest that Syndapin2 is required for the generation of MICAL-L1-decorated TRE, but EHD3 (and EHD1) is not required.

15.2 EHD3 stabilizes TRE

EHD3 interacts directly with both MICAL-L1 and Syndapin2. This interaction has lent support to the notion that EHD3 may be required to stabilize MICAL-L1 and Syndapin2 on the membranes, consequently stabilizing TRE. To assess the role of EHD3 in TRE stabilization over time, we monitored TRE levels 1–6 h after PLD inhibitor

washout in the absence of EHD3 (Fig. 4.2). In mock-treated cells, for up to 6 h after PLD inhibitor washout, the mean TRE levels continued to increase (Mock, quantified in Fig. 4.2B). In cells lacking Syndapin2, as anticipated, no TRE generation was observed at any point of time (Syndapin2 KD, quantified in Fig. 4.2 B). Surprisingly, despite the recovery of TRE generation in EHD3-depleted cells immediately following PLD inhibitor washout, within 1–4 h after washout, the TRE levels in these cells declined to pretreatment levels (EHD3-KD, quantified in Fig. 4.2B). These data suggest that although EHD3 is dispensable for TRE generation, it is required for continued stability of tubules within the cell. It is important to note, however, that these data do not provide direct information on the TRE half-life, because TRE could be undergoing multiple cycles of biogenesis and vesiculation in the course of recovery. On the other hand, in the absence of EHD1, as anticipated, the mean TRE area continued to increase 4–6 h after washout, further validating the role for EHD1 in TRE vesiculation (EHD1-KD, quantified in Fig. 4.2B). The transient recovery of TRE in EHD3 knockdown cells immediately following PLD inhibitor washout, followed by loss of TRE over 4–6 h time point post-washout and are consistent with a role for EHD3 in stabilization of TRE but indicate that this protein is not involved directly in TRE biogenesis.

15.3 The EH domain is responsible for the differential function of EHD1 and EHD3 in vesiculation and TRE stabilization, respectively.

Despite 86% amino acid identity between EHD3 and EHD1, remarkably these proteins display distinct cellular functions. Given that their ATP hydrolysis domains are highly conserved, and that the two proteins differentially interact with partners through their EH domains, we hypothesized that the EH domains may determine whether these proteins affect TRE stabilization or vesiculation. To evaluate the role of the EH domain in the stabilization or vesiculation of TREs, we knocked down EHD3 or EHD1 in HeLa cells

and respectively, rescued the expression with wild-type EHD3 (Fig. 4.3, A and B), wild-type EHD1 (Fig. 4.3, A and C), or a chimera of EHD3 containing the EH domain of EHD1 (EHD3-EH1, Fig 4.3D) and assessed their effect on mean TRE length. Endogenous Syndapin2 served as a bona fide marker for TRE. Average TRE length is quantified in Fig. 4.3E, which demonstrates that, although wild-type EHD3 localized to long TRE that were positive for Syndapin2 (Fig. 4.3B and 4.3E), EHD1 was associated with shorter and more fragmented TRE (Fig. 4.3C, quantified in Fig. 4.3E). Surprisingly, upon the expression of the EHD3-EH1 chimera, the TRE observed were not only shorter than those observed for wild-type EHD3, but also for those observed for wild-type EHD1 (Fig. 4.3D, quantified in Fig. 4.3E). These data support the notion that the EH domains are the prime determinants of differential EHD function.

15.4 Comparison of the binding affinity of the EHD1 EH domain and EHD3 EH domain for a MICAL-L1 NPF peptide by isothermal titration calorimetry (ITC)

Because both EHD1 and EHD3 interact with some of the same NPF-containing proteins, such as MICAL-L1 (Sharma et al., 2009; Sharma et al., 2010) and Syndapin2 (Braun et al., 2005), we hypothesized that their EH domains may have different affinities for these binding partners. Our rationale was that, initially, EHD3 might reside on TRE to stabilize these structures. Subsequently, EHD1, with a potentially higher affinity for MICAL-L1 and Syndapin2, might interact with these proteins and replace EHD3 in the complex. Eventually, EHD1 might play a more predominant role on the TRE, possibly leading to the onset of vesiculation. Accordingly, we used ITC to test the affinity of EH1 and EH3 for a MICAL-L1 NPF peptide. As demonstrated, the K_D for EH1 binding was calculated at 23.2 ± 3.2 μM (Fig. 4.4), very close to that observed previously for an NPF peptide from Rabankyrin-5 (Zhang e al., 2012). Interestingly, the K_D for EH3 binding is not significantly different from that of EH1 and was measured at 17.8 ± 3.7 μM (Fig. 4.4).

Nevertheless, based on these data, we cannot rule out different binding affinities for full-length EHD proteins or differences in affinity resulting from additional *in vivo* interactions and/or localizations. However, it appears unlikely that the recruitment of EHD1 and EHD3 to TRE is governed by simple differences in the binding affinity.

15.5 Identification of EH1 and EH3 residues responsible for their differential interactions with NPF-containing partners.

Given the role of the EH domain in dictating EHD1 versus EHD3 function, we set out to determine the specific residues in the EH domain that mediate differential function. On comparing the amino acid sequences of EH1 and EH3, we identified fourteen distinct residues between EH1 and EH3 and further divided them into six potential stretches of non-conserved amino acid residues for analysis (Fig. 4.5A, white highlights). As readout of differential function, we assessed the ability of EHD1, EHD3, and the substitution mutants to interact with binding partners using a selective yeast two-hybrid assay. For instance, wild-type EHD1 normally interacts with both Rabankyrin-5 and MICAL-L1, whereas wild-type EHD3 binds only to MICAL-L1 (Sharma et al., 2009; Zhang et al., 2012; Sharma et al., 2010) (Fig. 4.5B). We methodically swapped all the six non-conserved regions of EH3 with those found in EH1 (Fig. 4.5A), and then tested whether the EHD3 mutant protein displayed gain-of-function binding to Rabankyrin-5 (Fig. 4.5C). As expected, the selective two-hybrid binding assay showed that wild-type EHD1 bound to both MICAL-L1 and Rabankyrin-5, whereas EHD3 interacted exclusively with MICAL-L1 (Fig. 4.5C, dashed red rectangle). Of the six substitution mutations to render the EH3 domain similar to EH1, remarkably, only the NE519AD change resulted in a gain-of-function binding to Rabankyrin-5 (Fig. 4.5C, dashed red rectangle). Additionally, each of the single mutants (EHD3 N519A and EHD3 E520D) were also capable of inducing gain-of-binding of EHD3 to Rabankyrin-5 (Fig. 4.5E). We performed complementary GST

pulldown experiments to demonstrate that the GST-EH3 NE519AD mutant gained the ability to bind to Rabankyrin-5 *in vitro*. However, the binding was not as robust as that seen with wild-type GST-EH1 (Fig. 4.5D). This suggested that other residues in EH1 might carry out additional regulation. Indeed, the reverse substitution mutation in EHD1 (EHD1 AD519NE, Fig. 4.5E) was insufficient to cause a loss of binding to Rabankyrin-5. This observation further hints at involvement of additional residues in the EH domain of EHD1 in regulating the interaction between EHD1 and Rabankyrin-5.

15.6 The EHD3 NE519AD mutant is not competent to rescue the impaired transferrin trafficking phenotype observed in EHD3 knockdown cells.

Given that the EHD3 NE519AD mutant is capable of binding to an EHD1-specific interaction partner (Rabankyrin-5), we next asked whether the mutant EHD3 retains EHD3 function, or if the NE-to-AD mutations render it incapable of carrying out the function of EHD3. To test this, we used previously characterized functional assays in which labeled transferrin (Tf-568) is internalized continuously for 20 min in the presence or absence of EHD3 (Naslavsky et al., 2006). As depicted in the representative micrographs, in mock treated cells, internalized Tf-568 displayed clear accumulation at the ERC (Fig. 4.6, A, C, and F) regardless of whether wild-type EHD3 or EHD3 NE519AD was transfected (Fig. 4.6, B–D and E–G). However, upon EHD3 knockdown, consistent with our previous observation (Naslavsky et al., 2006), Tf-568 failed to reach the ERC and instead was maintained in the periphery in somewhat enlarged endosomal structures (Fig. 4.6, I and L; untransfected cells without yellow borders). Reintroduction of wild-type EHD3 restored the function of EHD3, allowing Tf-568 to accumulate at the ERC (Fig. 4.6I transfected cells with yellow borders and arrows indicating ERC accumulation). However, introduction of EHD3 NE519AD did not restore EHD3 function because transfected cells failed to show ERC accumulation and the Tf-568 remained

largely in the periphery (Fig. 4.6L, transfected cells with yellow borders). These data from three independent experiments were scored and quantified (Fig. 4.6, graph). In mock-treated cells, Tf-568 reached the ERC in almost 90% of cells. Upon EHD3 knockdown, less than 15% of the cells displayed Tf-568 at the ERC. Whereas, when wild-type EHD3 was reintroduced into the cells 75% of the cells had perinuclear Tf-568. However, upon transfection the EHD3 NE519AD mutant, only about 20% of the cells displayed Tf-568 at the ERC suggesting the mutant failed to rescue transferrin trafficking (Fig. 4.6, graph). These data led us to argue that residues 519 and 520 of EHD3 not only regulate its binding to NPF-containing protein partners, but also dictate its function *in vivo*.

15.7 The number of acidic residues after the NPF motif does not dictate binding to EHD3 or EHD1

Having identified residues in the EH domain responsible for the binding selectivity to Rabankyrin-5, we next wanted to assess the residues in Rabankyrin-5 and MICAL-L1 that mediate selective binding to EHDs. Previous studies from our laboratory and others identified a requirement for an NPF motif, followed by acidic residues for binding to EHDs (Kieken et al., 2007; Kieken et al., 2009; Kieken et al., 2010; Henry et al., 2010). Because the MICAL-L1 NPF motif is followed by six acidic residues (and binds to both EHD1 and EHD3), whereas the Rabankyrin-5 motif is followed by only two acidic residues (and binds only to EHD1), we postulated that for binding, EHD3 might require a NPF motif followed by more than two acidic residues (Fig. 4.7A). To this end, we first engineered Rabankyrin-5 proteins containing three, four, or five acidic residues after its single NPF motif. As shown by selective yeast two-hybrid binding assays (Fig. 4.7B), wild-type Rabankyrin-5 and the mutants with additional acidic residues all bound to EHD1 as anticipated. However, in the case of EHD3, even in a Rabankyrin-5 mutant

with five acidic residues following its NPF motif, no gain-of-binding was observed (Fig. 4.7B). We then decided to test whether reducing the number of acidic residues following the NPF motif of MICAL-L1 would lead to loss of binding to EHD3 (Fig. 4.7C). As demonstrated, although both EHD1 and EHD3 displayed loss of binding to MICAL-L1 in the absence of any acidic residues (NPFAAAAAA), EHD3 continued to bind to MICAL-L1 even when it contained only a single acidic residue after its NPF motif. On the other hand, EHD1 showed decreased binding to MICAL-L1 with only a single acidic residue after its NPF motif (NPFEAAAAA). Overall, these data suggest that the number of acidic residues following the NPF motif is not the factor governing binding selectivity of EHD1 and EHD3.

15.8 The binding difference between EHD1 and EHD3 is governed by residue differences upstream of the NPF motif.

Because our studies suggest that the binding selectivity of MICAL-L1 and Rabankyrin-5 for EHD proteins does not lie distal to the NPF motifs, we addressed the possibility that residues upstream of the NPF motif might dictate binding selectivity. We first hypothesized that the KPY residues immediately upstream of the MICAL-L1 NPF motif (Fig. 4.8A) might be responsible for more promiscuous binding than the QSV upstream of the Rabankyrin-5 NPF motif. Accordingly, we generated a mutant of Rabankyrin-5 with the QSV residues substituted with KPY. Next, we tested the binding of wild-type MICAL-L1, wild-type Rabankyrin-5, and a Rabankyrin-5 mutant containing KPYNPF instead of QSVNPF to EHD1 and EHD3 (in Fig. 4.6B). As expected, Rabankyrin-5 bound exclusively to EHD1, whereas MICAL-L1 bound to both EHD1 and EHD3. However, replacing the QSV with KPY upstream of the Rabankyrin-5 NPF motif led to a gain of binding to EHD3 (Fig. 4.8B). To further delineate the amino acid requirements upstream of the NPF motif for binding to EHD3, we then mutated individual

residues in the Rabankyrin-5 QSV motif (Fig. 4.8C). Substituting QSV to either KSV or QSY prior to the Rabankyrin-5 NPF motif was sufficient to induce gain of binding to EHD3 (in addition to EHD1). However, modifying QSV to QPV did not lead to gain of binding to EHD3. Indeed, even binding to EHD1 was lost. Together, these data suggest that although NPF followed by at least one to two acidic residues is required for EHD binding, the residues upstream of the NPF motif dictate the “fine-tuning” of binding to individual EHD proteins.

15.9 Atomic basis for the differential interaction of EHD1 and EHD3 with NPF-containing binding partners.

Since changing the Rabankyrin-5 QSVNPF motif to QSYNPF was sufficient to allow gain-of-function binding to EH3, we examined the three-dimensional structure of the EH1 domain and its binding to the NPF motif of MICAL-L1 (Kieken et al., 2007; Kieken et al., 2009; Kieken et al., 2010). The EH1 binding pocket is predicted to interact with the tyrosine of the NPF peptide via hydrogen bonds with glycine 494. We hypothesized that the valine residue of the Rabankyrin-5 QSVNPF motif, being a branched-carbon-chain containing amino acid, may display a weakened interaction with glycine 494. Accordingly, we predicted that including the non-branched alanine in the NPF peptide, and changing QSVNPF to QSANPF might allow gain-of-function binding to EH3. Indeed, as shown in Fig. 4.9A, yeast two-hybrid binding assays demonstrated that mutating the Rabankyrin-5 NPF motif from QSVNPF to QSANPF led to binding to EHD3.

16 Discussion

The EHDs are membrane curvature-sensing proteins that can induce membrane bending (Daumke et al., 2007), and are involved in promoting vesiculation through their intrinsic ATPase activity (Daumke et al., 2007; Naslavsky et al., 2006; Lee et al., 2005)

(Cai et al., 2012; Cai et al., 2013; Cai et al., 2014; Jakobsson et al., 2011). Indeed, chronic knockdown of EHD3 (over 48 h) leads to lack of cellular TRE, as determined by immunostaining with antibodies for either endogenous MICAL-L1 or Syndapin2, seemingly supporting a role for EHD3 in TRE biogenesis (Cai et al., 2013). Since we examined the TRE after chronic EHD3 loss, such studies do not allow us to differentiate between two distinct possibilities: failure of TRE to undergo biogenesis in the absence of EHD3, or loss of TRE stability over time upon EHD3 depletion. Recycling tubules (van Weering and Cullen, 2014) enhance the efficiency of membrane sorting by providing a high surface-to-volume ratio, and thus play an important role in endosomal trafficking (Maxfield and McGraw, 2004). Indeed, TRE are required for efficient recycling of a variety of receptor cargos, including integrins and major histocompatibility complex class I (MHCI) proteins, which often take tens of minutes to recycle (Jovic et al., 2009; Caplan et al., 2002; Jovic et al., 2007). MICAL-L1-, Syndapin2-, and EHD-decorated TRE display greater stability than most endosomal tubules (Sharma et al., 2009). Typically, we have observed that ≈75% of non-synchronized cells at steady state contain TRE decorated by endogenous MICAL-L1. Although we do not understand why all cells do not display such TRE, recent work from our laboratory leads us to suggest the possibility that the cell cycle is a factor in TRE biogenesis. Fittingly, it was recently shown that, in the course of mitosis, cells dramatically decrease their endocytic recycling (Boucrot et al., 2007). Although we can only speculate that 25% of unsynchronized cells lacking TRE may be entering mitosis, whether this is indeed the case, merits further investigation.

In this study, we describe a unique method of inducing acute TRE biogenesis that has allowed us to address the mechanistic role of EHD3. Having observed that inhibition of phosphatidic acid generation with PLD inhibitors causes TRE depletion from cells, we also noticed that washout of the inhibitors promotes a rapid recovery (burst) of

TRE within 20–30 min that goes on for several hours. Taking advantage of the acute and "synchronized" TRE biogenesis under these conditions, for the first time, we were able to determine that EHD3 is not required for TRE generation (unlike MICAL-L1 and Syndapin2 (Giridharan et al., 2013)). Because these experiments were performed under conditions where 85–95% of EHD3 was depleted, and because we have seen that chronic EHD3 knockdown of even 50% efficiency leads to loss of TRE after 48 h, TRE recovery following washout in EHD3-depleted cells is unlikely to result from residual EHD3. On the other hand, although EHD3 depletion did not prevent TRE generation upon inhibitor washout, the TRE remained stable for only 1–2 h, suggesting that EHD3 has a role in TRE stabilization. However, even though upon EHD3 depletion, TRE generation was possible after inhibitor washout, the TRE remained stable for only 1–2 h, suggesting that EHD3 has a role in TRE stabilization.

We do not anticipate that the very same tubules are maintained for many hours, but instead that overall TRE stability is enhanced in the presence of EHD3. We have demonstrated previously that TRE-decorating proteins such as EHD1 and MICAL-L1 can remain stably associated for 5–10 min (Sharma et al., 2009), measuring the TRE life span is difficult because of dynamic fusion and fission events that may occur at the TRE tips or along the length of the tubule. Although we cannot pin down the precise mechanism for TRE stabilization by EHD3, we rationalize that the ability of EHD3 to interact with both MICAL-L1 and Syndapin2 via NPF-EH interactions, it physically stabilizes these two proteins on TRE membranes, preventing their dissociation and degradation.

Another open question is what differences in NPF-containing proteins, such as MICAL-L1 and Rabankyrin-5, determine their ability to interact with different EHD proteins. Our initial hypothesis was that the number of acidic residues following the NPF motif might influence the ability to bind to certain EHDs. Indeed, six acidic residues

follow the first NPF motif of MICAL-L1, and it interacts with both EHD1 and EHD3. On the other hand, Rabankyrin-5 has only two acidic residues after its NPF motif, and it binds only to EHD1. However, neither reducing the number of acidic residues following the NPF motif of MICAL-L1, nor increasing the number of acidic residues following the NPF motif of Rabankyrin-5 had any impact on the binding pattern to EHD1 and EHD3. This indicates that, although NPF motifs flanked by acidic residues are necessary for EHD binding (Kieken et al., 2010; Henry et al., 2010), the precise number of acidic residues is not a factor in fine-tuning the binding to select EHDs.

The remarkable likeness of EHD1 and EHD3 raises interesting questions of how two proteins that share 86% identity carry out such disparate functions. Given that their ATP hydrolysis domains are nearly identical, we predicted that the distinct function of these EHD proteins may be attributed to differences in their EH domains, possibly resulting in binding to distinct subsets of interaction partners. Although both EHD1 and EHD3 bind to MICAL-L1 (Sharma et al., 2009) and Syndapin2 (Braun et al., 2005), Rabankyrin-5 binds exclusively to EHD1 (Zhang et al., 2012). Hence, binding to Rabankyrin-5 is a distinguishing factor between EHD1 and EHD3. We were able to map this differential binding to a pair of residues (Ala-519/Asp-520 for EHD1 and Asn-519/Glu-520 for EHD3). Remarkably, of the entire 534 EHD residues, a simple reversal of EHD3 Asn-519/Glu-520 to AD (as found in EHD1) led to its ability to bind to Rabankyrin-5. Notably, the switching of EHD3 residues 519 and 520 from NE to AD had a direct functional effect on EHD3. Depletion of EHD3 normally causes a failure of internalized receptors, such as the transferrin, to reach the perinuclear ERC from peripheral sorting endosomes (Fig. 4.6, I and L). Remarkably, the NE-to-AD EHD3 mutant failed to rescue this phenotype (as did wild-type EHD3), highlighting the significance of these residues functionally. Nonetheless, it remains to be determined what connection, if any, exists between Rabankyrin-5 binding and the membrane

trafficking functions of these EHD proteins.

The possible explanation for the significance of these two residues is provided by the examination of the EH1 NMR solution structure. Both Ala-519 and Asp-520 reside within 5 Å of Leu-487, likely forming a hydrogen bond. Although Leu-487 does not localize to the surface of the EH1 binding pocket, it does compose the back part (helix 3) of the binding pocket (helix 3 of the helix 2-loop-helix 3 pocket) (Fig. 4.9B). Indeed, such an interaction might alter the alignment of amino acids that make direct contact with the NPF peptide, the Lys-486 and the critical Trp-485. Thus, we hypothesize that hydrogen bonds between Ala-519/Asp-520 and Leu-487 impact the crucial Trp-485 and serve to stabilize the pocket in a conformation that maintains affinity for both the MICAL-L1 KPYNPF motif and the Rabankyrin-5 QSVNPF motif. Indeed, it appears as though reversal of Asn-519 of EHD3 to Ala or Glu-520 to Asp was sufficient to induce gain of binding to Rabankyrin-5. However, the lack of the Ala-519/Asp-520 residues in the EHD3 EH domain and the absence of the upstream tyrosine prior to the Rabankyrin-5 peptide NPF motif to interact with Gly-494 likely lead to low binding affinity between EHD3 and the peptide. It is intriguing that, upon mutating EHD1 from AD to NE (at residues 519/520), we did not discern a loss of EHD1 binding to Rabankyrin-5 as we initially anticipated (Fig. 4.5E). Although further experimentation will be needed to fully understand the reason for this anomaly, it is clear that other residues that are distinct from EHD3 within the EHD1 EH domain must play a role in maintaining EH1 binding pocket affinity for the Rabankyrin-5 NPF peptide.

Surprisingly, we observed that the residues immediately upstream of the NPF motif are able to dictate binding to select EHDs. The QSVNPFED motif of Rabankyrin-5 bound to EHD1 but not EHD3. However, when mutated to KPYNPFED (the KPY is upstream to the MICAL-L1 NPF motif), binding was observed with both EHD1 and EHD3. What is the atomic mechanism to explain the differential binding? Based on our

previous NMR solution structure of EH1 with NPF-containing peptides (Kieken et al., 2007; Kieken et al., 2009; Kieken et al., 2010), there are hydrogen bonds between glycine 494 of the binding pocket and the tyrosine (and potentially lysine) residue of the KPYNPF motif of MICAL-L1. We anticipate that a similar mechanism explains the binding between the QSVNPF motif of Rabankyrin-5 and EH1. In the case of EH3, it is plausible that the weakened affinity of the pocket (resulting from Asn-519/Glu-520 instead of Ala-519/Asp-520) causes a failure of EH3 binding to QSVNPF. However, we also considered that the branched valine residue of the QSVNPF peptide might create a geometry that is not conducive to hydrogen bonds with the backbone at Gly-494. Indeed, mutation of the Rabankyrin-5 to QSANPF without the branched valine induces a gain of binding to EH3.

Although Rabankyrin-5 binding only serves as a model to illustrate how subtle residue changes can lead to differential binding, and additional studies will need to be done to determine how such binding might affect EHD function in vesiculation and/or TRE stabilization, our findings provide a unique window to understand how two proteins that were likely generated through gene duplication evolved in higher eukaryotes to perform distinct functions. Based on our findings in previous studies by our group and others and the current study, a basic model for TRE function is emerging. TRE are essential for efficient recycling (Jovic et al., 2009) and appear to regulate trafficking steps both from sorting endosomes to the ERC (Xie et al., 2016) and from the ERC to the plasma membrane (Caplan et al., 2002). The biogenesis of TRE occurs when phosphatidic acid is generated on membranes by one of several pathways (Cai et al., 2012; Giridharan et al., 2013; Xie et al., 2014). The phosphatidic acid binding proteins MICAL-L1 and Syndapin2 are then recruited to the membrane, where they interact. Syndapin2 also has an F-BAR domain that induces membrane curvature (Giridharan et al., 2013). Although the loss of TRE by chronic depletion of EHD3 initially suggested that

this protein is required for TRE biogenesis, and a recent study maintains that EHD3 binds directly to phosphatidic acid and induces curvature (Henmi et al., 2016), this study reveals that EHD3 is not required for TRE biogenesis and likely plays a role in stabilizing TRE, possibly by strengthening the MICAL-L1-Syndapin2 interactions. Following cargo sorting within the TRE, the most likely scenario, based on various studies supporting a role for EHD1 in TRE fission (Cai et al., 2013; Cai et al., 2014), is that TRE stability is decreased by a temporal replacement of EHD3 by EHD1. The mechanism and specific triggers for this EHD switch and recruitment of EHD1 remain unknown and appear to be unrelated to EHD affinity for the MICAL-L1 NPF motif because both EH1 and EH3 bind with similar affinities (Fig. 4.4). We speculate that post-translational modifications, such as EHD3 sumoylation (Cabasso et al., 2015) and potentially, desumoylation may regulate this process. Alternatively, specific signaling triggers through receptors (i.e., epidermal growth factor receptor) may also promote EHD1 replacement of EHD3 and TRE fission (Reinecke et al., 2015; Reinecke et al., 2014). Ultimately, TRE are cleaved, either at their tips or potentially along the entire membrane, and the resulting vesicles are transported along microtubules back to the plasma membrane.

In summary, we provide a deeper understanding of the mechanism of EHD3 function. First, we have demonstrated that EHD3 is not required for TRE biogenesis but instead is involved in maintenance of TRE stability over time. Next, we characterized the differential function of EHD1 and EHD3 and found important differences in EH domain residues that led to differential binding with NPF-containing proteins. These residues likely promote optimal hydrogen bonds with hydrophobic residues immediately upstream of the NPF motifs. Although future studies will be needed to determine how differential binding partners control TRE vesiculation versus stability, these results provide novel insight into the atomic mechanisms of EHD function.

Figure 4.1. TRE biogenesis occurs in the absence of EHD3.

A, using MICAL-L1 as a marker, TRE biogenesis was assessed in mock-treated cells (first column), Syndapin2 knockdown cells (second column), EHD3 knockdown cells (third column), and EHD1 knockdown cells (fourth column). Top row, pretreatment shows TRE status under the corresponding knockdown conditions. Center row, 30-min treatment with PLD inhibitors (100 µM CAY 10593 and CAY 10594 for 30 min at37°C). Bottom row, 30-min treatment with PLD inhibitors followed by 20-min washout of the inhibitor. A representative field of cells (in the top half of each micrograph) is also depicted by an inverted-contrast image (bottom) to better visualize TRE. Note that there is initiation of TRE formation (burst) at the 20-minwashout for all treatments except Syndapin2-KD. Scale bar=10µm**. B,** immunoblot analysis depicting the efficiency of knockdown for endogenous EHD1 and Syndapin2 and transfected EHD3. Actin is shown as a loading control.

Figure 4.1

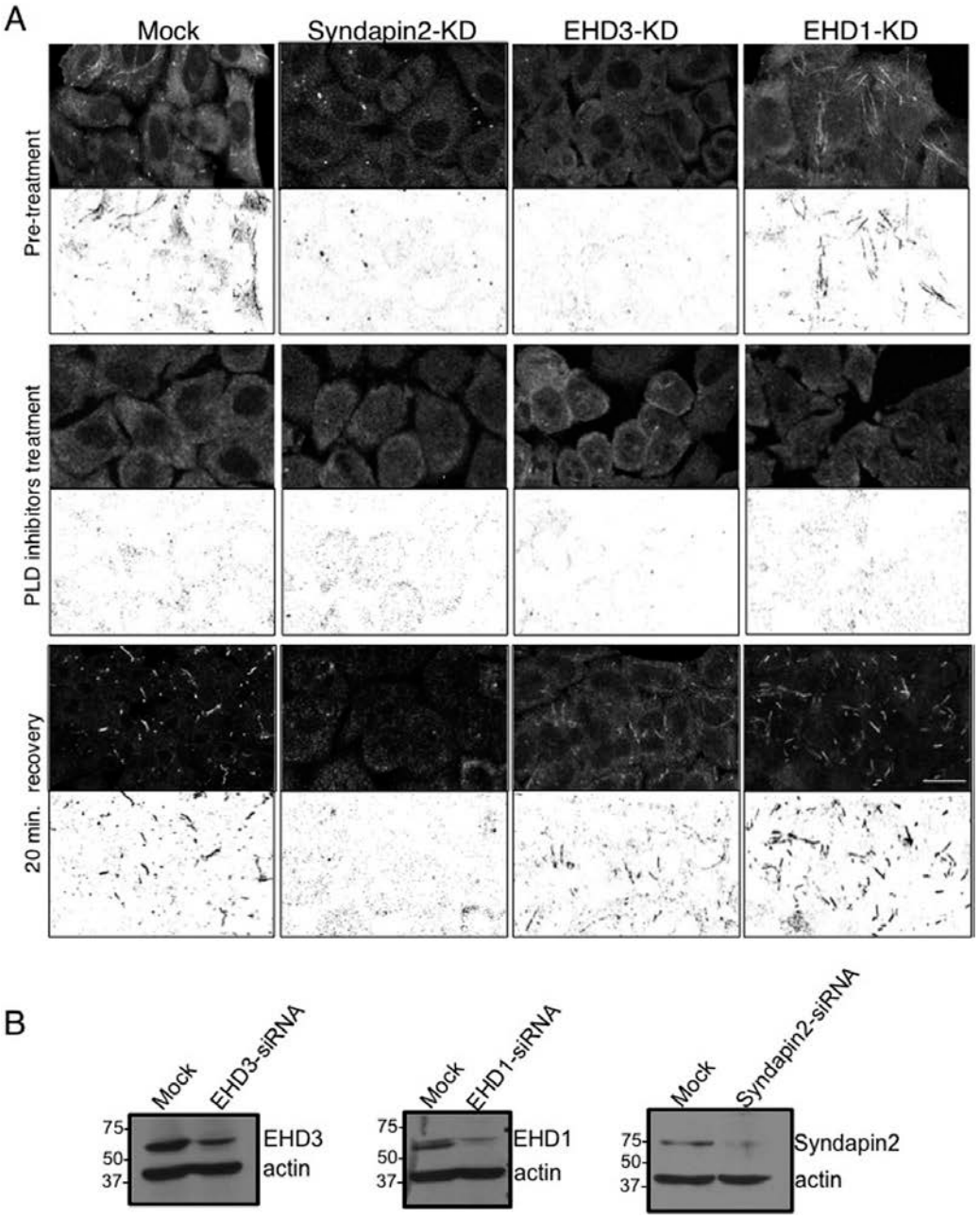
A
Mock
Syndapin2-KD
EHD3-KD
EHD1-KD
Pre-treatment
PLD inhibitors treatment
20 min. recovery
B
Mock
EHD3-siRNA
75
50
37
EHD3
actin
Mock
EHD1-siRNA
75
50
37
EHD1
actin
Mock
Syndapin2-siRNA
75
50
37
Syndapin2
actin

Figure 4.2. EHD3 stabilizes TRE.

A, mock-treated cells (first column), Syndapin2 knockdown cells (second column), EHD3 knockdown cells (third column), andEHD1 knockdown cells (fourth column) were subjected to PLD inhibitor treatment and washout (as described in Fig. 1) and then incubated for 1 h (top row), 4 h (center row), or 6 h (bottom row) after washout. A single red asterisk depicts the maximum biogenesis of TRE in EHD3 knockdown cells after 1-h washout. Two red asterisks (4 h after washout, center panel) highlight the disappearance of the newly formed TRE in EHD3 knockdown cells, whereas TRE in mock-treated and EHD1 knockdown cells are increasingly abundant 4–6 h after washout. A field of cells (in the top half of each micrograph) is also represented as an inverted contrast image to better visualize TRE (bottom half of each micrograph). **B**, quantitative analysis of 100 cells from three independent experiments, measuring mean TRE area in PLD inhibitor washout experiments. The red and purple dashed lines denote the increase in mean TRE length for EHD1 knockdown cells over time, whereas the black dashed line depicts the increase and subsequent decrease in mean TRE length over time for EHD3 knockdown cells. Significance was assessed by analysis of variance*, $p < 0.01$. Scale bar =10μm.

Figure 4.2

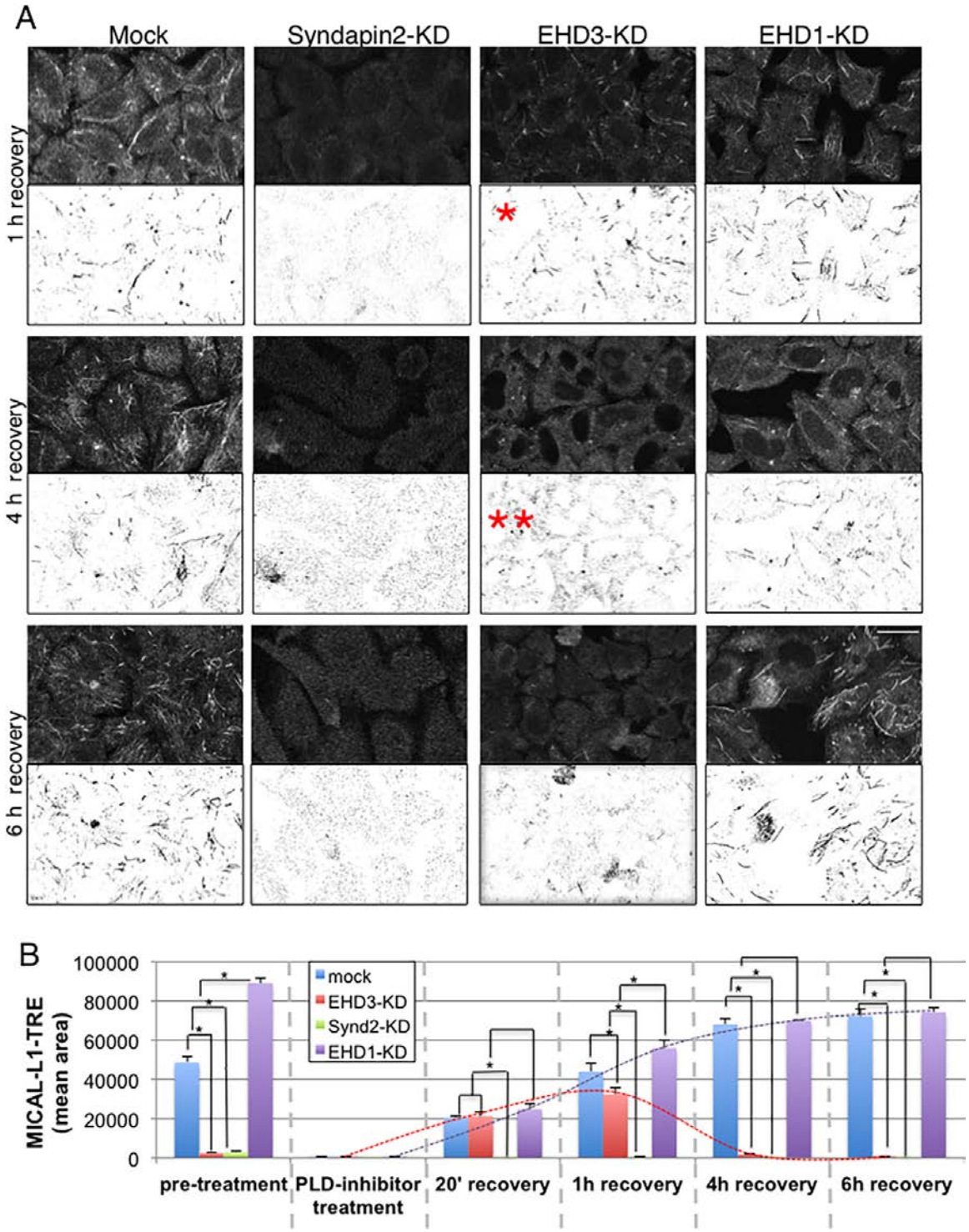
A
Mock
Syndapin2-KD
EHD3-KD
EHD1-KD
1 h recovery
4 h recovery
6 h recovery
*
**
B
MICAL-L1-TRE (mean area)
100000
80000
60000
40000
20000
0
mock
EHD3-KD
Synd2-KD
EHD1-KD
pre-treatment
PLD-inhibitor treatment
20' recovery
1h recovery
4h recovery
6h recovery

Figure 4.3. The EH domain is responsible for the differential function of EHD1 and EHD3 in vesiculation and TRE stabilization, respectively.

(A), the C-terminal EHD proteins EHD1 and EHD3 share 86% identity and have a conserved domain architecture comprised of four domains: two helical domains, a G domain, and a C-terminal EH domain**. (B—D),** HeLa cells were treated with EHD3 siRNA (B and D) or EHD1 siRNA C for 48 h. Cells were then transfected with (B) siRNA-resistant GFP-myc-EHD3 (WT), (**C)** siRNA-resistant GFP-myc-EHD1 (WT), and (D) siRNA-resistant GFP-myc-EHD3-EH1. TRE morphology was assessed by immunostaining with endogenous Syndapin2. Note that untransfected cells in C and D lack TRE. E, quantitative analysis of mean TRE length was measured in 100 cells from three independent experiments as in B–D. Significance was assessed by analysis of variance.*, $p < 0.01$. Scale bar = 10m.

Figure 4.3

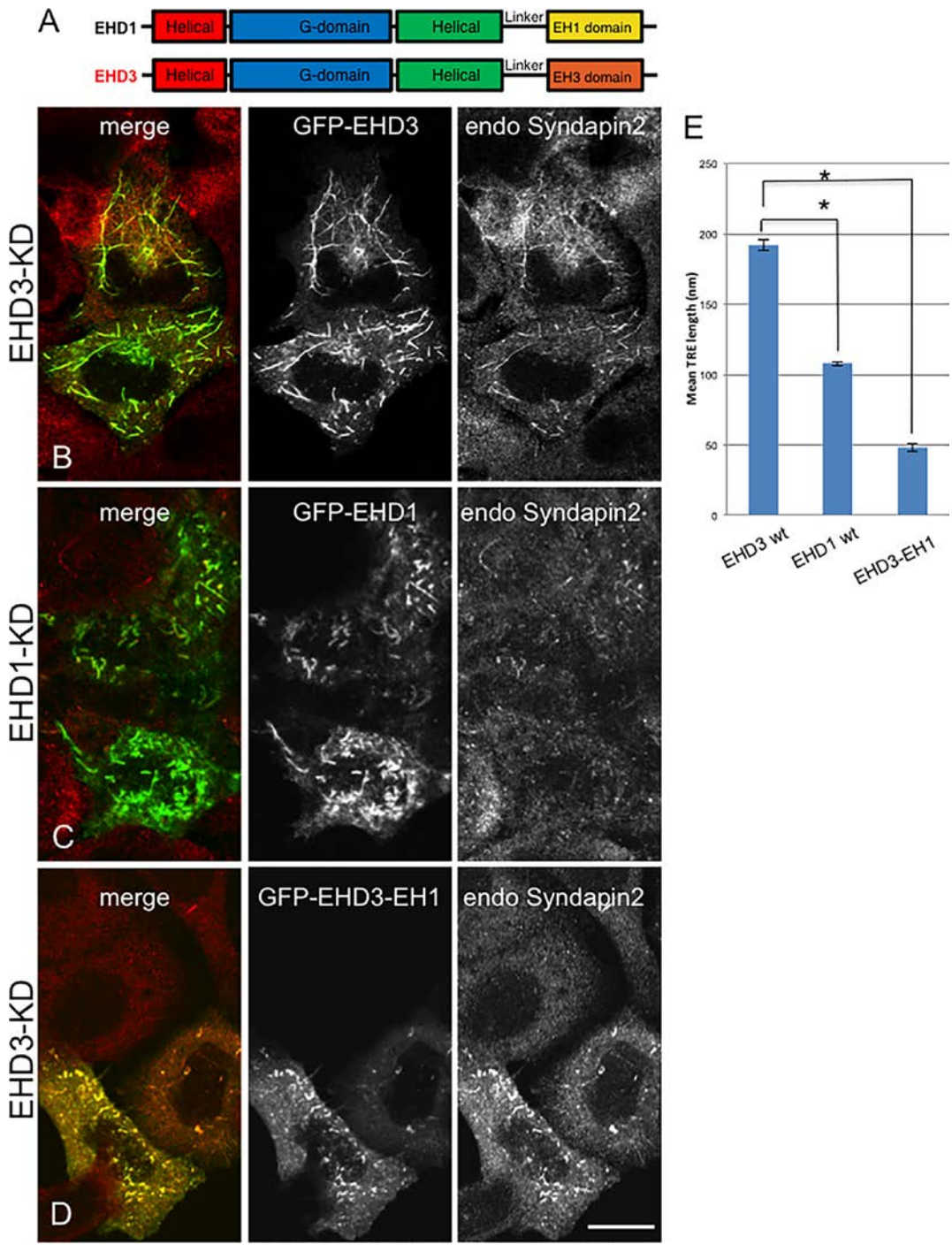
A
EHD1
Helical
G-domain
Helical
Linker
EH1 domain
EHD3
Helical
G-domain
Helical
Linker
EH3 domain
EHD3-KD
merge
GFP-EHD3
endo Syndapin2
B
EHD1-KD
merge
GFP-EHD1
endo Syndapin2
C
EHD3-KD
merge
GFP-EHD3-EH1
endo Syndapin2
D
E
Mean TRE length (nm)
250
200
150
100
50
0
*
*
EHD3 wt
EHD1 wt
EHD3-EH1

Figure 4.4. Comparison of the binding affinity of the EHD1 EH domain and EHD3 EH domain for a MICAL-L1 NPF peptide by isothermal titration calorimetry.

Solutions containing 90 µM purified EH domains of EHD1 or EHD3 were injected with 930 µM MICAL-L1 peptide, and ITC binding isotherms were collected. K_D values obtained by fitting the titration curves are indicated for each EH domain.

Figure 4.4

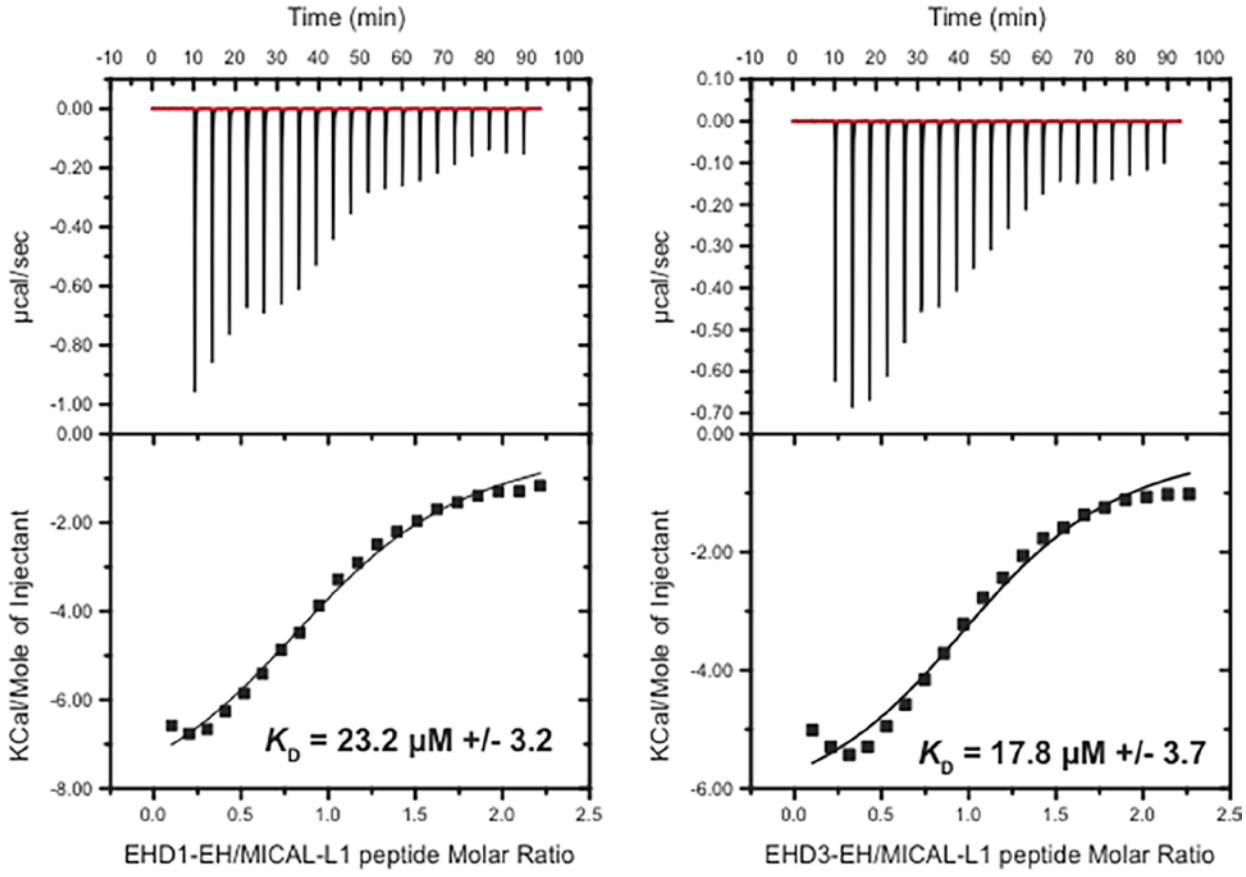
Time (min)
µcal/sec
KCal/Mole of Injectant
K_D = 23.2 µM +/- 3.2
EHD1-EH/MICAL-L1 peptide Molar Ratio
Time (min)
µcal/sec
KCal/Mole of Injectant
K_D = 17.8 µM +/- 3.7
EHD3-EH/MICAL-L1 peptide Molar Ratio

Figure 4.5. Identification of EH1 and EH3 residues responsible for their differential interactions with NPF-containing partners.

A, comparison of EH1 and EH3, exhibiting homologous (green) and non-homologous (white) residues. Six key regions containing non-conserved residues chosen for analysis are depicted. **B,** schematic showing the interaction of EHD1 with both Rabankyrin-5 and MICAL-L1, whereas EHD3 interacts only with MICAL-L1. **C**, the *S.cerevisiae* yeast strain AH109 was co-transformed with the following Gal4bd fusion constructs: Gal4bd-p53 (control), MICAL-L1 and Rabankyrin-5 along with Gal4ad fusion constructs Gal4ad-SV40 (control), Gal4ad-EHD1 (WT), Gal4ad-EHD3 (WT), Gal4ad-EHD3 (NE519AD), Gal4ad-EHD3 (AHLL523PHLV), Gal4ad-EHD3(D459N), Gal4adEHD3(M447T), Gal4ad-EHD3(A437V), and Gal4ad-EHD3(KVAE523RHE). **D**, HeLa cells were transfected with HA-Rabankyrin-5 (R-5) and lysed after 24 h. The GST-EH domains indicated were used to pull down Rabankyrin-5 from HeLa cell lysates. The protein pulled down was detected by immunoblotting with anti-HA, and anti-GST was used as a control for equal loading of proteins. The immunoblot shown is a representative of four individual experiments**. E,** the *S.cerevisiae* yeast strain AH109 was co-transformed with the following Gal4bd fusion constructs: Gal4bd-p53 (control), MICAL-L1, and Rank-5 along with the Gal4ad fusion constructs Gal4ad-SV40 (control), Gal4ad-EHD1 (WT), Gal4ad-EHD3 (WT), Gal4ad-EHD3 (NE519AD), Gal4ad-EHD1(AD519NE), Gal4ad-EHD3(N519A), and Gal4ad-EHD3(E519D). Co-transformants from C and E were plated on non-selective (+HIS) and selective (-HIS) agar plates. Dotted white lines indicate where two different scanned agar plates have been compiled into the same image. The dashed red rectangle in C shows the gain of binding by the EHD3 NE519AD mutant. A representative from four experiments is depicted.

Figure 4.5

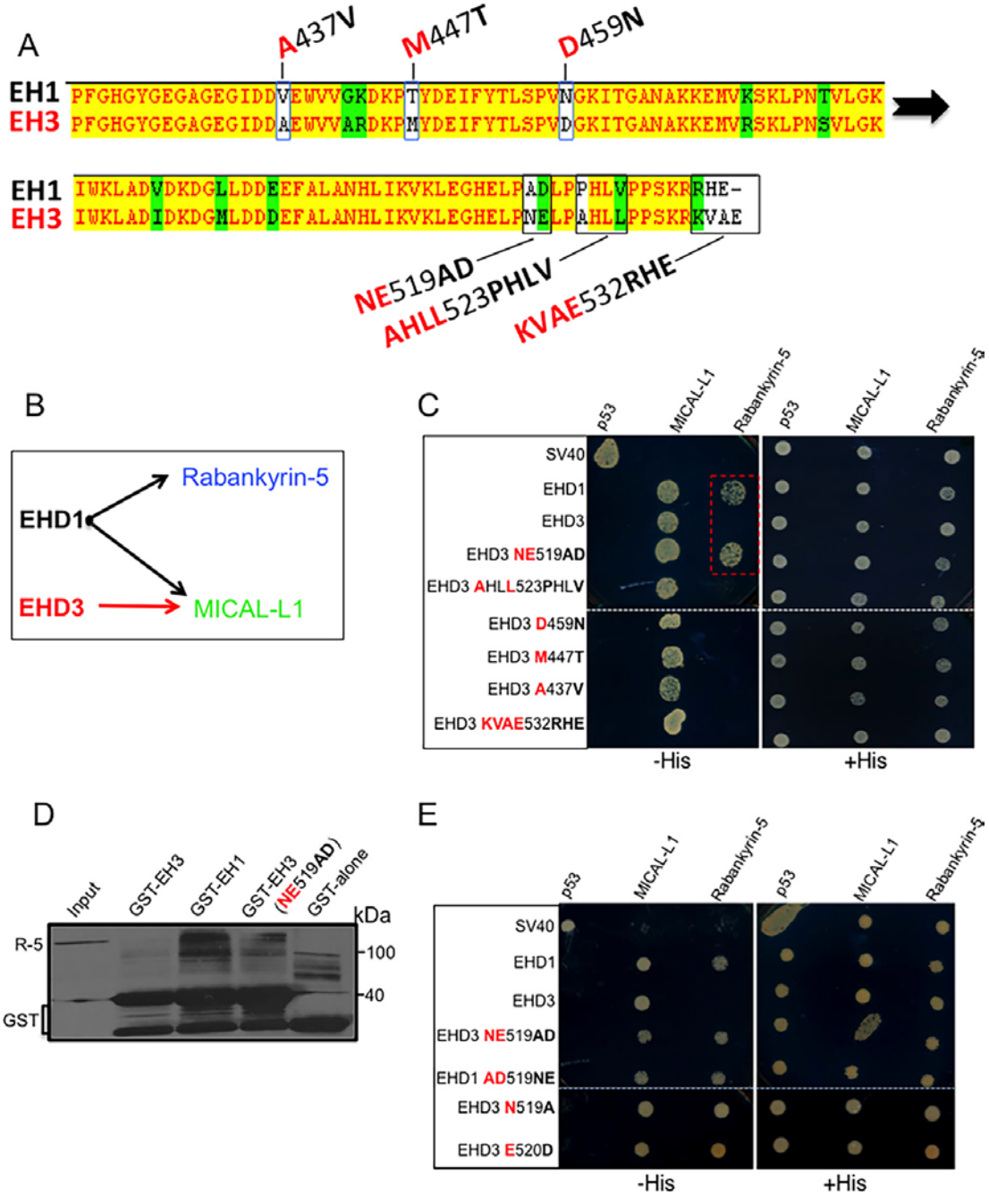
A
A437V
M447T
D459N
EH1 PFGHGYGEGAGEGIDDVEWVVGKDKPTYDEIFYTLSPVNGKITGANAKKEMVKSKLPNTVLGK
EH3 PFGHGYGEGAGEGIDDAEWVVARDKPMYDEIFYTLSPVDGKITGANAKKEMVRSKLPNSVLGK
EH1 IWKLADVDKDGLLDDEEFALANHLIKVKLEGHELFADLPPHLVPPSKRRHE-
EH3 IWKLADIDKDGMLDDDEFALANHLIKVKLEGHELFNELPAHLLPPSKRKVAE
NE519AD
AHLL523PHLV
KVAE532RHE
B
EHD1
Rabankyrin-5
EHD3
MICAL-L1
C
p53
MICAL-L1
Rabankyrin-5
SV40
EHD1
EHD3
EHD3 NE519AD
EHD3 AHLL523PHLV
EHD3 D459N
EHD3 M447T
EHD3 A437V
EHD3 KVAE532RHE
-His
+His
D
Input
GST-EH3
GST-EH1
GST-EH3 (NE519AD)
GST-alone
kDa
R-5
GST
100
40
E
p53
MICAL-L1
Rabankyrin-5
SV40
EHD1
EHD3
EHD3 NE519AD
EHD1 AD519NE
EHD3 N519A
EHD3 E520D
-His
+His

Figure 4.6. Wild-type EHD3, but not the EHD3NE519AD mutant, rescues the impaired transferrin trafficking phenotype observed in EHD3 knockdown cells.

HeLa cells were either mock-treated **(A–G)** or treated with EHD3 siRNA oligonucleotides (H–M) for 48 h. After the first 24 h, cells were transfected with either WT GFP-EHD3 (B–D and H–J) or GFP-EHD3 NE519AD **(E–G and K–M)** and then subjected to a 20-min uptake with Tf-568 prior to fixation and microscopic analysis. Mock-treated cells typically display accumulation of Tf-568 in the perinuclear ERC **(A, C, and F).** Upon EHD3 knockdown, Tf-568 failed to reach the ERC (I, non-labeled cells). **I,** wild-typeGFP-EHD3-transfectedcells are marked with a yellow border, and arrows highlight the rescued Tf-568 trafficking and arrival at the ERC.L, yellow borders indicate EHD3 KD cells transfected withGFP-EHD3NE519AD. Arrows are not shown because Tf-568 does not reach the ERC. The graph (top right) displays quantification of the percentage of cells in which Tf reaches the ERC (within 20 min), comparing wild-type and EHD3 NE519 AD-transfected cells. At least 50 cells from each treatment were scored from three individual experiments. Confirmation was done by “blind scoring.” Significance was assessed by analysis of variance. *, $p<0.01$.

Figure 4.6

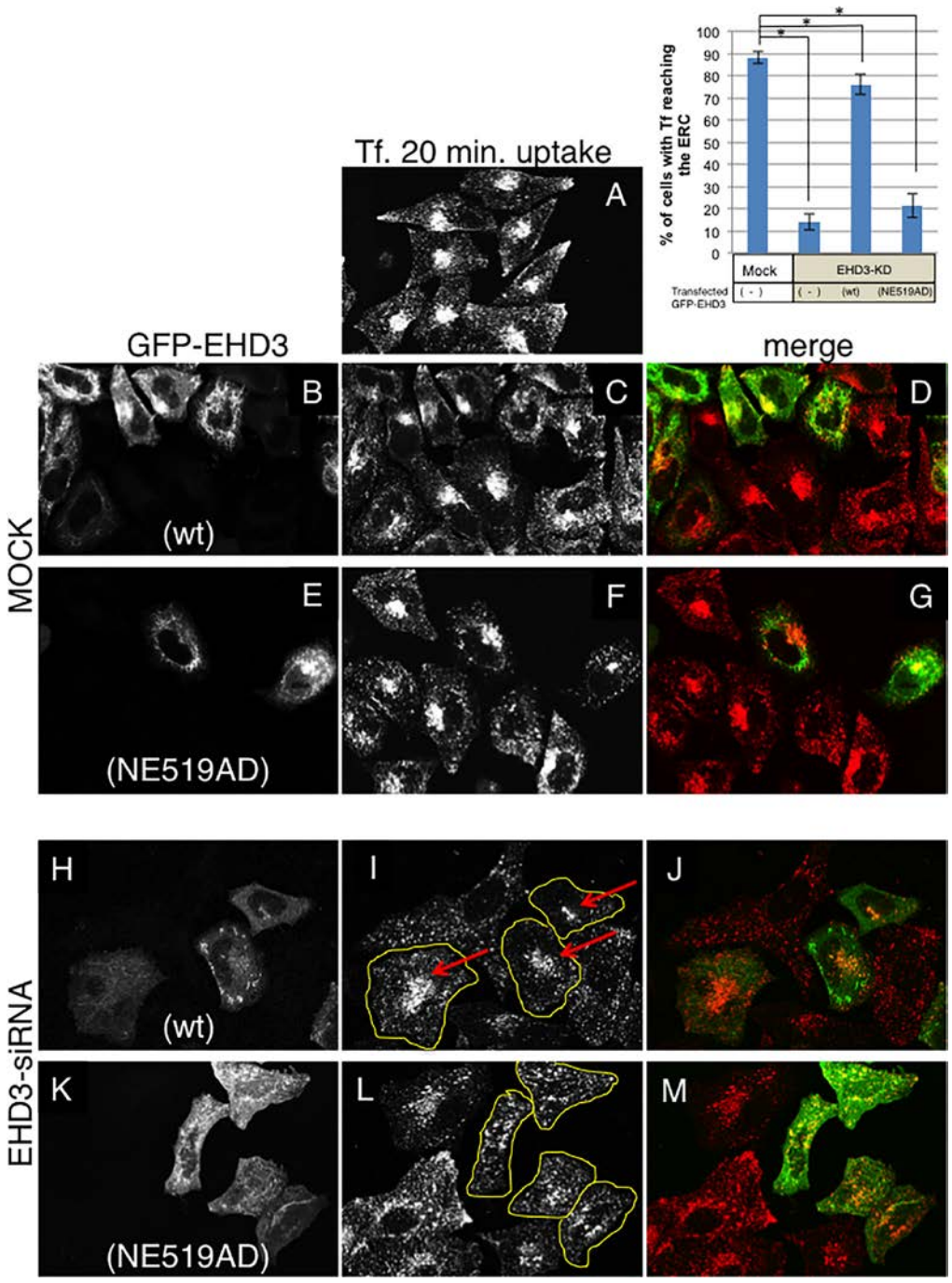
Tf. 20 min. uptake
A
% of cells with Tf reaching the ERC
100
90
80
70
60
50
40
30
20
10
0
Mock
EHD3-KD
Transfected GFP-EHD3
(-)
(-)
(wt)
(NE519AD)
GFP-EHD3
merge
MOCK
B
C
D
(wt)
E
F
G
(NE519AD)
EHD3-siRNA
H
I
J
(wt)
K
L
M
(NE519AD)

Figure 4.7. The number of acidic residues after the NPF motif does not discriminate between binding to EHD1 or EHD3.

A, comparison of the number of acidic residues (blue letters) following the NPF motif (red letters) of MICAL-L1 (NPFDEEEEEE) and Rabankyrin-5 (NPFED). **B**, the *S. cerevisiae* yeast strain AH109 was co-transformed with the following Gal4bd fusion constructs: Gal4bd-p53 (control), Gal4bd-Rabankyrin-5 (WT) (NPFEDV), Gal4bd-Rabankyrin-5(NPFEDV to NPFEDE), Gal4bd-Rabankyrin-5 (NPFEDV to NPFEDEE), and Rabankyrin-5 (NPFEDV to NPFEDEEE) along with the Gal4ad fusion constructs Gal4ad-SV40 (control), Gal4ad-EHD1 (WT), and Gal4ad-EHD3 (WT). Co-transformants were plated on non-selective (+ HIS) and selective (- HIS) agar plates. **C,** the S. cerevisiae yeast strain AH109 was co-transformed with the following Gal4bd fusion constructs: Gal4bd-p53 (control), Gal4bd-MICAL-L1 (WT) (NPFDEEEEE), Gal4bd-MICAL-L1 (NPFDEEEEE to NPFDEEEEA), Gal4bd-MICAL-L1(NPFDEEEEE to NPFDEEEAA), Gal4bd- MICAL-L1(NPFDEEEEE to NPFDEEAAA), Gal4bd-MICAL-L1(NPFDEEEEE to NPFDEAAAA), Gal4bd-MICAL-L1(NPFDEEEEE to NPFDAAAAA), and Gal4bd- MICAL-L1(NPFDEEEEE to NPFAAAAAA) along with the Gal4ad fusion constructs Gal4ad-SV40 (control), Gal4ad-EHD1 (WT) and Gal4ad-EHD3 (WT). A representative from four experiments is depicted.

Figure 4.7

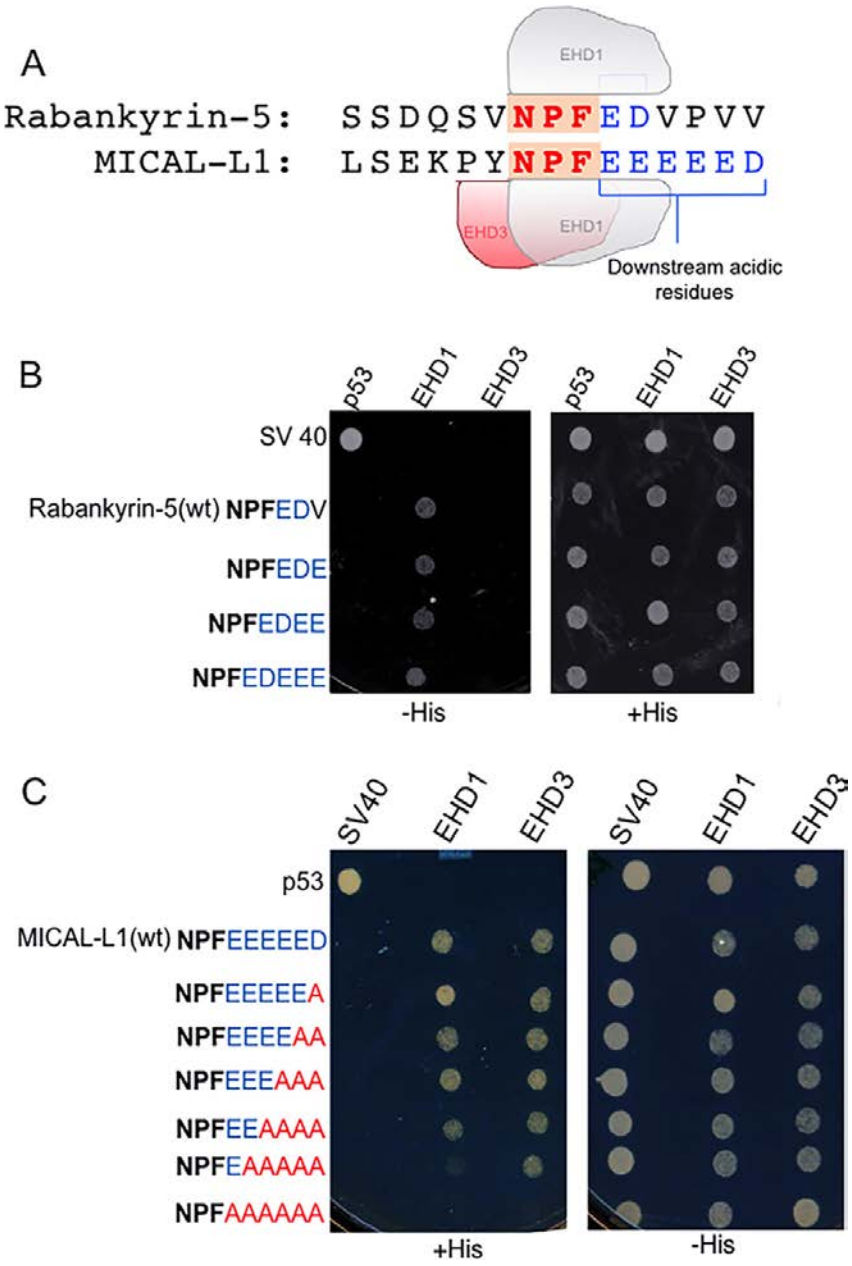
A
Rabankyrin-5: SSDQSVNPFEDVPVV
MICAL-L1: LSEKPYNPFEEEEED
EHD1
EHD3
EHD1
Downstream acidic residues
B
p53
EHD1
EHD3
p53
EHD1
EHD3
SV 40
Rabankyrin-5(wt) NPFEDV
NPFEDE
NPFEDEE
NPFEDEEE
-His
+His
C
SV40
EHD1
EHD3
SV40
EHD1
EHD3
p53
MICAL-L1(wt) NPFEEEEED
NPFEEEEEA
NPFEEEEAA
NPFEEEAAA
NPFEEAAAA
NPFEAAAAA
NPFAAAAAA
+His
-His

Figure 4.8. Residue differences upstream of the NPF motif govern binding difference between EHD1 and EHD3.

A, comparison of the residues upstream of the NPF motif (green) between MICAL-L1 (KPY) and Rabankyrin-5 (QSV). **B,** the *S. cerevisiae* yeast strain AH109 was co-transformed with the following Gal4bd fusion constructs: Gal4bd-p53 (control) and Gal4bd-EHD1 (WT), Gal4bd-EHD3 (WT) along with the Gal4ad fusion constructs Gal4ad-SV40 (control), Gal4ad-MICAL-L1 (WT), Gal4ad-Rabankyrin-5 (WT), and Gal4ad-Rabankyrin-5 (QSV to KPY). **C,** the S. cerevisiae yeast strain AH109 was co-transformed with the following Gal4bd fusion constructs: Gal4bd-p53 (control), Gal4bd-EHD1 (WT), or Gal4bd-EHD3 (WT) along with the Gal4ad fusion constructs Gal4ad-SV40 (control), Gal4ad-MICAL-L1 (WT) and Gal4ad- Rabankyrin-5 (WT), Gal4ad-Rabankyrin-5 (QSV to KPY), Gal4ad-Rabankyrin-5 (QSV to KSV), Gal4ad-Rabankyrin-5 (QSV to QPV), and Gal4ad-Rabankyrin-5 (QSV to QSY). Co-transformants were plated on non-selective (+ HIS) and selective (- HIS) agar plates. A representative from four experiments is depicted

Figure 4.8

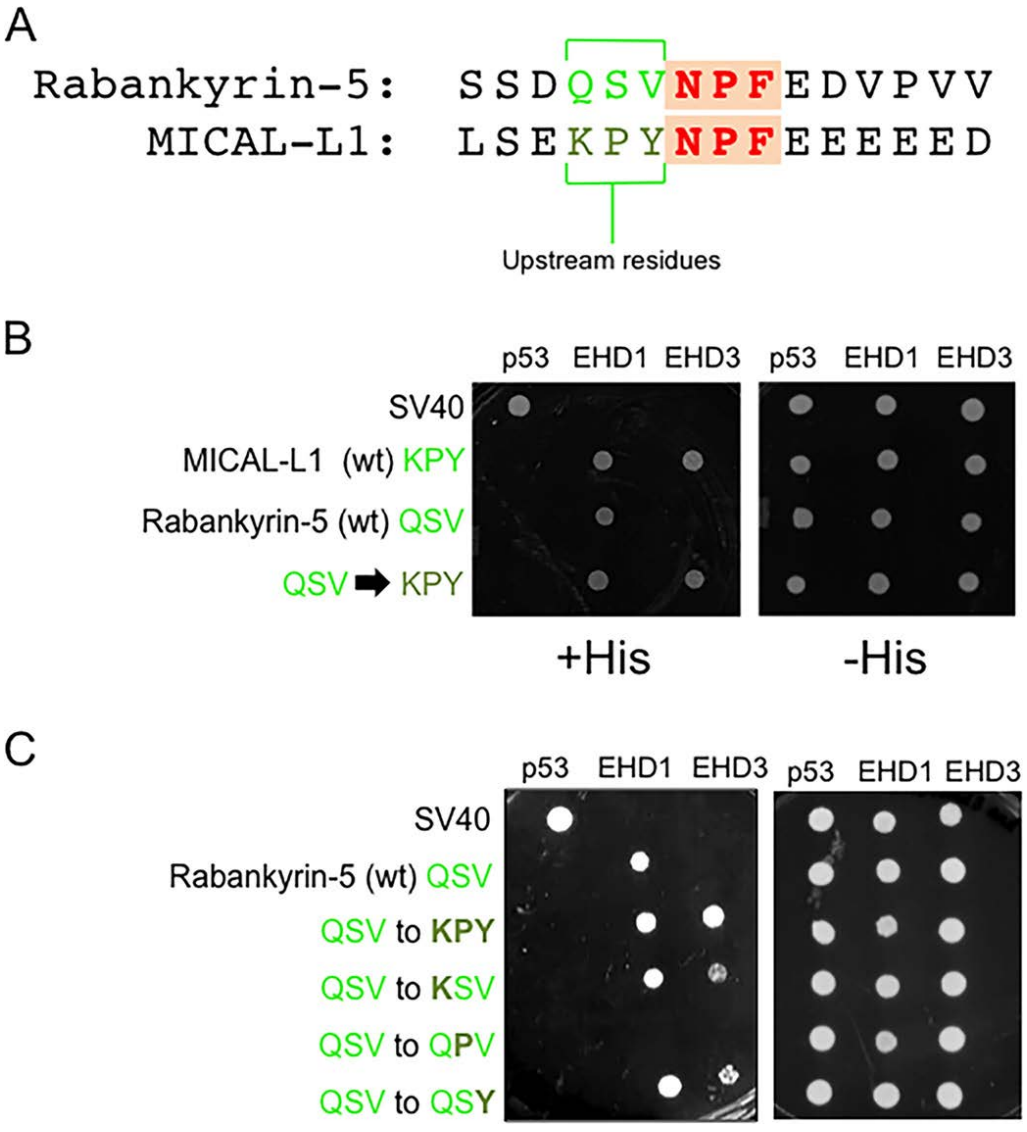
A
Rabankyrin-5: S S D Q S V N P F E D V P V V
MICAL-L1: L S E K P Y N P F E E E E E D
Upstream residues
B
p53 EHD1 EHD3 p53 EHD1 EHD3
SV40
MICAL-L1 (wt) KPY
Rabankyrin-5 (wt) QSV
QSV ➡ KPY
+His
-His
C
p53 EHD1 EHD3 p53 EHD1 EHD3
SV40
Rabankyrin-5 (wt) QSV
QSV to KPY
QSV to KSV
QSV to QPV
QSV to QSY

Figure 4.9. Atomic basis for the differential interaction of EHD1 and EHD3 with NPF-containing binding partners.

A, the *S. cerevisiae* yeast AH109 strain was co-transformed with the following Gal4bd fusion constructs: Gal4bd-p53 (control), Gal4bd-EHD1 (WT), and Gal4bd-EHD3 (WT) along with the Gal4ad fusion constructs Gal4ad-SV40 (control), Gal4ad-MICAL-L1 (WT) and Rabankyrin-5(WT), and Gal4ad-Rabankyrin-5 (QSV to QSV). Co-transformants were plated on non-selective (+ HIS) and selective (- HIS) agar plates. A representative from four experiments is depicted. **B,** model of the EHD1 EH domain with the MICAL-L1 KPYNPFEEEEED peptide, based on the NMR solution structure. Red depicts oxygen atoms in the Asp-520 side chain.

Figure 4.9

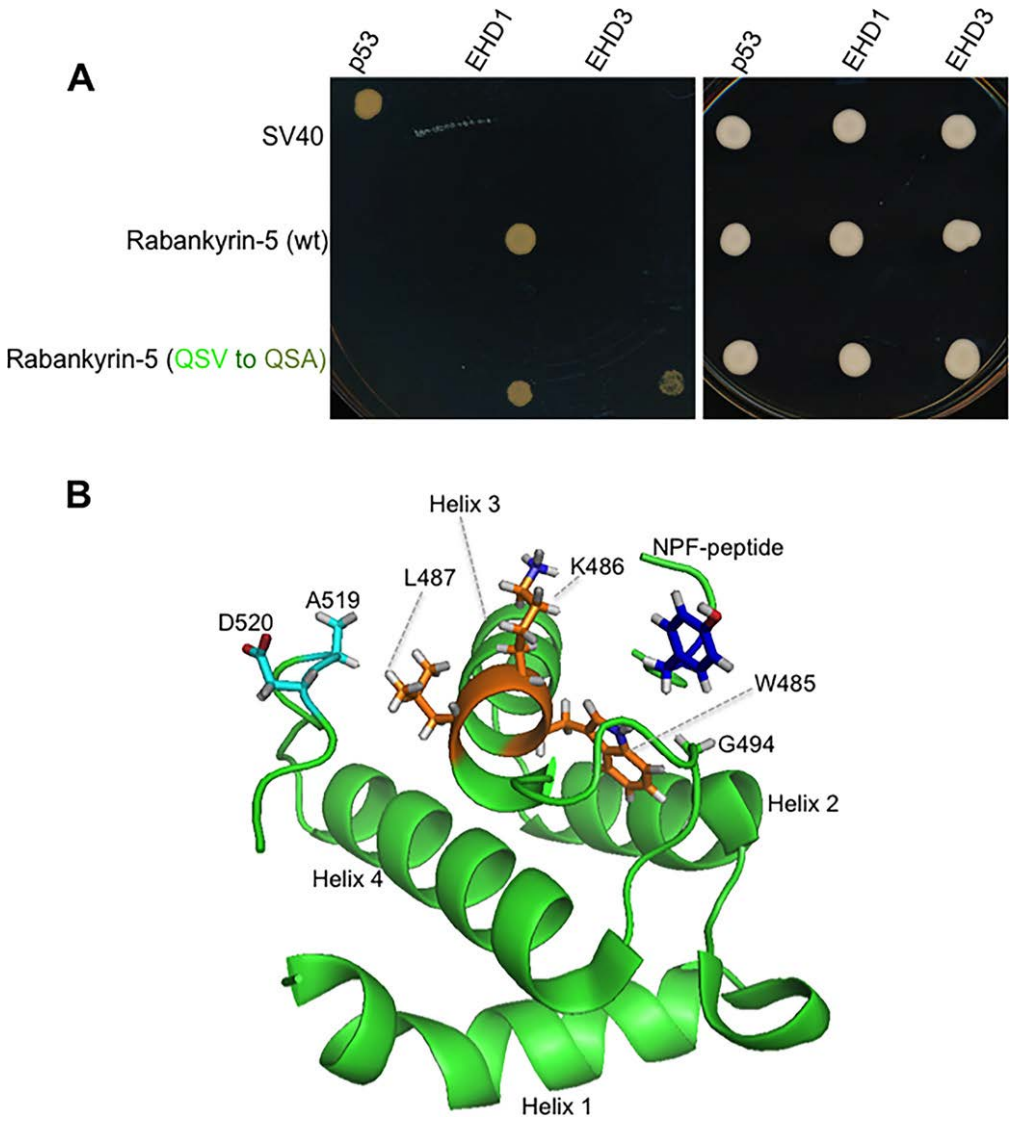
A
p53
EHD1
EHD3
p53
EHD1
EHD3
SV40
Rabankyrin-5 (wt)
Rabankyrin-5 (QSV to QSA)
B
Helix 3
NPF-peptide
K486
L487
A519
D520
W485
G494
Helix 2
Helix 4
Helix 1

Chapter V

Summary and Future Directions

17 Summary

Endocytic trafficking, which involves the internalization, sorting, degradation and recycling of macromolecules, is an integral process for maintaining cellular homeostasis and the regulation of diverse cellular processes such as signaling, migration, and cell division. The C-terminal Eps 15 Homology Domain proteins (EHD1-4) play an important role in regulating distinct steps of endocytic trafficking. EHD1, EHD3 and EHD4 are localized to intracellular tubular/vesicular membranes (Naslavsky and Caplan, 2011). In contrast, EHD2 localizes to the cytoplasmic interface of the plasma membrane, specifically the plasma membrane invaginations, caveolae. While EHD1, EHD3 and EHD4 are capable of forming hetero-oligomers, EHD2 exclusively forms homo-oligomers (Simone et al., 2013). Indeed, EHD2 is the most distinct of the four EHDs.

The crystal structure of EHD2 has been solved and it contains a partially conserved unstructured loop consisting of two proline-phenylalanine (PF) motifs: KPFRKLNPF (Daumke et al., 2007). Despite EHD2 having nearly 70% amino acid identity with its paralogs, EHD1, EHD3 and EHD4 (Naslavsky and Caplan, 2011), the latter proteins contain only a single KPF or RPF motif, but no NPF motif in their unstructured loop. We wanted to delineate the precise role of the KPFRKLNPF unstructured loop, in dimerization, protein binding, and subcellular localization.

Overall, in this study, we have demonstrated that the phenylalanine residue of EHD2 NPF is crucial for the localization of EHD2 to the plasma membrane and the cavolae. On the other hand, the proline residue is essential for the EHD2 dimerization and binding to NPF-containing protein partners. Furthermore, these studies support the recently proposed model, in which the EHD2 N-terminal region may regulate the availability of the unstructured loop for interactions with neighboring EHD2 dimers, thus promoting oligomerization. Interestingly, EHD1 has a single RPF motif that aligns with the KPF motif of EHD2. This led to the hypothesis that the RPF motif might be crucial for

binding and localization functions of EHD1. Indeed, EHD1's single RPF motif has a critical role in dimerization, binding to MICAL-L1 and Syndapin2, and localization to the tubular recycling endosomes (TRE). Moreover, recycling assays demonstrated that EHD1 RPF-to-APA was incapable of supporting normal receptor recycling.

The elaborate network of dynamic lipid membranes known as TRE orchestrates the process of endocytic recycling in mammalian cells (Jovic et al., 2009). Electron microscopy studies have determined that the tubular structures containing EHD1 are 200 nm wide and up to 10 μm long (Caplan et al, 2002). The EHD proteins have been implicated in the bending and fission of TREs, thus regulating endocytic recycling (Cai et al., 2013). EHD proteins have a C-terminal EH domain that preferentially interacts with proteins containing an asparagine-proline-phenylalanine (NPF) motif followed by acidic residues (Kieken et al., 2010; Henry et al., 2010). We had previously demonstrated that NPF-containing EHD1 interaction partners, such as molecules interacting with CasL-Like1 (MICAL-L1) and Syndapin2, are essential for TRE biogenesis (Sharma et al., 2009; Giridharan et al., 2013). Also crucial for TRE biogenesis is the generation of phosphatidic acid (PA). PA is an essential lipid component of TRE that serves as a docking point for MICAL-L1 and Syndapin2 (Giridharan et al., 2013). EHD1 and EHD3 have 86% amino acid identity; they homo- and hetero-dimerize, and partially co-localize to TRE (Galperin et al., 2002). Despite their remarkable identity, they have distinct mechanistic functions: EHD1 induces membrane vesiculation, whereas EHD3 supports TRE biogenesis and/or stabilization by an unknown mechanism. While using phospholipase D inhibitors (which block the conversion of glycerophospholipids to PA) to deplete cellular TRE, we observed that upon inhibitor washout there was a rapid and dramatic regeneration of MICAL-L1-marked TRE. Using this "de-novo synchronized" TRE biogenesis system, we determined that EHD3 is involved in the stabilization of TRE rather than their biogenesis. Moreover, we identified the residues Ala-519/Asp-520 of

EHD1 and Asp-519/Glu-520 of EHD3, governing the selectivity of these two paralogs for NPF-containing binding partners, and we presented a model to explain the atomic mechanism and provide new insight into their differential roles in vesiculation and tubulation, respectively.

In addition, our study has broader scientific relevance. It serves as a general model to resolve how highly similar proteins, which are likely to have evolved through gene duplication, have diverged within mammalian cells to carry out distinct, but related functions.

18 Future Directions

18.1 Role of NPF motif of KPFRKLNPF loop in caveolar mobility

Recent studies have demonstrated that EHD2 forms dimers with the previously proposed G-domain interface (Daumke et al., 2007) and the conserved KPFRKLNPF loop in the G domain plays a role in oligomerization. Furthermore, EHD2 is assembled into oligomeric ring-like structures (Melo et al., 2017). These structures create a scaffold that generates and/or stabilizes membrane curvature. Another study demonstrated the contribution of ATP in enhancing the oligomerization of EHD2 (Hoerneke et al., 2017). Recent evidence also supports a role of EHD2 in controlling the movement of small vesicles under the plasma membrane that are enriched in sphingolipids and cholesterol and known as caveolae (Stoeber et al., 2012; Moren et al., 2012). Moreover, regulating the formation of functional EHD2 oligomers at the membrane plays a key role in maintaining caveolae in a static and immobile state (Melo et al., 2017). We have recently demonstrated that EHD2 NPF to NAF mutants display impaired dimerization of EHD2 and binding with interaction partners. The effect of this mutant on caveolar mobility remains unknown. We will test whether the EHD2 NAF is required to regulate caveolar

mobility or more precisely, their stabilization. Our readout will use transfected GFP-caveolin1 to measure the mobility of caveolae by fluorescence recovery after photobleaching (FRAP), as we have previously done (Pelkmans et al., 2005; Sharma et al., 2009).

18.2 How does EHD2 link caveolae to the actin cytoskeleton?

Our previous studies have suggested that the binding of EHD2 to PIP2 connects caveolae to the actin microfilaments (Simone et al., 2013). Additionally, EHD2 interacting proteins may contribute to the tethering of caveolae to actin. Indeed, we show that caveolin1 is dispersed across the plasma membrane in EHBP1-depleted cells, suggesting that EHBP1 may co-operate with EHD2 in linking caveolae to actin microfilaments (Simone et al., 2013). However, the dimerization of EHD2 is not required for binding to EHBP1. The multifaceted relationship between the unstructured loop, localization of caveolae and the binding partners EHBP1 and Syndapin2 remains unclear. We will focus on understanding the connection between EHD2 oligomerization and actin cytoskeleton.

18.3 Spatio-temporal regulation of EHD1 and EHD3

EHD1 and EHD3 are capable of hetero-dimerization; it is possible that EHD1 is on TRE, but initially inactive until it receives a signal to induce vesiculation. This is a competing idea to the one proposing temporal binding, and if necessary, we will address potential post-translational modifications. The role of SUMOylation of EHD3 on TRE has already been addressed (Cabasso et al., 2015). We will address the effect of deSUMOylation of EHD3 and phosphorylation of EHD1. There is also a possibility that since EHD1 binds to a wider range of NPF-containing proteins than EHD3, including Rabankyrin-5 (Zhang et al., 2012), and that such proteins might ‘sequester’ EHD1 *in vivo*

(away from TRE) and prevent it from competing with EHD3 for TRE binding. To this aim, we will knock-down Rabankyrin-5 and determine whether the TRE become shorter, fewer, and/or less elaborate.

18.4 Identification of Residues in EH1 that govern binding of EHD1 with Rabankyrin-5

We have previously demonstrated that upon mutating EHD1, from AD to NE (at residues 519/520), did not discern a loss of EHD1 binding to Rabankyrin-5, as we initially anticipated. It is clear that other residues that are distinct from EHD3 within the EHD1 EH domain must play a role in maintaining EH1 binding pocket affinity for the Rabankyrin-5 NPF peptide. In order to evaluate the role of other residues in the EH1 binding pocket, we will generate double mutants of the six cassettes of the residues that are distinct between EH1 and EH3. Our readout will be the loss-of-binding of EHD1 with Rabankyrin-5.

18.5 Structure of EH-3

In order to gain insight into the structure-function relationship of EH3, we plan to do structural studies of EH3 with MICAL-L1 NPF peptide, which we used previously. In that regard, the solution structure of EH domain of EHD1 has already been solved (Kieken et al., 2010). The chemical shift resonances for the EH3 have been assigned (Spagnol et al., 2014). Solution of the structures of EH3 domains will be extremely useful in analyzing the mechanisms responsible for the functional role played by EHD3 and its localization.

References

- Aderem, A., & Underhill, D. M. (1999). Mechanisms of phagocytosis in macrophages. *Annual Review of Immunology, 17*, 593-623. doi:10.1146/annurev.immunol.17.1.593 [doi]
- Allantaz, F., Chaussabel, D., Stichweh, D., Bennett, L., Allman, W., Mejias, A., Pascual, V. (2007). Blood leukocyte microarrays to diagnose systemic onset juvenile idiopathic arthritis and follow the response to IL-1 blockade. *The Journal of Experimental Medicine, 204*(9), 2131-2144. doi:jem.20070070 [pii]
- Anderson, R. G. (1998). The caveolae membrane system. *Annual Review of Biochemistry, 67*, 199-225. doi:10.1146/annurev.biochem.67.1.199 [doi]
- Babst, M., Katzmann, D. J., Estepa-Sabal, E. J., Meerloo, T., & Emr, S. D. (2002)(a). Escrt-III: An endosome-associated heterooligomeric protein complex required for mvb sorting. *Developmental Cell, 3*(2), 271-282. doi:S1534-5807(02)00220-4 [pii]
- Babst, M., Katzmann, D. J., Snyder, W. B., Wendland, B., & Emr, S. D. (2002)(b). Endosome-associated complex, ESCRT-II, recruits transport machinery for protein sorting at the multivesicular body. *Developmental Cell, 3*(2), 283-289. doi:S1534-5807(02)00219-8 [pii]
- Bahl, K., Naslavsky, N., & Caplan, S. (2015). Role of the EHD2 unstructured loop in dimerization, protein binding and subcellular localization. *PloS One, 10*(4), e0123710. doi:10.1371/journal.pone.0123710 [doi]
- Bahl, K., Xie, S., Spagnol, G., Sorgen, P., Naslavsky, N., & Caplan, S. (2016). EHD3 protein is required for tubular recycling endosome stabilization, and an asparagine-glutamic acid residue pair within its Eps15 homology (EH) domain

dictates its selective binding to NPF peptides. *The Journal of Biological Chemistry, 291*(26), 13465-13478. doi:10.1074/jbc.M116.716407 [doi]

- Barriere, H., Nemes, C., Lechardeur, D., Khan-Mohammad, M., Fruh, K., & Lukacs, G. L. (2006). Molecular basis of oligoubiquitin-dependent internalization of membrane proteins in mammalian cells. *Traffic (Copenhagen, Denmark), 7*(3), 282-297. doi:TRA384 [pii]
- Bastiani, M., & Parton, R. G. (2010). Caveolae at a glance. *Journal of Cell Science, 123*(Pt 22), 3831-3836. doi:10.1242/jcs.070102 [doi]
- Behnia, R., & Munro, S. (2005). Organelle identity and the signposts for membrane traffic. *Nature, 438*(7068), 597-604. doi:nature04397 [pii]
- Bennett, M. K. (1995). SNAREs and the specificity of transport vesicle targeting. *Current Opinion in Cell Biology, 7*(4), 581-586. doi:0955-0674(95)80016-6 [pii]
- Blume, J. J., Halbach, A., Behrendt, D., Paulsson, M., & Plomann, M. (2007). EHD proteins are associated with tubular and vesicular compartments and interact with specific phospholipids. *Experimental Cell Research, 313*(2), 219-231. doi:S0014-4827(06)00423-X [pii]
- Bock, J. B., Matern, H. T., Peden, A. A., & Scheller, R. H. (2001). A genomic perspective on membrane compartment organization. *Nature, 409*(6822), 839-841. doi:10.1038/35057024 [doi]
- Bonifacino, J. S., & Glick, B. S. (2004). The mechanisms of vesicle budding and fusion. *Cell, 116*(2), 153-166. doi:S0092867403010791 [pii]
- Bonifacino, J. S., & Hurley, J. H. (2008). Retromer. *Current Opinion in Cell Biology, 20*(4), 427-436. doi:10.1016/j.ceb.2008.03.009 [doi]

- Bonifacino, J. S., & Rojas, R. (2006). Retrograde transport from endosomes to the trans-golgi network. *Nature Reviews.Molecular Cell Biology, 7*(8), 568-579. doi:nrm1985 [pii]
- Bonifacino, J. S., & Traub, L. M. (2003). Signals for sorting of transmembrane proteins to endosomes and lysosomes. *Annual Review of Biochemistry, 72*, 395-447. doi:10.1146/annurev.biochem.72.121801.161800 [doi]
- Boucrot, E., & McMahon, H. T. (2011). Nucleation of clathrin-coated pits at work. *Medecine Sciences : M/S, 27*(2), 122-125. doi:10.1051/medsci/2011272122 [doi]
- Braell, W. A., Schlossman, D. M., Schmid, S. L., & Rothman, J. E. (1984). Dissociation of clathrin coats coupled to the hydrolysis of ATP: Role of an uncoating ATPase. *The Journal of Cell Biology, 99*(2), 734-741.
- Brandhorst, D., Zwilling, D., Rizzoli, S. O., Lippert, U., Lang, T., & Jahn, R. (2006). Homotypic fusion of early endosomes: SNAREs do not determine fusion specificity. *Proceedings of the National Academy of Sciences of the United States of America, 103*(8), 2701-2706. doi:0511138103 [pii]
- Braun, A., Pinyol, R., Dahlhaus, R., Koch, D., Fonarev, P., Grant, B. D., . . . Qualmann, B. (2005). EHD proteins associate with syndapin I and II and such interactions play a crucial role in endosomal recycling. *Molecular Biology of the Cell, 16*(8), 3642-3658. doi:E05-01-0076 [pii]
- Brown, F. D., Rozelle, A. L., Yin, H. L., Balla, T., & Donaldson, J. G. (2001). Phosphatidylinositol 4,5-bisphosphate and Arf6-regulated membrane traffic. *The Journal of Cell Biology, 154*(5), 1007-1017. doi:10.1083/jcb.200103107 [doi]
- Buggia-Prevot, V., Fernandez, C. G., Udayar, V., Vetrivel, K. S., Elie, A., Roseman, J., . . . Thinakaran, G. (2013). A function for EHD family proteins in unidirectional retrograde dendritic transport of BACE1 and alzheimer's disease

abeta production. *Cell Reports, 5*(6), 1552-1563. doi:10.1016/j.celrep.2013.12.006 [doi]

- Cabasso, O., Pekar, O., & Horowitz, M. (2015). SUMOylation of EHD3 modulates tubulation of the endocytic recycling compartment. *PloS One, 10*(7), e0134053. doi:10.1371/journal.pone.0134053 [doi]
- Cai, B., Caplan, S., & Naslavsky, N. (2012). cPLA2alpha and EHD1 interact and regulate the vesiculation of cholesterol-rich, GPI-anchored, protein-containing endosomes. *Molecular Biology of the Cell, 23*(10), 1874-1888. doi:10.1091/mbc.E11-10-0881 [doi]
- Cai, B., Giridharan, S. S., Zhang, J., Saxena, S., Bahl, K., Schmidt, J. A., . . . Caplan, S. (2013). Differential roles of C-terminal Eps15 homology domain proteins as vesiculators and tubulators of recycling endosomes. *The Journal of Biological Chemistry, 288*(42), 30172-30180. doi:10.1074/jbc.M113.488627 [doi]
- Cai, B., Xie, S., Caplan, S., & Naslavsky, N. (2014). GRAF1 forms a complex with MICAL-L1 and EHD1 to cooperate in tubular recycling endosome vesiculation. *Frontiers in Cell and Developmental Biology, 2*, 22. doi:10.3389/fcell.2014.00022 [doi]
- Cai, B., Xie, S., Liu, F., Simone, L. C., Caplan, S., Qin, X., & Naslavsky, N. (2014). Rapid degradation of the complement regulator, CD59, by a novel inhibitor. *The Journal of Biological Chemistry, 289*(17), 12109-12125. doi:10.1074/jbc.M113.547083 [doi]
- Cai, H., Reinisch, K., & Ferro-Novick, S. (2007). Coats, tethers, rabs, and SNAREs work together to mediate the intracellular destination of a transport vesicle. *Developmental Cell, 12*(5), 671-682. doi:S1534-5807(07)00152-9 [pii]

- Campelo, F., Fabrikant, G., McMahon, H. T., & Kozlov, M. M. (2010). Modeling membrane shaping by proteins: Focus on EHD2 and N-BAR domains. *FEBS Letters, 584*(9), 1830-1839. doi:10.1016/j.febslet.2009.10.023 [doi]
- Cantalupo, G., Alifano, P., Roberti, V., Bruni, C. B., & Bucci, C. (2001). Rab-interacting lysosomal protein (RILP): The Rab7 effector required for transport to lysosomes. *The EMBO Journal, 20*(4), 683-693. doi:10.1093/emboj/20.4.683 [doi]
- Caplan, S., Naslavsky, N., Hartnell, L. M., Lodge, R., Polishchuk, R. S., Donaldson, J. G., & Bonifacino, J. S. (2002). A tubular EHD1-containing compartment involved in the recycling of major histocompatibility complex class I molecules to the plasma membrane. *The EMBO Journal, 21*(11), 2557-2567. doi:10.1093/emboj/21.11.2557 [doi]
- Chaudhuri, R., Lindwasser, O. W., Smith, W. J., Hurley, J. H., & Bonifacino, J. S. (2007). Downregulation of CD4 by human immunodeficiency virus type 1 nef is dependent on clathrin and involves direct interaction of nef with the AP2 clathrin adaptor. *Journal of Virology, 81*(8), 3877-3890. doi:JVI.02725-06 [pii]
- Chen, Y. A., & Scheller, R. H. (2001). SNARE-mediated membrane fusion. *Nature Reviews.Molecular Cell Biology, 2*(2), 98-106. doi:10.1038/35052017 [doi]
- Cheng, Z. J., Singh, R. D., Marks, D. L., & Pagano, R. E. (2006). Membrane microdomains, caveolae, and caveolar endocytosis of sphingolipids. *Molecular Membrane Biology, 23*(1), 101-110. doi:K7006VL47M683150 [pii]
- Christoforidis, S., Miaczynska, M., Ashman, K., Wilm, M., Zhao, L., Yip, S. C., . . . Zerial, M. (1999). Phosphatidylinositol-3-OH kinases are Rab5 effectors. *Nature Cell Biology, 1*(4), 249-252. doi:10.1038/12075 [doi]

- Chukkapalli, S., Amessou, M., Dekhil, H., Dilly, A. K., Liu, Q., Bandyopadhyay, S., . . . Kandouz, M. (2014). Ehd3, a regulator of vesicular trafficking, is silenced in gliomas and functions as a tumor suppressor by controlling cell cycle arrest and apoptosis. *Carcinogenesis, 35*(4), 877-885. doi:10.1093/carcin/bgt399 [doi]
- Colicelli, J. (2004). Human RAS superfamily proteins and related GTPases. *Science's STKE : Signal Transduction Knowledge Environment, 2004*(250), RE13. doi:10.1126/stke.2502004re13 [doi]
- Conner, S. D., & Schmid, S. L. (2003). Regulated portals of entry into the cell. *Nature, 422*(6927), 37-44. doi:10.1038/nature01451 [doi]
- Dai, J., Li, J., Bos, E., Porcionatto, M., Premont, R. T., Bourgoin, S., . . . Hsu, V. W. (2004). ACAP1 promotes endocytic recycling by recognizing recycling sorting signals. *Developmental Cell, 7*(5), 771-776. doi:S1534-5807(04)00362-4 [pii]
- Daro, E., van der Sluijs, P., Galli, T., & Mellman, I. (1996). Rab4 and cellubrevin define different early endosome populations on the pathway of transferrin receptor recycling. *Proceedings of the National Academy of Sciences of the United States of America, 93*(18), 9559-9564.
- Daumke, O., Lundmark, R., Vallis, Y., Martens, S., Butler, P. J., & McMahon, H. T. (2007). Architectural and mechanistic insights into an EHD ATPase involved in membrane remodelling. *Nature, 449*(7164), 923-927. doi:nature06173 [pii]
- de Beer, T., Carter, R. E., Lobel-Rice, K. E., Sorkin, A., & Overduin, M. (1998). Structure and asn-pro-phe binding pocket of the Eps15 homology domain. *Science (New York, N.Y.), 281*(5381), 1357-1360.
- de Beer, T., Hoofnagle, A. N., Enmon, J. L., Bowers, R. C., Yamabhai, M., Kay, B. K., & Overduin, M. (2000). Molecular mechanism of NPF recognition by EH domains. *Nature Structural Biology, 7*(11), 1018-1022. doi:10.1038/80924 [doi]

- de Renzis, S., Sonnichsen, B., & Zerial, M. (2002). Divalent rab effectors regulate the sub-compartmental organization and sorting of early endosomes. *Nature Cell Biology, 4*(2), 124-133. doi:10.1038/ncb744 [doi]
- Delprato, A., Merithew, E., & Lambright, D. G. (2004). Structure, exchange determinants, and family-wide rab specificity of the tandem helical bundle and Vps9 domains of rabex-5. *Cell, 118*(5), 607-617. doi:10.1016/j.cell.2004.08.009 [doi]
- Doherty, G. J., & McMahon, H. T. (2009). Mechanisms of endocytosis. *Annual Review of Biochemistry, 78*, 857-902. doi:10.1146/annurev.biochem.78.081307.110540 [doi]
- Doherty, G. J., Ahlund, M. K., Howes, M. T., Moren, B., Parton, R. G., McMahon, H. T., & Lundmark, R. (2011). The endocytic protein GRAF1 is directed to cell-matrix adhesion sites and regulates cell spreading. *Molecular Biology of the Cell, 22*(22), 4380-4389. doi:10.1091/mbc.E10-12-0936 [doi]
- Donaldson, J. G. (2003). Multiple roles for Arf6: Sorting, structuring, and signaling at the plasma membrane. *The Journal of Biological Chemistry, 278*(43), 41573-41576. doi:10.1074/jbc.R300026200 [doi]
- Doray, B., Lee, I., Knisely, J., Bu, G., & Kornfeld, S. (2007). The gamma/sigma1 and alpha/sigma2 hemicomplexes of clathrin adaptors AP-1 and AP-2 harbor the dileucine recognition site. *Molecular Biology of the Cell, 18*(5), 1887-1896. doi:E07-01-0012 [pii]
- Dorot, O., Steller, H., Segal, D., & Horowitz, M. (2017). Past1 modulates drosophila eye development. *PloS One, 12*(1), e0169639. doi:10.1371/journal.pone.0169639 [doi]

- Faraudo, J., & Travesset, A. (2007). Phosphatidic acid domains in membranes: Effect of divalent counterions. *Biophysical Journal, 92*(8), 2806-2818. doi:S0006-3495(07)71085-8 [pii]
- Fasshauer, D. (2003). Structural insights into the SNARE mechanism. *Biochimica Et Biophysica Acta, 1641*(2-3), 87-97. doi:S0167488903000909 [pii]
- Fasshauer, D., Sutton, R. B., Brunger, A. T., & Jahn, R. (1998). Conserved structural features of the synaptic fusion complex: SNARE proteins reclassified as Q- and R-SNAREs. *Proceedings of the National Academy of Sciences of the United States of America, 95*(26), 15781-15786.
- Ferguson, S. M., & De Camilli, P. (2012). Dynamin, a membrane-remodelling GTPase. *Nature Reviews.Molecular Cell Biology, 13*(2), 75-88. doi:10.1038/nrm3266 [doi]
- Fielding, A. B., Schonteich, E., Matheson, J., Wilson, G., Yu, X., Hickson, G. R., . . . Gould, G. W. (2005). Rab11-FIP3 and FIP4 interact with Arf6 and the exocyst to control membrane traffic in cytokinesis. *The EMBO Journal, 24*(19), 3389-3399. doi:7600803 [pii]
- Fjorback, A. W., Seaman, M., Gustafsen, C., Mehmedbasic, A., Gokool, S., Wu, C., . . . Andersen, O. M. (2012). Retromer binds the FANSHY sorting motif in SorLA to regulate amyloid precursor protein sorting and processing. *The Journal of Neuroscience : The Official Journal of the Society for Neuroscience, 32*(4), 1467-1480. doi:10.1523/JNEUROSCI.2272-11.2012 [doi]
- Francis, M. K., Holst, M. R., Vidal-Quadras, M., Henriksson, S., Santarella-Mellwig, R., Sandblad, L., & Lundmark, R. (2015). Endocytic membrane turnover at the leading edge is driven by a transient interaction between Cdc42 and

GRAF1. *Journal of Cell Science, 128*(22), 4183-4195. doi:10.1242/jcs.174417 [doi]

- Frost, A., Unger, V. M., & De Camilli, P. (2009). The BAR domain superfamily: Membrane-molding macromolecules. *Cell, 137*(2), 191-196. doi:10.1016/j.cell.2009.04.010 [doi]
- Galperin, E., Benjamin, S., Rapaport, D., Rotem-Yehudar, R., Tolchinsky, S., & Horowitz, M. (2002). EHD3: A protein that resides in recycling tubular and vesicular membrane structures and interacts with EHD1. *Traffic (Copenhagen, Denmark), 3*(8), 575-589. doi:tra030807 [pii]

- Galperin, E., Benjamin, S., Rapaport, D., Rotem-Yehudar, R., Tolchinsky, S., & Horowitz, M. (2002). EHD3: A protein that resides in recycling tubular and vesicular membrane structures and interacts with EHD1. *Traffic (Copenhagen, Denmark), 3*(8), 575-589. doi:tra030807 [pii]

- Ganley, I. G., Espinosa, E., & Pfeffer, S. R. (2008). A syntaxin 10-SNARE complex distinguishes two distinct transport routes from endosomes to the trans-golgi in human cells. *The Journal of Cell Biology, 180*(1), 159-172. doi:10.1083/jcb.200707136 [doi]
- George, M., Ying, G., Rainey, M. A., Solomon, A., Parikh, P. T., Gao, Q., . . . Band, H. (2007). Shared as well as distinct roles of EHD proteins revealed by biochemical and functional comparisons in mammalian cells and C. elegans. *BMC Cell Biology, 8*, 3. doi:1471-2121-8-3 [pii]

- George, M., Ying, G., Rainey, M. A., Solomon, A., Parikh, P. T., Gao, Q., . . . Band, H. (2007). Shared as well as distinct roles of EHD proteins revealed by biochemical and functional comparisons in mammalian cells and C. elegans. *BMC Cell Biology, 8*, 3. doi:1471-2121-8-3 [pii]

- Gesbert, F., Sauvonnet, N., & Dautry-Varsat, A. (2004). Clathrin-lndependent endocytosis and signalling of interleukin 2 receptors IL-2R endocytosis and signalling. *Current Topics in Microbiology and Immunology, 286*, 119-148.
- Giridharan, S. S., Cai, B., Naslavsky, N., & Caplan, S. (2012). Trafficking cascades mediated by Rab35 and its membrane hub effector, MICAL-L1. *Communicative & Integrative Biology, 5*(4), 384-387. doi:10.4161/cib.20064 [doi]
- Giridharan, S. S., Cai, B., Vitale, N., Naslavsky, N., & Caplan, S. (2013). Cooperation of MICAL-L1, syndapin2, and phosphatidic acid in tubular recycling endosome biogenesis. *Molecular Biology of the Cell, 24*(11), 1776-90, S1-15. doi:10.1091/mbc.E13-01-0026 [doi]
- Glebov, O. O., Bright, N. A., & Nichols, B. J. (2006). Flotillin-1 defines a clathrin-independent endocytic pathway in mammalian cells. *Nature Cell Biology, 8*(1), 46-54. doi:ncb1342 [pii]
- Gokool, S., Tattersall, D., & Seaman, M. N. (2007). EHD1 interacts with retromer to stabilize SNX1 tubules and facilitate endosome-to-golgi retrieval. *Traffic (Copenhagen, Denmark), 8*(12), 1873-1886. doi:TRA652 [pii]
- Goody, R. S., Rak, A., & Alexandrov, K. (2005). The structural and mechanistic basis for recycling of rab proteins between membrane compartments. *Cellular and Molecular Life Sciences : CMLS, 62*(15), 1657-1670. doi:10.1007/s00018-005-4486-8 [doi]
- Gorvel, J. P., Chavrier, P., Zerial, M., & Gruenberg, J. (1991). Rab5 controls early endosome fusion in vitro. *Cell, 64*(5), 915-925. doi:0092-8674(91)90316-Q [pii]

- Grant, B. D., & Caplan, S. (2008). Mechanisms of EHD/RME-1 protein function in endocytic transport. *Traffic (Copenhagen, Denmark), 9*(12), 2043-2052. doi:10.1111/j.1600-0854.2008.00834.x [doi]
- Grant, B. D., & Donaldson, J. G. (2009). Pathways and mechanisms of endocytic recycling. *Nature Reviews.Molecular Cell Biology, 10*(9), 597-608. doi:10.1038/nrm2755 [doi]
- Grosshans, B. L., Ortiz, D., & Novick, P. (2006). Rabs and their effectors: Achieving specificity in membrane traffic. *Proceedings of the National Academy of Sciences of the United States of America, 103*(32), 11821-11827. doi:0601617103 [pii]
- Gruenberg, J., Griffiths, G., & Howell, K. E. (1989). Characterization of the early endosome and putative endocytic carrier vesicles in vivo and with an assay of vesicle fusion in vitro. *The Journal of Cell Biology, 108*(4), 1301-1316.
- Guilherme, A., Soriano, N. A., Bose, S., Holik, J., Bose, A., Pomerleau, D. P., . . . Czech, M. P. (2004). EHD2 and the novel EH domain binding protein EHBP1 couple endocytosis to the actin cytoskeleton. *The Journal of Biological Chemistry, 279*(11), 10593-10605. doi:10.1074/jbc.M307702200 [doi]
- Haglund, K., Di Fiore, P. P., & Dikic, I. (2003). Distinct monoubiquitin signals in receptor endocytosis. *Trends in Biochemical Sciences, 28*(11), 598-603. doi:S0968-0004(03)00229-9 [pii]

- Haglund, K., Di Fiore, P. P., & Dikic, I. (2003). Distinct monoubiquitin signals in receptor endocytosis. *Trends in Biochemical Sciences, 28*(11), 598-603. doi:S0968-0004(03)00229-9 [pii]

- Hales, C. M., Griner, R., Hobdy-Henderson, K. C., Dorn, M. C., Hardy, D., Kumar, R., . . . Goldenring, J. R. (2001). Identification and characterization of a

family of Rab11-interacting proteins. *The Journal of Biological Chemistry, 276*(42), 39067-39075. doi:10.1074/jbc.M104831200 [doi]

- Hales, C. M., Vaerman, J. P., & Goldenring, J. R. (2002). Rab11 family interacting protein 2 associates with myosin vb and regulates plasma membrane recycling. *The Journal of Biological Chemistry, 277*(52), 50415-50421. doi:10.1074/jbc.M209270200 [doi]
- Hammer, J. A.,3rd, & Wu, X. S. (2002). Rabs grab motors: Defining the connections between rab GTPases and motor proteins. *Current Opinion in Cell Biology, 14*(1), 69-75. doi:S0955067401002964 [pii]
- Hansen, C. G., Bright, N. A., Howard, G., & Nichols, B. J. (2009). SDPR induces membrane curvature and functions in the formation of caveolae. *Nature Cell Biology, 11*(7), 807-814. doi:10.1038/ncb1887 [doi]
- Hanson, P. I., & Whiteheart, S. W. (2005). AAA+ proteins: Have engine, will work. *Nature Reviews.Molecular Cell Biology, 6*(7), 519-529. doi:nrm1684 [pii]
- Hawryluk, M. J., Keyel, P. A., Mishra, S. K., Watkins, S. C., Heuser, J. E., & Traub, L. M. (2006). Epsin 1 is a polyubiquitin-selective clathrin-associated sorting protein. *Traffic (Copenhagen, Denmark), 7*(3), 262-281. doi:TRA383 [pii]
- Henmi, Y., Oe, N., Kono, N., Taguchi, T., Takei, K., & Tanabe, K. (2016). Phosphatidic acid induces EHD3-containing membrane tubulation and is required for receptor recycling. *Experimental Cell Research, 342*(1), 1-10. doi:10.1016/j.yexcr.2016.02.011 [doi]
- Henry, G. D., Corrigan, D. J., Dineen, J. V., & Baleja, J. D. (2010). Charge effects in the selection of NPF motifs by the EH domain of EHD1. *Biochemistry, 49*(16), 3381-3392. doi:10.1021/bi100065r [doi]

- Hill, M. M., Bastiani, M., Luetterforst, R., Kirkham, M., Kirkham, A., Nixon, S. J., . . . Parton, R. G. (2008). PTRF-cavin, a conserved cytoplasmic protein required for caveola formation and function. *Cell, 132*(1), 113-124. doi:10.1016/j.cell.2007.11.042 [doi]
- Hinshaw, J. E., & Schmid, S. L. (1995). Dynamin self-assembles into rings suggesting a mechanism for coated vesicle budding. *Nature, 374*(6518), 190-192. doi:10.1038/374190a0 [doi]
- Horiuchi, H., Lippe, R., McBride, H. M., Rubino, M., Woodman, P., Stenmark, H., . . . Zerial, M. (1997). A novel Rab5 GDP/GTP exchange factor complexed to rabaptin-5 links nucleotide exchange to effector recruitment and function. *Cell, 90*(6), 1149-1159. doi:S0092-8674(00)80380-3 [pii]
- Huang, F., Kirkpatrick, D., Jiang, X., Gygi, S., & Sorkin, A. (2006). Differential regulation of EGF receptor internalization and degradation by multiubiquitination within the kinase domain. *Molecular Cell, 21*(6), 737-748. doi:S1097-2765(06)00120-1 [pii]
- Huotari, J., & Helenius, A. (2011). Endosome maturation. *The EMBO Journal, 30*(17), 3481-3500. doi:10.1038/emboj.2011.286 [doi]
- Hutagalung, A. H., & Novick, P. J. (2011). Role of rab GTPases in membrane traffic and cell physiology. *Physiological Reviews, 91*(1), 119-149. doi:10.1152/physrev.00059.2009 [doi]
- Itzen, A., & Goody, R. S. (2011). GTPases involved in vesicular trafficking: Structures and mechanisms. *Seminars in Cell & Developmental Biology, 22*(1), 48-56. doi:10.1016/j.semcdb.2010.10.003 [doi]

- Jackson, C. L., & Casanova, J. E. (2000). Turning on ARF: The Sec7 family of guanine-nucleotide-exchange factors. *Trends in Cell Biology, 10*(2), 60-67. doi:S0962-8924(99)01699-2 [pii]
- Jakobsson, J., Ackermann, F., Andersson, F., Larhammar, D., Low, P., & Brodin, L. (2011). Regulation of synaptic vesicle budding and dynamin function by an EHD ATPase. *The Journal of Neuroscience : The Official Journal of the Society for Neuroscience, 31*(39), 13972-13980. doi:10.1523/JNEUROSCI.1289-11.2011 [doi]
- Johannes, L., & Popoff, V. (2008). Tracing the retrograde route in protein trafficking. *Cell, 135*(7), 1175-1187. doi:10.1016/j.cell.2008.12.009 [doi]
- Johansson, M., Rocha, N., Zwart, W., Jordens, I., Janssen, L., Kuijl, C., . . . Neefjes, J. (2007). Activation of endosomal dynein motors by stepwise assembly of Rab7-RILP-p150Glued, ORP1L, and the receptor betalll spectrin. *The Journal of Cell Biology, 176*(4), 459-471. doi:jcb.200606077 [pii]
- Jordens, I., Fernandez-Borja, M., Marsman, M., Dusseljee, S., Janssen, L., Calafat, J., . . . Neefjes, J. (2001). The Rab7 effector protein RILP controls lysosomal transport by inducing the recruitment of dynein-dynactin motors. *Current Biology : CB, 11*(21), 1680-1685. doi:S0960-9822(01)00531-0 [pii]
- Jovanovic, O. A., Brown, F. D., & Donaldson, J. G. (2006). An effector domain mutant of Arf6 implicates phospholipase D in endosomal membrane recycling. *Molecular Biology of the Cell, 17*(1), 327-335. doi:E05-06-0523 [pii]
- Jovic, M., Kieken, F., Naslavsky, N., Sorgen, P. L., & Caplan, S. (2009). Eps15 homology domain 1-associated tubules contain phosphatidylinositol-4-phosphate and phosphatidylinositol-(4,5)-bisphosphate and are required for efficient

recycling. *Molecular Biology of the Cell, 20*(11), 2731-2743. doi:10.1091/mbc.E08-11-1102 [doi]

- Jovic, M., Naslavsky, N., Rapaport, D., Horowitz, M., & Caplan, S. (2007). EHD1 regulates beta1 integrin endosomal transport: Effects on focal adhesions, cell spreading and migration. *Journal of Cell Science, 120*(Pt 5), 802-814. doi:jcs.03383 [pii]
- Jovic, M., Sharma, M., Rahajeng, J., & Caplan, S. (2010). The early endosome: A busy sorting station for proteins at the crossroads. *Histology and Histopathology, 25*(1), 99-112. doi:10.14670/HH-25.99 [doi]
- Kahn, R. A., Cherfils, J., Elias, M., Lovering, R. C., Munro, S., & Schurmann, A. (2006). Nomenclature for the human arf family of GTP-binding proteins: ARF, ARL, and SAR proteins. *The Journal of Cell Biology, 172*(5), 645-650. doi:jcb.200512057 [pii]
- Kazazic, M., Bertelsen, V., Pedersen, K. W., Vuong, T. T., Grandal, M. V., Rodland, M. S.,Madshus, I. H. (2009). Epsin 1 is involved in recruitment of ubiquitinated EGF receptors into clathrin-coated pits. *Traffic (Copenhagen, Denmark), 10*(2), 235-245. doi:10.1111/j.1600-0854.2008.00858.x [doi]
- Kessels, M. M., Dong, J., Leibig, W., Westermann, P., & Qualmann, B. (2006). Complexes of syndapin II with dynamin II promote vesicle formation at the trans-golgi network. *Journal of Cell Science, 119*(Pt 8), 1504-1516. doi:jcs.02877 [pii]
- Kieken, F., Jovic, M., Tonelli, M., Naslavsky, N., Caplan, S., & Sorgen, P. L. (2009). Structural insight into the interaction of proteins containing NPF, DPF, and GPF motifs with the C-terminal EH-domain of EHD1. *Protein Science : A Publication of the Protein Society, 18*(12), 2471-2479. doi:10.1002/pro.258 [doi]

- Kieken, F., Sharma, M., Jovic, M., Giridharan, S. S., Naslavsky, N., Caplan, S., & Sorgen, P. L. (2010). Mechanism for the selective interaction of C-terminal Eps15 homology domain proteins with specific asn-pro-phe-containing partners. *The Journal of Biological Chemistry, 285*(12), 8687-8694. doi:10.1074/jbc.M109.045666 [doi]
- Kinchen, J. M., & Ravichandran, K. S. (2010). Identification of two evolutionarily conserved genes regulating processing of engulfed apoptotic cells. *Nature, 464*(7289), 778-782. doi:10.1038/nature08853 [doi]
- Kirchhausen, T. (1999). Adaptors for clathrin-mediated traffic. *Annual Review of Cell and Developmental Biology, 15*, 705-732. doi:10.1146/annurev.cellbio.15.1.705 [doi]
- Kirchhausen, T. (2000). Clathrin. *Annual Review of Biochemistry, 69*, 699-727. doi:69/1/699 [pii]
- Kirkham, M., Fujita, A., Chadda, R., Nixon, S. J., Kurzchalia, T. V., Sharma, D. K., . . . Parton, R. G. (2005). Ultrastructural identification of uncoated caveolin-independent early endocytic vehicles. *The Journal of Cell Biology, 168*(3), 465-476. doi:jcb.200407078 [pii]
- Kjaerulff, O., Verstreken, P., & Bellen, H. J. (2002). Synaptic vesicle retrieval: Still time for a kiss. *Nature Cell Biology, 4*(11), E245-8. doi:10.1038/ncb1102-e245 [doi]
- Koch, D., Westermann, M., Kessels, M. M., & Qualmann, B. (2012). Ultrastructural freeze-fracture immunolabeling identifies plasma membrane-localized syndapin II as a crucial factor in shaping caveolae. *Histochemistry and Cell Biology, 138*(2), 215-230. doi:10.1007/s00418-012-0945-0 [doi]

- Koles, K., Messelaar, E. M., Feiger, Z., Yu, C. J., Frank, C. A., & Rodal, A. A. (2015). The EHD protein Past1 controls postsynaptic membrane elaboration and synaptic function. *Molecular Biology of the Cell, 26*(18), 3275-3288. doi:10.1091/mbc.E15-02-0093 [doi]
- Kubo, K., Kobayashi, M., Nozaki, S., Yagi, C., Hatsuzawa, K., Katoh, Y., . . . Nakayama, K. (2015). SNAP23/25 and VAMP2 mediate exocytic event of transferrin receptor-containing recycling vesicles. *Biology Open, 4*(7), 910-920. doi:10.1242/bio.012146 [doi]
- Kucharczyk, R., Hoffman-Sommer, M., Piekarska, I., von Mollard, G. F., & Rytka, J. (2009). The saccharomyces cerevisiae protein Ccz1p interacts with components of the endosomal fusion machinery. *FEMS Yeast Research, 9*(4), 565-573. doi:10.1111/j.1567-1364.2009.00515.x [doi]
- Kumari, S., & Mayor, S. (2008). ARF1 is directly involved in dynamin-independent endocytosis. *Nature Cell Biology, 10*(1), 30-41. doi:ncb1666 [pii]
- Lamaze, C., Dujeancourt, A., Baba, T., Lo, C. G., Benmerah, A., & Dautry-Varsat, A. (2001). Interleukin 2 receptors and detergent-resistant membrane domains define a clathrin-independent endocytic pathway. *Molecular Cell, 7*(3), 661-671. doi:S1097-2765(01)00212-X [pii]
- Lapierre, L. A., Kumar, R., Hales, C. M., Navarre, J., Bhartur, S. G., Burnette, J. O., . . . Goldenring, J. R. (2001). Myosin vb is associated with plasma membrane recycling systems. *Molecular Biology of the Cell, 12*(6), 1843-1857.
- Lauffer, B. E., Melero, C., Temkin, P., Lei, C., Hong, W., Kortemme, T., & von Zastrow, M. (2010). SNX27 mediates PDZ-directed sorting from endosomes to the plasma membrane. *The Journal of Cell Biology, 190*(4), 565-574. doi:10.1083/jcb.201004060 [doi]

- Lee, A., Frank, D. W., Marks, M. S., & Lemmon, M. A. (1999). Dominant-negative inhibition of receptor-mediated endocytosis by a dynamin-1 mutant with a defective pleckstrin homology domain. *Current Biology : CB, 9*(5), 261-264. doi:S0960-9822(99)80115-8 [pii]
- Lee, D. W., Zhao, X., Scarselletta, S., Schweinsberg, P. J., Eisenberg, E., Grant, B. D., & Greene, L. E. (2005). ATP binding regulates oligomerization and endosome association of RME-1 family proteins. *The Journal of Biological Chemistry, 280*(17), 17213-17220. doi:M412751200 [pii]
- Leung, K. F., Baron, R., Ali, B. R., Magee, A. I., & Seabra, M. C. (2007). Rab GTPases containing a CAAX motif are processed post-geranylgeranylation by proteolysis and methylation. *The Journal of Biological Chemistry, 282*(2), 1487-1497. doi:M605557200 [pii]
- Levkowitz, G., Waterman, H., Zamir, E., Kam, Z., Oved, S., Langdon, W. Y., . . . Yarden, Y. (1998). c-Cbl/Sli-1 regulates endocytic sorting and ubiquitination of the epidermal growth factor receptor. *Genes & Development, 12*(23), 3663-3674.
- Lin, R. C., & Scheller, R. H. (1997). Structural organization of the synaptic exocytosis core complex. *Neuron, 19*(5), 1087-1094. doi:S0896-6273(00)80399-2 [pii]
- Lin, S. X., Grant, B., Hirsh, D., & Maxfield, F. R. (2001). Rme-1 regulates the distribution and function of the endocytic recycling compartment in mammalian cells. *Nature Cell Biology, 3*(6), 567-572. doi:10.1038/35078543 [doi]
- Lindsay, A. J., Hendrick, A. G., Cantalupo, G., Senic-Matuglia, F., Goud, B., Bucci, C., & McCaffrey, M. W. (2002). Rab coupling protein (RCP), a novel Rab4 and Rab11 effector protein. *The Journal of Biological Chemistry, 277*(14), 12190-12199. doi:10.1074/jbc.M108665200 [doi]

- Lippe, R., Miaczynska, M., Rybin, V., Runge, A., & Zerial, M. (2001). Functional synergy between Rab5 effector rabaptin-5 and exchange factor rabex-5 when physically associated in a complex. *Molecular Biology of the Cell, 12*(7), 2219-2228.
- Lu, Q., Insinna, C., Ott, C., Stauffer, J., Pintado, P. A., Rahajeng, J., . . . Westlake, C. J. (2015). Early steps in primary cilium assembly require EHD1/EHD3-dependent ciliary vesicle formation. *Nature Cell Biology, 17*(3), 228-240. doi:10.1038/ncb3109 [doi]
- Lundmark, R., Doherty, G. J., Howes, M. T., Cortese, K., Vallis, Y., Parton, R. G., & McMahon, H. T. (2008). The GTPase-activating protein GRAF1 regulates the CLIC/GEEC endocytic pathway. *Current Biology : CB, 18*(22), 1802-1808. doi:10.1016/j.cub.2008.10.044 [doi]
- Mammoto, A., Ohtsuka, T., Hotta, I., Sasaki, T., & Takai, Y. (1999). Rab11BP/Rabphilin-11, a downstream target of rab11 small G protein implicated in vesicle recycling. *The Journal of Biological Chemistry, 274*(36), 25517-25524.
- Marg, A., Schoewel, V., Timmel, T., Schulze, A., Shah, C., Daumke, O., & Spuler, S. (2012). Sarcolemmal repair is a slow process and includes EHD2. *Traffic (Copenhagen, Denmark), 13*(9), 1286-1294. doi:10.1111/j.1600-0854.2012.01386.x [doi]
- Matanis, T., Akhmanova, A., Wulf, P., Del Nery, E., Weide, T., Stepanova, T., . . . Hoogenraad, C. C. (2002). Bicaudal-D regulates COPI-independent golgi-ER transport by recruiting the dynein-dynactin motor complex. *Nature Cell Biology, 4*(12), 986-992. doi:10.1038/ncb891 [doi]

- Mattera, R., & Bonifacino, J. S. (2008). Ubiquitin binding and conjugation regulate the recruitment of rabex-5 to early endosomes. *The EMBO Journal, 27*(19), 2484-2494. doi:10.1038/emboj.2008.177 [doi]
- Maurer, M. E., & Cooper, J. A. (2006). The adaptor protein Dab2 sorts LDL receptors into coated pits independently of AP-2 and ARH. *Journal of Cell Science, 119*(Pt 20), 4235-4246. doi:jcs.03217 [pii]
- Maxfield, F. R., & McGraw, T. E. (2004). Endocytic recycling. *Nature Reviews.Molecular Cell Biology, 5*(2), 121-132. doi:10.1038/nrm1315 [doi]
- Mayor, S., & Pagano, R. E. (2007). Pathways of clathrin-independent endocytosis. *Nature Reviews.Molecular Cell Biology, 8*(8), 603-612. doi:nrm2216 [pii]
- Mayor, S., Parton, R. G., & Donaldson, J. G. (2014). Clathrin-independent pathways of endocytosis. *Cold Spring Harbor Perspectives in Biology, 6*(6), 10.1101/cshperspect.a016758. doi:10.1101/cshperspect.a016758 [doi]
- Mayor, S., Presley, J. F., & Maxfield, F. R. (1993). Sorting of membrane components from endosomes and subsequent recycling to the cell surface occurs by a bulk flow process. *The Journal of Cell Biology, 121*(6), 1257-1269.
- McBride, H. M., Rybin, V., Murphy, C., Giner, A., Teasdale, R., & Zerial, M. (1999). Oligomeric complexes link Rab5 effectors with NSF and drive membrane fusion via interactions between EEA1 and syntaxin 13. *Cell, 98*(3), 377-386. doi:S0092-8674(00)81966-2 [pii]
- McKenzie, J. E., Raisley, B., Zhou, X., Naslavsky, N., Taguchi, T., Caplan, S., & Sheff, D. (2012). Retromer guides STxB and CD8-M6PR from early to recycling endosomes, EHD1 guides STxB from recycling endosome to golgi. *Traffic*

(Copenhagen, Denmark), 13(8), 1140-1159. doi:10.1111/j.1600-0854.2012.01374.x [doi]

- McMahon, H. T., & Boucrot, E. (2011). Molecular mechanism and physiological function. *Nature Reviews.Molecular Cell Biology, 12*(8), 517-533. doi:10.1038/nrm3151 [doi]
- McMahon, H. T., & Gallop, J. L. (2005). Membrane curvature and mechanisms of dynamic cell membrane remodelling. *Nature, 438*(7068), 590-596. doi:nature04396 [pii]
- McMahon, K. A., Zajicek, H., Li, W. P., Peyton, M. J., Minna, J. D., Hernandez, V. J., . . . Anderson, R. G. (2009). SRBC/cavin-3 is a caveolin adapter protein that regulates caveolae function. *The EMBO Journal, 28*(8), 1001-1015. doi:10.1038/emboj.2009.46 [doi]
- Mellman, I. (1996). Membranes and sorting. *Current Opinion in Cell Biology, 8*(4), 497-498. doi:S0955-0674(96)80026-3 [pii]
- Melo, A. A., Hegde, B. G., Shah, C., Larsson, E., Isas, J. M., Kunz, S., . . . Daumke, O. (2017). Structural insights into the activation mechanism of dynamin-like EHD ATPases. *Proceedings of the National Academy of Sciences of the United States of America,* doi:201614075 [pii]
- Meng, Q., Xing, Y., Ren, T., Lu, H., Xi, Y., Jiang, Z., . . . Cai, L. (2016). Mammalian Eps15 homology domain 1 promotes metastasis in non-small cell lung cancer by inducing epithelial-mesenchymal transition. *Oncotarget,* doi:10.18632/oncotarget.11220 [doi]
- Miaczynska, M., & Zerial, M. (2002). Mosaic organization of the endocytic pathway. *Experimental Cell Research, 272*(1), 8-14. doi:10.1006/excr.2001.5401 [doi]

- Mintz, L., Galperin, E., Pasmanik-Chor, M., Tulzinsky, S., Bromberg, Y., Kozak, C. A., . . . Horowitz, M. (1999). EHD1--an EH-domain-containing protein with a specific expression pattern. *Genomics, 59*(1), 66-76. doi:10.1006/geno.1999.5800 [doi]
- Moren, B., Shah, C., Howes, M. T., Schieber, N. L., McMahon, H. T., Parton, R. G., . . . Lundmark, R. (2012). EHD2 regulates caveolar dynamics via ATP-driven targeting and oligomerization. *Molecular Biology of the Cell, 23*(7), 1316-1329. doi:10.1091/mbc.E11-09-0787 [doi]
- Murray, J. T., Panaretou, C., Stenmark, H., Miaczynska, M., & Backer, J. M. (2002). Role of Rab5 in the recruitment of hVps34/p150 to the early endosome. *Traffic (Copenhagen, Denmark), 3*(6), 416-427. doi:tra030605 [pii]
- Naslavsky, N., & Caplan, S. (2005). C-terminal EH-domain-containing proteins: Consensus for a role in endocytic trafficking, EH? *Journal of Cell Science, 118*(Pt 18), 4093-4101. doi:118/18/4093 [pii]
- Naslavsky, N., & Caplan, S. (2011). EHD proteins: Key conductors of endocytic transport. *Trends in Cell Biology, 21*(2), 122-131. doi:10.1016/j.tcb.2010.10.003 [doi]
- Naslavsky, N., Boehm, M., Backlund, P. S.,Jr, & Caplan, S. (2004). Rabenosyn-5 and EHD1 interact and sequentially regulate protein recycling to the plasma membrane. *Molecular Biology of the Cell, 15*(5), 2410-2422. doi:10.1091/mbc.E03-10-0733 [doi]
- Naslavsky, N., McKenzie, J., Altan-Bonnet, N., Sheff, D., & Caplan, S. (2009). EHD3 regulates early-endosome-to-golgi transport and preserves golgi morphology. *Journal of Cell Science, 122*(Pt 3), 389-400. doi:10.1242/jcs.037051 [doi]

- Naslavsky, N., Rahajeng, J., Chenavas, S., Sorgen, P. L., & Caplan, S. (2007). EHD1 and Eps15 interact with phosphatidylinositols via their Eps15 homology domains. *The Journal of Biological Chemistry, 282*(22), 16612-16622. doi:M609493200 [pii]
- Naslavsky, N., Rahajeng, J., Sharma, M., Jovic, M., & Caplan, S. (2006). Interactions between EHD proteins and Rab11-FIP2: A role for EHD3 in early endosomal transport. *Molecular Biology of the Cell, 17*(1), 163-177. doi:E05-05-0466 [pii]
- Naslavsky, N., Weigert, R., & Donaldson, J. G. (2003). Convergence of non-clathrin- and clathrin-derived endosomes involves Arf6 inactivation and changes in phosphoinositides. *Molecular Biology of the Cell, 14*(2), 417-431. doi:10.1091/mbc.02-04-0053 [doi]
- Naslavsky, N., Weigert, R., & Donaldson, J. G. (2004). Characterization of a nonclathrin endocytic pathway: Membrane cargo and lipid requirements. *Molecular Biology of the Cell, 15*(8), 3542-3552. doi:10.1091/mbc.E04-02-0151 [doi]
- Nielsen, E., Severin, F., Backer, J. M., Hyman, A. A., & Zerial, M. (1999). Rab5 regulates motility of early endosomes on microtubules. *Nature Cell Biology, 1*(6), 376-382. doi:10.1038/14075 [doi]
- Numrich, J., & Ungermann, C. (2014). Endocytic rabs in membrane trafficking and signaling. *Biological Chemistry, 395*(3), 327-333. doi:10.1515/hsz-2013-0258 [doi]
- Ohno, H., Stewart, J., Fournier, M. C., Bosshart, H., Rhee, I., Miyatake, S., . . . Bonifacino, J. S. (1995). Interaction of tyrosine-based sorting signals with clathrin-associated proteins. *Science (New York, N.Y.), 269*(5232), 1872-1875.

- Olswang-Kutz, Y., Gertel, Y., Benjamin, S., Sela, O., Pekar, O., Arama, E., . . . Segal, D. (2009). Drosophila Past1 is involved in endocytosis and is required for germline development and survival of the adult fly. *Journal of Cell Science, 122*(Pt 4), 471-480. doi:10.1242/jcs.038521 [doi]
- Otto, G. P., & Nichols, B. J. (2011). The roles of flotillin microdomains--endocytosis and beyond. *Journal of Cell Science, 124*(Pt 23), 3933-3940. doi:10.1242/jcs.092015 [doi]
- Owen, D. J., Collins, B. M., & Evans, P. R. (2004). Adaptors for clathrin coats: Structure and function. *Annual Review of Cell and Developmental Biology, 20*, 153-191. doi:10.1146/annurev.cellbio.20.010403.104543 [doi]
- Pal, A., Severin, F., Lommer, B., Shevchenko, A., & Zerial, M. (2006). Huntingtin-HAP40 complex is a novel Rab5 effector that regulates early endosome motility and is up-regulated in huntington's disease. *The Journal of Cell Biology, 172*(4), 605-618. doi:jcb.200509091 [pii]
- Pant, S., Sharma, M., Patel, K., Caplan, S., Carr, C. M., & Grant, B. D. (2009). AMPH-1/Amphiphysin/Bin1 functions with RME-1/Ehd1 in endocytic recycling. *Nature Cell Biology, 11*(12), 1399-1410. doi:10.1038/ncb1986 [doi]
- Paoluzi, S., Castagnoli, L., Lauro, I., Salcini, A. E., Coda, L., Fre', S., . . . Cesareni, G. (1998). Recognition specificity of individual EH domains of mammals and yeast. *The EMBO Journal, 17*(22), 6541-6550. doi:10.1093/emboj/17.22.6541 [doi]
- Parton, R. G., & Simons, K. (2007). The multiple faces of caveolae. *Nature Reviews.Molecular Cell Biology, 8*(3), 185-194. doi:nrm2122 [pii]
- Peter, B. J., Kent, H. M., Mills, I. G., Vallis, Y., Butler, P. J., Evans, P. R., & McMahon, H. T. (2004). BAR domains as sensors of membrane curvature: The

amphiphysin BAR structure. *Science (New York, N.Y.), 303*(5657), 495-499. doi:10.1126/science.1092586 [doi]

- Pitto, M., Brunner, J., Ferraretto, A., Ravasi, D., Palestini, P., & Masserini, M. (2000). Use of a photoactivable GM1 ganglioside analogue to assess lipid distribution in caveolae bilayer. *Glycoconjugate Journal, 17*(3 -4), 215-222.
- Polo, S., Sigismund, S., Faretta, M., Guidi, M., Capua, M. R., Bossi, G., . . . Di Fiore, P. P. (2002). A single motif responsible for ubiquitin recognition and monoubiquitination in endocytic proteins. *Nature, 416*(6879), 451-455. doi:10.1038/416451a [doi]
- Popoff, V., Mardones, G. A., Bai, S. K., Chambon, V., Tenza, D., Burgos, P. V., . . . Johannes, L. (2009). Analysis of articulation between clathrin and retromer in retrograde sorting on early endosomes. *Traffic (Copenhagen, Denmark), 10*(12), 1868-1880. doi:10.1111/j.1600-0854.2009.00993.x [doi]
- Posey, A. D.,Jr, Pytel, P., Gardikiotes, K., Demonbreun, A. R., Rainey, M., George, M., . . . McNally, E. M. (2011). Endocytic recycling proteins EHD1 and EHD2 interact with fer-1-like-5 (Fer1L5) and mediate myoblast fusion. *The Journal of Biological Chemistry, 286*(9), 7379-7388. doi:10.1074/jbc.M110.157222 [doi]
- Powelka, A. M., Sun, J., Li, J., Gao, M., Shaw, L. M., Sonnenberg, A., & Hsu, V. W. (2004). Stimulation-dependent recycling of integrin beta1 regulated by ARF6 and Rab11. *Traffic (Copenhagen, Denmark), 5*(1), 20-36. doi:150 [pii]
- Prasad, K., Barouch, W., Greene, L., & Eisenberg, E. (1993). A protein cofactor is required for uncoating of clathrin baskets by uncoating ATPase. *The Journal of Biological Chemistry, 268*(32), 23758-23761.

- Prekeris, R., Davies, J. M., & Scheller, R. H. (2001). Identification of a novel Rab11/25 binding domain present in eferin and rip proteins. *The Journal of Biological Chemistry, 276*(42), 38966-38970. doi:10.1074/jbc.M106133200 [doi]
- Prekeris, R., Klumperman, J., & Scheller, R. H. (2000). A Rab11/Rip11 protein complex regulates apical membrane trafficking via recycling endosomes. *Molecular Cell, 6*(6), 1437-1448. doi:S1097-2765(00)00140-4 [pii]
- Rahajeng, J., Giridharan, S. S., Cai, B., Naslavsky, N., & Caplan, S. (2010). Important relationships between rab and MICAL proteins in endocytic trafficking. *World Journal of Biological Chemistry, 1*(8), 254-264. doi:10.4331/wjbc.v1.i8.254 [doi]
- Raiborg, C., & Stenmark, H. (2002). Hrs and endocytic sorting of ubiquitinated membrane proteins. *Cell Structure and Function, 27*(6), 403-408.
- Randazzo, P. A., & Hirsch, D. S. (2004). Arf GAPs: Multifunctional proteins that regulate membrane traffic and actin remodelling. *Cellular Signalling, 16*(4), 401-413. doi:S0898656803001918 [pii]
- Rapaport, D., Auerbach, W., Naslavsky, N., Pasmanik-Chor, M., Galperin, E., Fein, A., . . . Horowitz, M. (2006). Recycling to the plasma membrane is delayed in EHD1 knockout mice. *Traffic (Copenhagen, Denmark), 7*(1), 52-60. doi:TRA359 [pii]
- Rink, J., Ghigo, E., Kalaidzidis, Y., & Zerial, M. (2005). Rab conversion as a mechanism of progression from early to late endosomes. *Cell, 122*(5), 735-749. doi:S0092-8674(05)00697-5 [pii]
- Robinson, M. S. (2015). Forty years of clathrin-coated vesicles. *Traffic (Copenhagen, Denmark), 16*(12), 1210-1238. doi:10.1111/tra.12335 [doi]

- Roland, J. T., Kenworthy, A. K., Peranen, J., Caplan, S., & Goldenring, J. R. (2007). Myosin vb interacts with Rab8a on a tubular network containing EHD1 and EHD3. *Molecular Biology of the Cell, 18*(8), 2828-2837. doi:E07-02-0169 [pii]
- Rotem-Yehudar, R., Galperin, E., & Horowitz, M. (2001). Association of insulin-like growth factor 1 receptor with EHD1 and SNAP29. *The Journal of Biological Chemistry, 276*(35), 33054-33060. doi:10.1074/jbc.M009913200 [doi]
- Salcini, A. E., Confalonieri, S., Doria, M., Santolini, E., Tassi, E., Minenkova, O., . . . Di Fiore, P. P. (1997). Binding specificity and in vivo targets of the EH domain, a novel protein-protein interaction module. *Genes & Development, 11*(17), 2239-2249.
- Sandvig, K., & van Deurs, B. (1994). Endocytosis without clathrin. *Trends in Cell Biology, 4*(8), 275-277. doi:0962892494902119 [pii]
- Santy, L. C., & Casanova, J. E. (2001). Activation of ARF6 by ARNO stimulates epithelial cell migration through downstream activation of both Rac1 and phospholipase D. *The Journal of Cell Biology, 154*(3), 599-610. doi:10.1083/jcb.200104019 [doi]
- Sato, M., Grant, B. D., Harada, A., & Sato, K. (2008). Rab11 is required for synchronous secretion of chondroitin proteoglycans after fertilization in caenorhabditis elegans. *Journal of Cell Science, 121*(Pt 19), 3177-3186. doi:10.1242/jcs.034678 [doi]
- Sato, M., Sato, K., Liou, W., Pant, S., Harada, A., & Grant, B. D. (2008). Regulation of endocytic recycling by C. elegans Rab35 and its regulator RME-4, a coated-pit protein. *The EMBO Journal, 27*(8), 1183-1196. doi:10.1038/emboj.2008.54 [doi]

- Schnatwinkel, C., Christoforidis, S., Lindsay, M. R., Uttenweiler-Joseph, S., Wilm, M., Parton, R. G., & Zerial, M. (2004). The Rab5 effector rabankyrin-5 regulates and coordinates different endocytic mechanisms. *PLoS Biology, 2*(9), E261. doi:10.1371/journal.pbio.0020261 [doi]
- Schonteich, E., Wilson, G. M., Burden, J., Hopkins, C. R., Anderson, K., Goldenring, J. R., & Prekeris, R. (2008). The Rip11/Rab11-FIP5 and kinesin II complex regulates endocytic protein recycling. *Journal of Cell Science, 121*(Pt 22), 3824-3833. doi:10.1242/jcs.032441 [doi]
- Seaman, M. N. (2007). Identification of a novel conserved sorting motif required for retromer-mediated endosome-to-TGN retrieval. *Journal of Cell Science, 120*(Pt 14), 2378-2389. doi:120/14/2378 [pii]
- Senju, Y., Itoh, Y., Takano, K., Hamada, S., & Suetsugu, S. (2011). Essential role of PACSIN2/syndapin-II in caveolae membrane sculpting. *Journal of Cell Science, 124*(Pt 12), 2032-2040. doi:10.1242/jcs.086264 [doi]
- Shah, C., Hegde, B. G., Moren, B., Behrmann, E., Mielke, T., Moenke, G., . . . Langen, R. (2014). Structural insights into membrane interaction and caveolar targeting of dynamin-like EHD2. *Structure (London, England : 1993), 22*(3), 409-420. doi:10.1016/j.str.2013.12.015 [doi]
- Shao, Y., Akmentin, W., Toledo-Aral, J. J., Rosenbaum, J., Valdez, G., Cabot, J. B., . . . Halegoua, S. (2002). Pincher, a pinocytic chaperone for nerve growth factor/TrkA signaling endosomes. *The Journal of Cell Biology, 157*(4), 679-691. doi:10.1083/jcb.200201063 [doi]
- Sharma, M., Giridharan, S. S., Rahajeng, J., Naslavsky, N., & Caplan, S. (2009). MICAL-L1 links EHD1 to tubular recycling endosomes and regulates receptor

recycling. *Molecular Biology of the Cell, 20*(24), 5181-5194. doi:10.1091/mbc.E09-06-0535 [doi]

- Sharma, M., Jovic, M., Kieken, F., Naslavsky, N., Sorgen, P., & Caplan, S. (2009). A model for the role of EHD1-containing membrane tubules in endocytic recycling. *Communicative & Integrative Biology, 2*(5), 431-433.
- Shestakova, A., Hanono, A., Drosner, S., Curtiss, M., Davies, B. A., Katzmann, D. J., & Babst, M. (2010). Assembly of the AAA ATPase Vps4 on ESCRT-III. *Molecular Biology of the Cell, 21*(6), 1059-1071. doi:10.1091/mbc.E09-07-0572 [doi]
- Shin, J., Monti, S., Aires, D. J., Duvic, M., Golub, T., Jones, D. A., & Kupper, T. S. (2007). Lesional gene expression profiling in cutaneous T-cell lymphoma reveals natural clusters associated with disease outcome. *Blood, 110*(8), 3015-3027. doi:blood-2006-12-061507 [pii]
- Short, B., Preisinger, C., Schaletzky, J., Kopajtich, R., & Barr, F. A. (2002). The Rab6 GTPase regulates recruitment of the dynactin complex to golgi membranes. *Current Biology : CB, 12*(20), 1792-1795. doi:S0960-9822(02)01221-6 [pii]
- Simone, L. C., Caplan, S., & Naslavsky, N. (2013). Role of phosphatidylinositol 4,5-bisphosphate in regulating EHD2 plasma membrane localization. *PloS One, 8*(9), e74519. doi:10.1371/journal.pone.0074519 [doi]
- Simone, L. C., Naslavsky, N., & Caplan, S. (2014). Scratching the surface: Actin' and other roles for the C-terminal Eps15 homology domain protein, EHD2. *Histology and Histopathology, 29*(3), 285-292. doi:10.14670/HH-29.285 [doi]

- Simonsen, A., Gaullier, J. M., D'Arrigo, A., & Stenmark, H. (1999). The Rab5 effector EEA1 interacts directly with syntaxin-6. *The Journal of Biological Chemistry, 274*(41), 28857-28860.
- Skop, A. R., Bergmann, D., Mohler, W. A., & White, J. G. (2001). Completion of cytokinesis in C. elegans requires a brefeldin A-sensitive membrane accumulation at the cleavage furrow apex. *Current Biology : CB, 11*(10), 735-746. doi:S0960-9822(01)00231-7 [pii]
- Sollner, T. (1995). SNAREs and targeted membrane fusion. *FEBS Letters, 369*(1), 80-83. doi:0014-5793(95)00594-Y [pii]
- Sollner, T., Bennett, M. K., Whiteheart, S. W., Scheller, R. H., & Rothman, J. E. (1993). A protein assembly-disassembly pathway in vitro that may correspond to sequential steps of synaptic vesicle docking, activation, and fusion. *Cell, 75*(3), 409-418. doi:0092-8674(93)90376-2 [pii]
- Sonnichsen, B., De Renzis, S., Nielsen, E., Rietdorf, J., & Zerial, M. (2000). Distinct membrane domains on endosomes in the recycling pathway visualized by multicolor imaging of Rab4, Rab5, and Rab11. *The Journal of Cell Biology, 149*(4), 901-914.
- Sorkin, A. (2004). Cargo recognition during clathrin-mediated endocytosis: A team effort. *Current Opinion in Cell Biology, 16*(4), 392-399. doi:10.1016/j.ceb.2004.06.001 [doi]
- Stein, M. P., Dong, J., & Wandinger-Ness, A. (2003). Rab proteins and endocytic trafficking: Potential targets for therapeutic intervention. *Advanced Drug Delivery Reviews, 55*(11), 1421-1437. doi:S0169409X03001613 [pii]
- Stoeber, M., Schellenberger, P., Siebert, C. A., Leyrat, C., Helenius, A., & Grunewald, K. (2016). Model for the architecture of caveolae based on a flexible,

net-like assembly of Cavin1 and caveolin discs. *Proceedings of the National Academy of Sciences of the United States of America, 113*(50), E8069-E8078. doi:1616838113 [pii]

- Stoeber, M., Stoeck, I. K., Hanni, C., Bleck, C. K., Balistreri, G., & Helenius, A. (2012). Oligomers of the ATPase EHD2 confine caveolae to the plasma membrane through association with actin. *The EMBO Journal, 31*(10), 2350-2364. doi:10.1038/emboj.2012.98 [doi]
- Sztul, E., & Lupashin, V. (2006). Role of tethering factors in secretory membrane traffic. *American Journal of Physiology.Cell Physiology, 290*(1), C11-26. doi:290/1/C11 [pii]
- Takei, K., Mundigl, O., Daniell, L., & De Camilli, P. (1996). The synaptic vesicle cycle: A single vesicle budding step involving clathrin and dynamin. *The Journal of Cell Biology, 133*(6), 1237-1250.
- Taniwaki, M., Daigo, Y., Ishikawa, N., Takano, A., Tsunoda, T., Yasui, W., . . . Nakamura, Y. (2006). Gene expression profiles of small-cell lung cancers: Molecular signatures of lung cancer. *International Journal of Oncology, 29*(3), 567-575.
- Tong, D., Liang, Y. N., Stepanova, A. A., Liu, Y., Li, X., Wang, L., . . . Vasilyeva, N. V. (2017). Increased Eps15 homology domain 1 and RAB11FIP3 expression regulate breast cancer progression via promoting epithelial growth factor receptor recycling. *Tumour Biology : The Journal of the International Society for Oncodevelopmental Biology and Medicine, 39*(2), 1010428317691010. doi:10.1177/1010428317691010 [doi]

- Ullrich, O., Reinsch, S., Urbe, S., Zerial, M., & Parton, R. G. (1996). Rab11 regulates recycling through the pericentriolar recycling endosome. *The Journal of Cell Biology, 135*(4), 913-924.
- Umebayashi, K., Stenmark, H., & Yoshimori, T. (2008). Ubc4/5 and c-cbl continue to ubiquitinate EGF receptor after internalization to facilitate polyubiquitination and degradation. *Molecular Biology of the Cell, 19*(8), 3454-3462. doi:10.1091/mbc.E07-10-0988 [doi]
- Ungewickell, E. (1999). Clathrin: A good view of a shapely leg. *Current Biology : CB, 9*(1), R32-5. doi:S0960-9822(99)80040-2 [pii]
- Vallis, Y., Wigge, P., Marks, B., Evans, P. R., & McMahon, H. T. (1999). Importance of the pleckstrin homology domain of dynamin in clathrin-mediated endocytosis. *Current Biology : CB, 9*(5), 257-260. doi:S0960-9822(99)80114-6 [pii]
- van der Bliek, A. M., Redelmeier, T. E., Damke, H., Tisdale, E. J., Meyerowitz, E. M., & Schmid, S. L. (1993). Mutations in human dynamin block an intermediate stage in coated vesicle formation. *The Journal of Cell Biology, 122*(3), 553-563.
- Van Der Sluijs, P., Hull, M., Zahraoui, A., Tavitian, A., Goud, B., & Mellman, I. (1991). The small GTP-binding protein rab4 is associated with early endosomes. *Proceedings of the National Academy of Sciences of the United States of America, 88*(14), 6313-6317.
- van Ijzendoorn, S. C. (2006). Recycling endosomes. *Journal of Cell Science, 119*(Pt 9), 1679-1681. doi:119/9/1679 [pii]
- van Kerkhof, P., Lee, J., McCormick, L., Tetrault, E., Lu, W., Schoenfish, M., . . . Bu, G. (2005). Sorting nexin 17 facilitates LRP recycling in the early endosome. *The EMBO Journal, 24*(16), 2851-2861. doi:7600756 [pii]

- van Weering, J. R., Sessions, R. B., Traer, C. J., Kloer, D. P., Bhatia, V. K., Stamou, D., . . . Cullen, P. J. (2012). Molecular basis for SNX-BAR-mediated assembly of distinct endosomal sorting tubules. *The EMBO Journal, 31*(23), 4466-4480. doi:10.1038/emboj.2012.283 [doi]
- Vitale, G., Rybin, V., Christoforidis, S., Thornqvist, P., McCaffrey, M., Stenmark, H., & Zerial, M. (1998). Distinct rab-binding domains mediate the interaction of rabaptin-5 with GTP-bound Rab4 and Rab5. *The EMBO Journal, 17*(7), 1941-1951. doi:10.1093/emboj/17.7.1941 [doi]
- Vonderheit, A., & Helenius, A. (2005). Rab7 associates with early endosomes to mediate sorting and transport of semliki forest virus to late endosomes. *PLoS Biology, 3*(7), e233. doi:04-PLBI-RA-0777R2 [pii]
- Wallace, D. M., Lindsay, A. J., Hendrick, A. G., & McCaffrey, M. W. (2002). The novel Rab11-FIP/Rip/RCP family of proteins displays extensive homo- and hetero-interacting abilities. *Biochemical and Biophysical Research Communications, 292*(4), 909-915. doi:10.1006/bbrc.2002.6736 [doi]
- Wallace, D. M., Lindsay, A. J., Hendrick, A. G., & McCaffrey, M. W. (2002). Rab11-FIP4 interacts with Rab11 in a GTP-dependent manner and its overexpression condenses the Rab11 positive compartment in HeLa cells. *Biochemical and Biophysical Research Communications, 299*(5), 770-779. doi:S0006291X02027201 [pii]
- Walseng, E., Bakke, O., & Roche, P. A. (2008). Major histocompatibility complex class II-peptide complexes internalize using a clathrin- and dynamin-independent endocytosis pathway. *The Journal of Biological Chemistry, 283*(21), 14717-14727. doi:10.1074/jbc.M801070200 [doi]

- Wang, C. W., Stromhaug, P. E., Shima, J., & Klionsky, D. J. (2002). The Ccz1-Mon1 protein complex is required for the late step of multiple vacuole delivery pathways. *The Journal of Biological Chemistry, 277*(49), 47917-47927. doi:10.1074/jbc.M208191200 [doi]
- Wang, E., Brown, P. S., Aroeti, B., Chapin, S. J., Mostov, K. E., & Dunn, K. W. (2000). Apical and basolateral endocytic pathways of MDCK cells meet in acidic common endosomes distinct from a nearly-neutral apical recycling endosome. *Traffic (Copenhagen, Denmark), 1*(6), 480-493. doi:tra010606 [pii]
- Whyte, J. R., & Munro, S. (2002). Vesicle tethering complexes in membrane traffic. *Journal of Cell Science, 115*(Pt 13), 2627-2637.
- Wichmann, H., Hengst, L., & Gallwitz, D. (1992). Endocytosis in yeast: Evidence for the involvement of a small GTP-binding protein (Ypt7p). *Cell, 71*(7), 1131-1142. doi:S0092-8674(05)80062-5 [pii]
- Williams, K. C., McNeilly, R. E., & Coppolino, M. G. (2014). SNAP23, Syntaxin4, and vesicle-associated membrane protein 7 (VAMP7) mediate trafficking of membrane type 1-matrix metalloproteinase (MT1-MMP) during invadopodium formation and tumor cell invasion. *Molecular Biology of the Cell, 25*(13), 2061-2070. doi:10.1091/mbc.E13-10-0582 [doi]
- Wong, W. T., Schumacher, C., Salcini, A. E., Romano, A., Castagnino, P., Pelicci, P. G., & Di Fiore, P. P. (1995). A protein-binding domain, EH, identified in the receptor tyrosine kinase substrate Eps15 and conserved in evolution. *Proceedings of the National Academy of Sciences of the United States of America, 92*(21), 9530-9534.
- Xie, S., Bahl, K., Reinecke, J. B., Hammond, G. R., Naslavsky, N., & Caplan, S. (2016). The endocytic recycling compartment maintains cargo segregation

acquired upon exit from the sorting endosome. *Molecular Biology of the Cell, 27*(1), 108-126. doi:10.1091/mbc.E15-07-0514 [doi]

- Xie, S., Naslavsky, N., & Caplan, S. (2014). Diacylglycerol kinase alpha regulates tubular recycling endosome biogenesis and major histocompatibility complex class I recycling. *The Journal of Biological Chemistry, 289*(46), 31914-31926. doi:10.1074/jbc.M114.594291 [doi]
- Yang, X., Ren, H., Yao, L., Chen, X., & He, A. (2015). Role of EHD2 in migration and invasion of human breast cancer cells. *Tumour Biology : The Journal of the International Society for Oncodevelopmental Biology and Medicine, 36*(5), 3717-3726. doi:10.1007/s13277-014-3011-9 [doi]
- Yap, C. C., Lasiecka, Z. M., Caplan, S., & Winckler, B. (2010). Alterations of EHD1/EHD4 protein levels interfere with L1/NgCAM endocytosis in neurons and disrupt axonal targeting. *The Journal of Neuroscience : The Official Journal of the Society for Neuroscience, 30*(19), 6646-6657. doi:10.1523/JNEUROSCI.5428-09.2010 [doi]
- Yoshida, Y., Kinuta, M., Abe, T., Liang, S., Araki, K., Cremona, O., . . . Takei, K. (2004). The stimulatory action of amphiphysin on dynamin function is dependent on lipid bilayer curvature. *The EMBO Journal, 23*(17), 3483-3491. doi:10.1038/sj.emboj.7600355 [doi]
- Zeng, J., Ren, M., Gravotta, D., De Lemos-Chiarandini, C., Lui, M., Erdjument-Bromage, H., . . . Sabatini, D. D. (1999). Identification of a putative effector protein for rab11 that participates in transferrin recycling. *Proceedings of the National Academy of Sciences of the United States of America, 96*(6), 2840-2845.

- Zerial, M., & McBride, H. (2001). Rab proteins as membrane organizers. *Nature Reviews.Molecular Cell Biology, 2*(2), 107-117. doi:10.1038/35052055 [doi]
- Zhang, J., Naslavsky, N., & Caplan, S. (2012). EHDs meet the retromer: Complex regulation of retrograde transport. *Cellular Logistics, 2*(3), 161-165. doi:10.4161/cl.20582 [doi]
- Zhang, J., Naslavsky, N., & Caplan, S. (2012)(a). EHDs meet the retromer: Complex regulation of retrograde transport. *Cellular Logistics, 2*(3), 161-165. doi:10.4161/cl.20582 [doi]
- Zhang, J., Reiling, C., Reinecke, J. B., Prislan, I., Marky, L. A., Sorgen, P. L., . . . Caplan, S. (2012)(b). Rabankyrin-5 interacts with EHD1 and Vps26 to regulate endocytic trafficking and retromer function. *Traffic (Copenhagen, Denmark), 13*(5), 745-757. doi:10.1111/j.1600-0854.2012.01334.x [doi]
- Zhang, X. M., Ellis, S., Sriratana, A., Mitchell, C. A., & Rowe, T. (2004). Sec15 is an effector for the Rab11 GTPase in mammalian cells. *The Journal of Biological Chemistry, 279*(41), 43027-43034. doi:10.1074/jbc.M402264200 [doi]
- Zwilling, D., Cypionka, A., Pohl, W. H., Fasshauer, D., Walla, P. J., Wahl, M. C., & Jahn, R. (2007). Early endosomal SNAREs form a structurally conserved SNARE complex and fuse liposomes with multiple topologies. *The EMBO Journal, 26*(1), 9-18. doi:7601467 [pii]